Wide Area Differential GPS (WADGPS)

Kee, Changdon, Ph.D.

Stanford University, 1994

WIDE AREA DIFFERENTIAL GPS (WADGPS)

A DISSERTATION

SUBMITTED TO THE DEPARTMENT OF AERONAUTICS AND ASTRONAUTICS

AND THE COMMITTEE ON GRADUATE STUDIES

OF STANFORD UNIVERSITY

IN PARTIAL FULFILLMENT OF THE REQUIREMENTS

FOR THE DEGREE OF

DOCTOR OF PHILOSOPHY
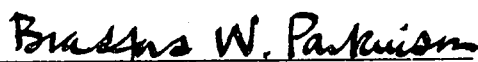
By

Changdon Kee

December 1993
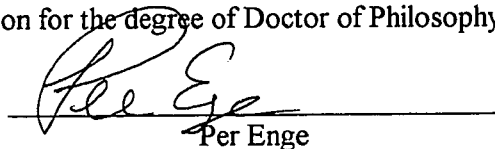
I certify that I have read this thesis and that in my opinion it is fully adequate, in scope and in quality, as a dissertation for the degree of Doctor of Philosophy.

_____
Bradford W. Parkinson
(Principal Adviser)

I certify that I have read this thesis and that in my opinion it is fully adequate, in scope and in quality, as a dissertation for the degree of Doctor of Philosophy.

_____
Per Enge

I certify that I have read this thesis and that in my opinion it is fully adequate, in scope and in quality, as a dissertation for the degree of Doctor of Philosophy.

_____
J. David Powell

I certify that I have read this thesis and that in my opinion it is fully adequate, in scope and in quality, as a dissertation for the degree of Doctor of Philosophy.

_____
C. W. Francis Everitt
(W. W. Hansen Experimental Physics Laboratory)

Approved for the University Committee on Graduate Studies:

_____
Dean of Graduate Studies

iii

ABSTRACT

The Global Positioning System (GPS) has proven to be an extremely accurate positioning sensor. A stand-alone civilian user enjoys an accuracy of 100 meters, which is adequate, for a wide variety of applications. However in some situations, such as aircraft precision approaches and taxi-way guidance, higher accuracy is required.

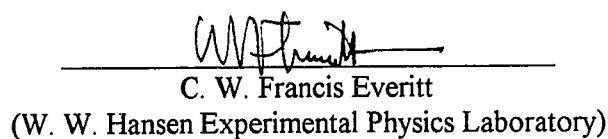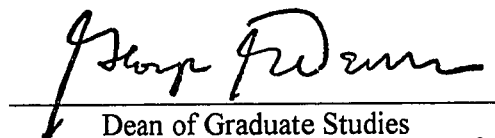Conventional Differential GPS (DGPS) usually has an accuracy of 2 to 5 meters within 100 kilometers of the stationary calibration receiver, even with the expected levels of induced Selective Availability (SA) errors. To implement DGPS on a large scale, the total number of monitor stations needed to cover the United States Continent to this accuracy would exceed 500. Wide Area Differential GPS (WADGPS) is a system that can limit the number of necessary monitor stations to 15 while achieving the same accuracy. WADGPS can reduce the installation cost and the operational cost of the system dramatically. The WADGPS system comprises a master station and monitor stations distributed across the United States. It calculates and transmits a vector of error corrections to the users preferably via satellite. This correction vector consists of parameters describing the three-dimensional ephemeris errors, the satellite clock offsets including SA, and optionally the ionospheric time delay.

The performance of a 15-station WADGPS network was investigated by simulation for users at sites across the United States, and the results indicated that normal GPS positioning errors can potentially be reduced to about one meter using WADGPS.

Experimental results from field tests using six monitor stations with a 1600km minimum baseline from a dual frequency user showed a submeter positioning accuracy, provided the data link had no time delay. These results strongly support the potential of

WADGPS to give high positioning accuracy at a cost substantially lower than that of conventional DGPS.

ACKNOWLEDGMENTS

TABLE OF CONTENTS

LIST OF TABLES

LIST OF FIGURES

LIST OF SYMBOLS

A_i	coefficient in Klobuchar's ionospheric model
b	satellite clock offset (m)
B	receiver clock offset (m)
d	physical distance between receiver and satellite (m)
D	the distance from the user to the GPS satellite (m)
D_{ij}	range vector from i-th monitor station to j-th satellite
e_{ij}	range unit vector
h_{ij}	ionospheric time delay from i-th station to j-th satellite (m)
I	ionospheric parameter vector
I_0	nominal ionospheric parameter vector
k	averaging constant in Hatch/Eshenbach filter
m	multipath error (m)
n	epoch or measurement noise
N	cycle ambiguity (cycles)
Q_{ij}	obliquity factor from i-th station to j-th satellite
R_j	j-th satellite position vector calculated from the GPS message
S_i	known position vector of the i-th monitor station
t	tropospheric error (m)
T_{gd}	satellite interfrequency bias
T_{ij}	ionospheric time delay in vertical direction at intersection of ionosphere with line from i-th station to j-th satellite (m)
v	measurement noise (m)

x_1	clock offset (second)
x_2	average frequency

Greek Symbols

α_i	ionospheric parameter
β_i	ionospheric parameter
δd	ephemeris error (m)
δI	increment of ionospheric parameter vector
δR	the magnitude of the satellite ephemeris error (m)
δR_{error}	range error difference between monitor station and user (m)
δR_j	ephemeris error vector of j-th satellite
δt	latency (sec)
ε_ρ	pseudorange noise (m)
ε_ϕ	continuous carrier phase noise (m)
ε_{SA}	SA induced range error (m)
$\dot{\varepsilon}_{SA}$	SA induced velocity error (m/s)
$\ddot{\varepsilon}_{SA}$	SA induced acceleration error (m²/s)
θ	elevation angle (rad)
λ	wave length of carrier (m)
ρ	raw pseudorange (m)
ρ_1	pseudorange in L1 frequency (m)
ρ_2	pseudorange in L2 frequency (m)
τ	local time or sampling time (sec)
ϕ	continuous carrier phase (m)

ϕ_i	raw continuous carrier phase (m)
ϕ_M	geomagnetic latitude of ionosphere subpoint

Abbreviations

BLS	batch least-squares
bps	bit per second
C/A	coarse acquisition
CIGNET	cooperative international GPS network
DGPS	differential global positioning system
DoD	Department of Defense
DOP	dilution of precision
FAA	federal aviation administration
GDOP	geometric dilution of precision
GPS	global positioning system
HDOP	horizontal dilution of precision
ID	identification
IERS	international earth rotation service
ITRF	international terrestrial reference frame
JPL	jet propulsion laboratory
LADGPS	local area differential global positioning system
Mcps	mega-chip per second
NSE	nonlinear static estimation
OOP	object oriented programming

PDOP	position dilution of precision
PRN	pseudo random noise
RINEX	receiver-independent exchange
RMS	root mean square
PST	pacific standard time
RTCM	radio technical commission for maritime services
SA	selective availability
SV	space vehicle
US	United States
VDOP	vertical dilution of precision
WADGPS	wide area differential global positioning system
WGS	world geodetic system

Conventions

$\wedge$	a hat over a symbol indicates an estimate
$\mathbf{x}$	bold and small letter indicates a vector
$\mathbf{X}$	bold and capital letter indicates a matrix

CHAPTER 1. INTRODUCTION

1.1 Motivation

The Global Positioning System (GPS) greatly increases the accuracy and reduces the cost and complexity of navigation for land, marine, and air and space users. Under normal operating conditions, it is able to provide positioning accuracies in the range of 15-25m. However, with Selective Availability (SA), a deliberate degradation of the signal for national security purposes, the errors incurred by typical civilian users have been found to be 100 m or more [Larkin, 1988]. In some situations, for example harbor navigation or precision approach of an aircraft, these accuracies are not sufficient. Table 1.1 describes the details of precision approach requirements of an aircraft.

Teasley et al. [1980] proposed the Differential GPS (DGPS) navigation concept based on the differential techniques developed for Loran C, OMEGA, and TRANSIT. DGPS is a potential means for improving navigation accuracy in a local area. A single DGPS monitor station at a known location can compute range error corrections for all GPS satellites in view. These error corrections are then broadcast to users in the vicinity. By applying the corrections to the signals received, a user within a 100km range can typically improve the accuracy down to the 2 to 5m level [Chou, 1991]. However, as the distance between the user and the monitor station increases, range decorrelation occurs and accuracy degrades. Beyond a separation distance of 100 km, a range error correction is not sufficiently accurate for the user to be able to take advantage of the full potential of DGPS. In fact, over 500 monitor stations would be required to provide conventional

1

DGPS aiding across the entire United States. The total cost of such a system would be too high and the system would not provide high reliability because of the large number of monitor stations.

Table 1.1 Aviation Navigation Accuracy Requirements

Phase	Sub-phase		Decision Height (feet)	Accuracy (2drms, meters)	
				Lateral	Vertical
Approach and Landing	Non-precision		250-3,000	100.0	
	Precision	CAT I	200	±17.1	±4.1
		CAT II	100	±5.2	±1.7
		CAT III	0-50	±4.1	±0.6

Wide Area Differential GPS (WADGPS) is a system that will reduce the number of monitor stations necessary to 10-15 while achieving virtually the same accuracy. WADGPS will reduce the operational cost and the overall cost of the system dramatically and will also increase the system's reliability and integrity. The WADGPS system calculates and transmits a vector of error corrections to the users via satellite. This correction vector consists of parameters describing the three-dimensional ephemeris errors, the satellite clock offsets including SA, and optionally the ionospheric time delay. As a result, the accuracy of WADGPS does not depend on the distance between a single monitor station and user. WADGPS provides a powerful means for bridging the gap between unaided performance and high accuracy navigation in the vicinity of a correction station.

Now the Federal Aviation Administration (FAA) is planning to implement WADGPS in the navigation system by 2000.

1.2 Previous Work

- Teasley et al. [1980] proposed the concept of DGPS and presented some preliminary experimental results. They also pointed out some potential uses of DGPS.

- Beser and Parkinson [1982] gave a very extensive review on DGPS. The history, policy, and the status of selective availability was reviewed in this paper. In addition, they listed the requirements of the civilian community and provided a comprehensive list of potential uses of DGPS.

- Kalafus et al. [1986] proposed the RTCM SC-104 recommendations for DGPS Service. Their document defined the recommended data structure of the DGPS correction message. It also recommended the radio communication link to be used.

- Kremer et al. [1990] presented experimental results concerning the effect of SA on DGPS. This is the first paper about the effect of SA based on real data. They concluded that the current RTCM SC-104 specification was sufficient to provide five-meter positioning service (95% accuracy).

- Parkinson and Kee [1990] first introduced the WADGPS concept.

- Loomis et al. [1990] introduced worldwide differential GPS, an extension of WADGPS. They proposed worldwide differential GPS for emergency space shuttle landings and showed their results.

- Kee et al. [1991] showed that WADGPS can achieve a positioning accuracy as good as that of DGPS over a wide area. They ran extensive simulations and

showed promising results. They showed that with only 15 monitor stations, WADGPS can cover the continental United States with the same accuracy as DGPS.

- Kee et al. [1992] presented WADGPS algorithms, implementations, and experimental results. They achieved two-meter accuracy using WADGPS with IERS '91 Campaign data.

- Kee et al. [1993] presented experimental results with the GPS Global Tracking Network data from P-code receivers. They postprocessed the data and achieved submeter accuracy using WADGPS, provided the data link had no time delay.

This dissertation draws on the three latter papers.

1.3 Thesis Outline

Chapter 2 is an introduction to the principles of operation of GPS, DGPS, and WADGPS. GPS basics, GPS observables, and GPS error sources are introduced and explained. Required items of equipment and data streams in monitor stations as well as users of WADGPS are discussed. Satellite ephemeris errors, satellite clock offset, and ionospheric time delay as well as their models are also introduced. Techniques for estimating those errors in the master station are described. The message contents for error corrections of WADGPS transmitted to the user from the master station are discussed.

In Chapter 3 the real-time algorithms and the real-time implementation of WADGPS are presented, and important factors in designing the WADGPS real-time algorithms are discussed. Three different algorithms are introduced and their performances are discussed. The last section presents how WADGPS is implemented.

Chapter 4 describes our simulations of WADGPS. Four different modules in the WADGPS simulation — the GPS satellite module, the monitor station module, the master station module, and the user module — are depicted. The results of ionospheric error estimation are also shown in this chapter. Finally, the navigation performance of WADGPS simulations is discussed and summarized.

Chapter 5 describes the experiments and their test results and has two parts. The first part is for the field tests with the IERS '91 Campaign data and the second part used the GPS Global Tracking Network data. Both parts explain the networks, what kinds of receivers were used in this campaign, and how the experiments were conducted. Then we describe the campaign data contents and the receiver locations for monitor stations and users. The results of the experiments and their navigation performances are discussed and summarized. Finally the effect of the latency is discussed.

Chapter 6 presents conclusions from the results of this research.

1.4 Contributions

The main contribution of the current work is the development of the WADGPS concept, algorithms, implementation, and verification by field tests. The contributions may be summarized as follows:

1. These studies were the first extensive WADGPS simulations and showed that the normal GPS positioning error can be reduced to about one meter using WADGPS. This strongly indicates the potential of WADGPS for improving positioning accuracy.

2. These studies contain the first detailed WADGPS experiments and prove the potential of WADGPS.

3. I designed several different WADGPS implementation algorithms, evaluated their performances, and found the accurate algorithm.

4. The experiments achieved a submeter WADGPS positioning accuracy for 1632km minimum baseline in the experiments provided the data link had no time delay, which is about the accuracy of DGPS with less than a 100km baseline.

5. A study of the latency–defined as the time taken to estimate the correction parameters plus the time spent for the error corrections to arrive at the users–showed that 2-3m of three-dimensional RMS positioning accuracy can be achieved with 5-10 seconds of latency, which result in 10-20 seconds of maximum age, if P-code mode is selected and WADGPS is used with error-rate corrections.

6. A statistics of the ionospheric time delay measurement noise for P-code and cross-correlation mode led us to predict the WADGPS test results with 5-10 seconds of latency and using the receivers in cross-correlation mode as 3-5m of three-dimensional positioning errors.

7. I developed the Matrix, GPS, and WADGPS libraries, all of which are written in the C++ language, using the Object Oriented Programming (OOP) concept. OOP facilitates the implementation of the new concept and provides an excellent environment for enhancements and extensions.

CHAPTER 2. WIDE AREA DIFFERENTIAL GPS (WADGPS) ARCHITECTURE

2.1 Introduction

GPS is a satellite-based passive positioning system currently under deployment by the United States Air Force. It will be fully operational in the mid-1990s [Green, et al., 1989], and will provide positioning service with an accuracy of 100m (2drms) to any number of users, at all times, anywhere on or near the surface of the Earth. In its planned configuration it will consist of a constellation of 24 satellites in 12-hour orbits at an altitude of 20,183km, each broadcasting a highly accurate ranging signal and its own orbital parameters, which will enable the user to calculate the position of each satellite at the time of transmission of the signal. It will also have five Monitor Stations, which track all GPS signals, a Master Control Station, which takes the measurements from the Monitor Stations and computes satellite ephemerides and satellite clock corrections, and Upload Stations, which transmit data up to the satellites, including new ephemerides, clock corrections, and other broadcast message data. The signal consists of an L-band carrier, modulated by C/A code, which provides civilian users with an easy lock-on to the GPS signal, and P code, which provides mostly military users with precise positioning. A user who receives ranging signals from four or more satellites can passively determine his own position, velocity, and time. Further information on GPS can be found in references such as Milliken [1980], ION [1980, 1984, 1987], and Wells et al. [1986].

The following sections describe the basics of GPS and give definitions of GPS observables, and error sources in GPS measurements. This is followed by an introduction to DGPS and WADGPS, which has its own master station, monitor stations, and upload link. Each functional component of WADGPS is described and the procedures used at the master station for estimating ionospheric time delay parameters and ephemeris and satellite clock errors are discussed. Then the user message content and its format are proposed. Finally, the chapter ends with a brief summary.

2.2 GPS Overview

The underlying principle of GPS navigation is very simple. If a user knows the distance to four GPS satellites with known positions, it can determine its position and time by solving the four distance equations [Milliken, 1980]. However, the realization of this simple concept is very complex. The concept poses three problems. The first is how to let the user know the position of the satellites. The second is how to find the distance between the user and the satellites. The third is how to provide enough satellites to users (anytime and anyplace) on or close to the surface of the earth.

To provide a solution to the first problem, the Master Control Station processes the data from four Monitor Stations, estimates the ephemeris and clock model parameters for each Space Vehicle (SV), i.e., GPS satellite, and sends them to the Upload Station. The Upload Station then utilizes an S-band command-and-control uplink to upload data into satellite navigation processors [Russel, 1980]. The SVs broadcast the navigation data at a data rate of 50 bits per second. The navigation data include information on the status of the space vehicle, the parameters for computing the clock correction, the ephemeris of the space vehicle and estimated corrections for delays in the propagation of the signal through the atmosphere. In addition, it contains almanac information that defines the approximate

ephemerides and status of all the other space vehicles, which is required for use in signal acquisitions. From the navigation data the users can calculate a given satellite's position very precisely.

The distance problem is solved by use of a Pseudo Random Noise (PRN) code family for which the cross correlations are small. A correlator used in conjunction with this pattern facilitates finding the time difference between transmission and reception [Spilker, 1979]. The GPS uses two types of PRN codes. The first, the precision (P) code, is the one with longer period (38 weeks), higher chip rate (10.23Mcps), and higher resolution (0.3m). The second, the clear acquisition (C/A) code, has a period of one ms, a chip rate of 1.023Mcps, and a resolution of about three meters. The modulo two sum of the navigation data and code is then used to modulate the carrier to generate the GPS signal. The carriers used by GPS are in the L-band and have frequencies of 1575.42MHz (L1) and 1227.60MHz (L2). Under most circumstances, the C/A code is transmitted with the L1 frequency only and the P code is transmitted with both the L1 and the L2 frequencies. Most civilian receivers are set up to use the C/A code rather than the P code. For security reasons, access to the P code may be limited to authorized users only. However, the C/A code will always be available [Ward, 1989].

The coverage problem is solved by the use of 24 satellites, with four satellites in each of six 55°-inclined, equally spaced orbital planes. This GPS satellite configuration is called the 21 Primary Satellite Constellation [Green, 1989], which is optimized to provide the best coverage in the event of any single satellite's failure. The 21 Primary Satellite Constellation will be fully implemented sometime during 1994.

2.3 GPS Observables

The measurements a user can get from a GPS receiver are code phase and carrier phase. The pseudorange is equal to the sum of the code phase and an unknown integer number of C/A code epochs multiplied by the speed of light. Because the signal can travel about 299.79 km in a C/A code epoch, this integer is not hard to find and current receivers output pseudorange with the integer already determined. The pseudorange from receiver i to satellite j at one epoch can be written as

$$\rho_{ij} = d_{ij} + \delta d_{ij} + h_{ij} + t_{ij} + m_{ij} - b_j + B_i + \varepsilon_\rho \qquad (2.1)$$

where

ρ: measured pseudorange (m)

d: physical distance between receiver and satellite (m)

δd: ephemeris error (m)

h: ionospheric time delay (m)

t: tropospheric error (m)

m: multipath error (m)

b: satellite clock offset (m)

B: receiver clock offset (m)

ε_ρ: pseudorange noise (m)

In a real-time application the receivers usually provide the cumulative sum of the carrier phase rather than the carrier phase itself. This measurement is called the continuous carrier phase. Because the initial value of the continuous carrier phase is an unknown, there is an initial cycle ambiguity. This cycle ambiguity is difficult to resolve in real-time. The reason is that most of the measurement error in code is bigger than the

wavelength of the carrier (19 cm for L1). The continuous carrier phase of satellite j

relative to receiver i at a certain epoch can be written as

$$\phi_{ij} = d_{ij} + \delta d_{ij} + h_{ij} + t_{ij} + m_{ij} - b_j + B_i + N_{ij} \cdot \lambda + \varepsilon_\phi \qquad (2.2)$$

where

ϕ: continuous carrier phase (m)

N: cycle ambiguity (cycles)

λ: wave length of carrier (m)

ε_ϕ: continuous carrier phase noise (m)

If the code is smoothed with the continuous carrier phase, it becomes more precise,

and the result is more accurate positioning.

2.4 Error Sources in GPS measurements

The sources of errors in GPS measurements are summarized as follows in order of

decreasing severity:

1. Selective Availability (SA) --- This is an artificial error implemented by the

    Department of Defense (DoD) for security reasons [Beser, 1982]. The error is

    about 100 meters (2 drms). The SA is implemented by dithering the SV clock and

    broadcasting degraded ephemeris data [Kremer, 1990]. The correlation time of

    SA is about 200 seconds. Chou [1990] identified the parameters of a second-order

    Markov process which characterize the observed SA effects. Chou modeled SA-

    induced range error (ε_{SA}) as follows:

$$\frac{d^2 \varepsilon_{SA}}{dt^2} + 2\beta \frac{d\varepsilon_{SA}}{dt} + \beta^2 \varepsilon_{SA} = w_{SA} \qquad (2.3)$$

$$\text{where } w_{SA} = N(0, 4\beta^2\sigma^2),$$

and he determined β=0.011sec^{-1} and σ=14.3m. The correlation time, τ, which is $\dfrac{2.146}{\beta}$, is about 200 seconds. These numbers typically vary by about 10%. SA is the most rapidly changing error in GPS, and it cannot be corrected by the stand-alone user. The SA parameters probably can be changed frequently.

2. Ionospheric Delay --- The signal propagating in the ionosphere is refracted by ions. As a result, the code encounters a phase lag; whereas the carrier experiences a phase advance. The vertical delay is about 20-30 meters during the day and three to six meters at night. The correlation time for this error is several hours. Dual frequency users can eliminate most of the ionospheric delay by using the time differential delay between L1 and L2. Single frequency users can eliminate about 60% of the ionospheric delay by using the Klobuchar ionospheric model [Klobuchar, 1986] [Stephen, 1986].

3. Tropospheric Delay --- This delay occurs in the lower atmosphere up to 80km. It is approximately 30 meters at low satellite elevation angles. The main cause is the altitude variation of the refractive index, which is a function of local temperature, pressure, and humidity. Thus tropospheric error is divided into dry and wet components. The dry component contains approximately 90% of the total zenith range error, and may be estimated from surface pressure data with an accuracy of about 0.2%. The wet component, on the other hand, depends on the atmospheric conditions all along the signal path. These conditions are not necessarily well correlated with surface conditions. Typically, the wet component will be about 30cm or more for a 20-degree elevation angle. To achieve very high positioning

accuracy, water vapor radiometers need to be used to infer the integrated water vapor content along the lines of sight to the satellites. This is because the atmospheric water vapor content is likely to be quite variable in time and inhomogeneous spatially in many locations. When the elevation angle is above 5°, the tropospheric delay can be corrected with an uncertainty of typically about 5cm by Black's Model [Black, 1978].

4. Ephemeris Error — This error is the difference between the actual satellite position and the position predicted by broadcast navigational messages [Greenspan, 1986]. Normally it is below three meters. Since the period of a GPS satellite is about 12 hours, the ephemeris error changes slowly with time. The stand-alone user cannot correct this error.

5. Satellite Clock Error — This error is the difference between the time of the actual clock and that of the clock model identified by the master control station [Greenspan, 1986]. For the highly accurate cesium oscillator used on SVs, this error is by itself very small (the drift rate is 10^{-13}sec/sec). But since satellite clock error and SA are lumped together the net effect is very large (~100m). The stand-alone user cannot correct this error.

6. Multipath Effect — This error is caused by the fact that both the direct and the reflected signal are received [Bishop, 1985]. Because spread spectrum systems can reject signals delayed by more than one code chip [Dixon, 1984], the multipath error occurs when the reflected signal path is less than 450 meters for the C/A code and less than 45 meters for the P code. With great care the multipath error for code tracking receivers can be reduced to less than a meter externally or inside the receiver. The external reduction involves reducing the multipath error by

antenna gain shaping through a ground plate or a choke ring or by the antenna being placed at an obstacle-free site. The internal reduction involves reducing the multipath error inside the receiver by using narrow correlator spacing [van Dierendonck, et al., 1992] or using a multipath estimating delay lock loop (installing multi-correlators to each channel to be able to track several paths simultaneously instead of a single path) [van Nee, 1993].

7. Receiver Clock Error --- *This error is caused by the oscillator used in the receiver,* typically a quartz crystal oscillator with a drift rate of 10^{-8}-10^{-9}sec/sec. Many receivers also accept external timing from an atomic clock, usually a rubidium clock (10^{-12}sec/sec). Most of the receiver clock error can be eliminated in navigation solutions.

8. Interchannel Bias --- This error is specific to multichannel receivers [Greenspan, 1986] [Knight, 1987]. Because of the differences in the hardware of each channel, a bias exists between the channels. Calibration can eliminate the interchannel biases.

9. Receiver Interfrequency Bias --- This error exists only in dual-frequency receivers. Because the L1 and L2 signals are not synchronized inside the receiver, there is a bias between the L1 and L2 frequency [Wilson, 1993]. Since interfrequency bias is constant for all the channels, the bias acts like a receiver clock error in navigation solutions. Calibration can eliminate the interfrequency bias.

10. Satellite Interfrequency Bias --- Because the L1 and L2 signals are not synchronized inside the GPS satellite, there is a bias (as big as 1.2m), T_{gd}, between the L1 and L2 frequency. T_{gd} is included in the ionospheric time delay

measurement from dual-frequency receiver unless it is carefully calibrated and taken off from the raw ionospheric time delay measurement [Wilson, 1993]. Since T_{gd} value of each GPS satellite is constant for all the channels, the bias acts like a satellite clock error. Estimation of T_{gd} value for each GPS satellite can eliminate the satellite interfrequency bias.

11. Receiver Noise --- This error is composed of thermal noise, a quantization error and the residuals of modeling. It can be approximated as a white Gaussian noise. Standard deviation of the typical receiver noise is approximately 1m and 0.001m for code and carrier, respectively. Because of its white characteristics, it can be reduced by averaging filters.

2.5 Differential GPS

The above summary of the GPS measurement error sources suggests that these sources can be fit into two categories. The first category consists of SA, the ionospheric delay, the tropospheric delay, the ephemeris and the SV clock. These errors are more or less common to receivers in a given area and are therefore called common errors. The second category is composed of the multipath effect, the interchannel bias, interfrequency bias, the receiver clock error, and the receiver noise. These errors depend on either the environment or the hardware of the receivers, and they are called noncommon errors. One distinction between these two categories is that the common errors constitute a large part of the total error and are hard to eliminate by models only for the stand-alone user whereas the noncommon errors can be reduced drastically if proper measures are taken.

Fig. 2.1 shows the basic concept of DGPS. The key element of DGPS is a receiver at a surveyed location, which is called a reference station or a monitor station. Because the

exact position of the reference station is known, the common errors can be estimated. Within certain spatial and temporal limits, users can cancel a large portion of the common errors in a local area and can greatly improve navigation accuracy. A single DGPS monitor station at a known location can compute a range error correction for each GPS satellite in view. These error corrections are then broadcast to users in the vicinity as depicted in Figure 2.1. By applying the corrections to the signals received, a user can typically improve the accuracy down to a level of two to five meters [Chou, 1991].

However, as the distance between the user and the monitor station increases, range decorrelation occurs and accuracy is degraded. This increased error is due to the fact that projection of the ephemeris error onto the user-satellite line of sight is no longer the same as the projection onto the monitor station-satellite line of sight. This is illustrated in Figure 2.2.

The maximum range error difference, δR_{error}, between the monitor and user is given by,

$$max(\delta R_{error}) \approx \frac{d}{D}\delta R \qquad (2.4)$$

where δR is the magnitude of the satellite ephemeris error, d is the separation between the user and the monitor station, and D is the distance from the user to the GPS satellite.
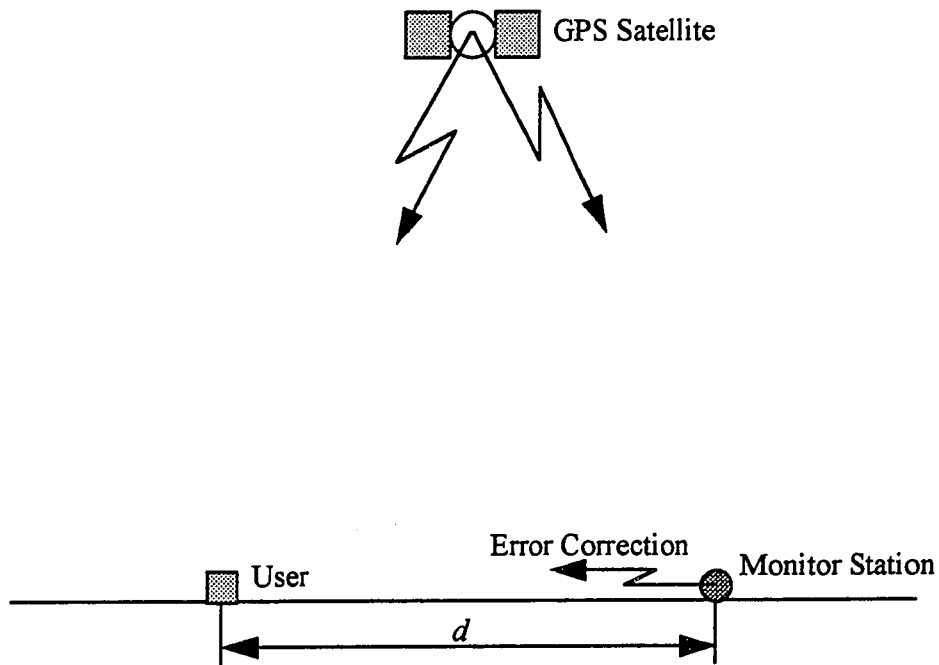
Figure 2.1 Overview of Differential GPS

In addition, if the user and the monitor station are widely separated, the lines of sight through the ionosphere are also different, resulting in differences in the ionospheric delay observed. A similar, but smaller effect occurs for the tropospheric delay.

Beyond a separation distance of 100km, a range error correction is not sufficiently accurate for the user to take full advantage of DGPS. In fact, over 500 monitor stations--assuming that the area of the continental U.S. is 2200km times 4500km and the distance between the monitor stations is 141km--would be required to provide standard single station DGPS aiding across the entire United States. The total cost of such a system would be too high and the system would not provide high reliability because of the large number of monitor stations. Wide Area Differential GPS (WADGPS) solves this problem, as the next section will show.
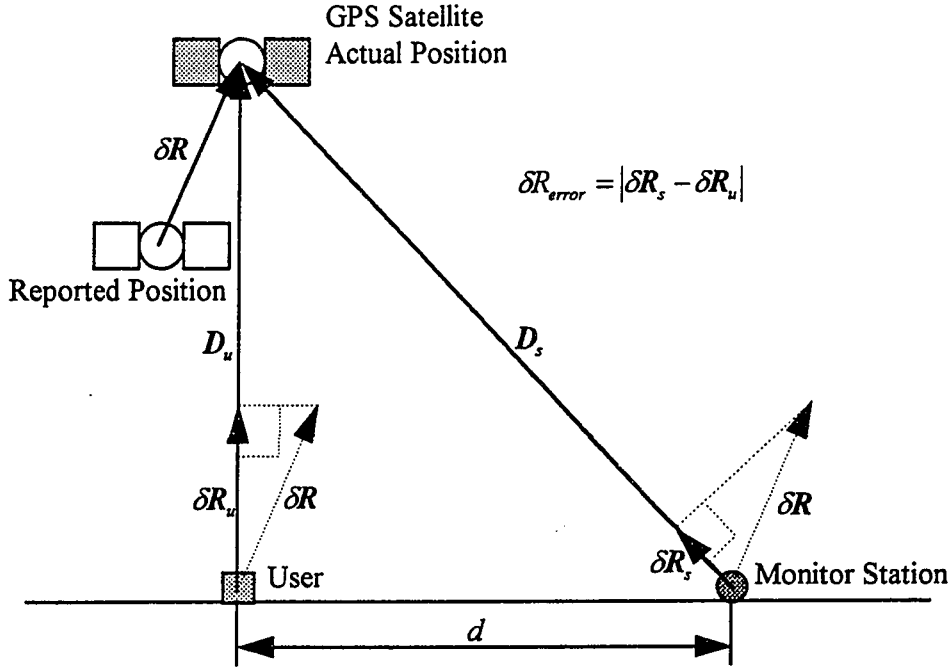
Figure 2.2 Degradation of DGPS Accuracy with Distance.

The accuracy of the range correction broadcast by a DGPS monitor station degrades with distance. The figure shows an ephemeris error δR that produces a small range error, δR_s, at the monitor station but a larger range error, δR_u, at the user location. If the user were to employ the range correction broadcast by the monitor station, a residual range error of $\delta R_s - \delta R_u$ would remain.

2.6 Wide Area Differential GPS (WADGPS) Architecture

Instead of calculating a scalar range error correction for each satellite, as is done in DGPS, WADGPS provides a vector of error corrections comprised of a three-dimensional ephemeris error and clock offset for each GPS satellite, and, optionally, ionospheric time delay parameters. The accuracy of the WADGPS correction is consistent within the monitored region and degrades gracefully on the perimeter.
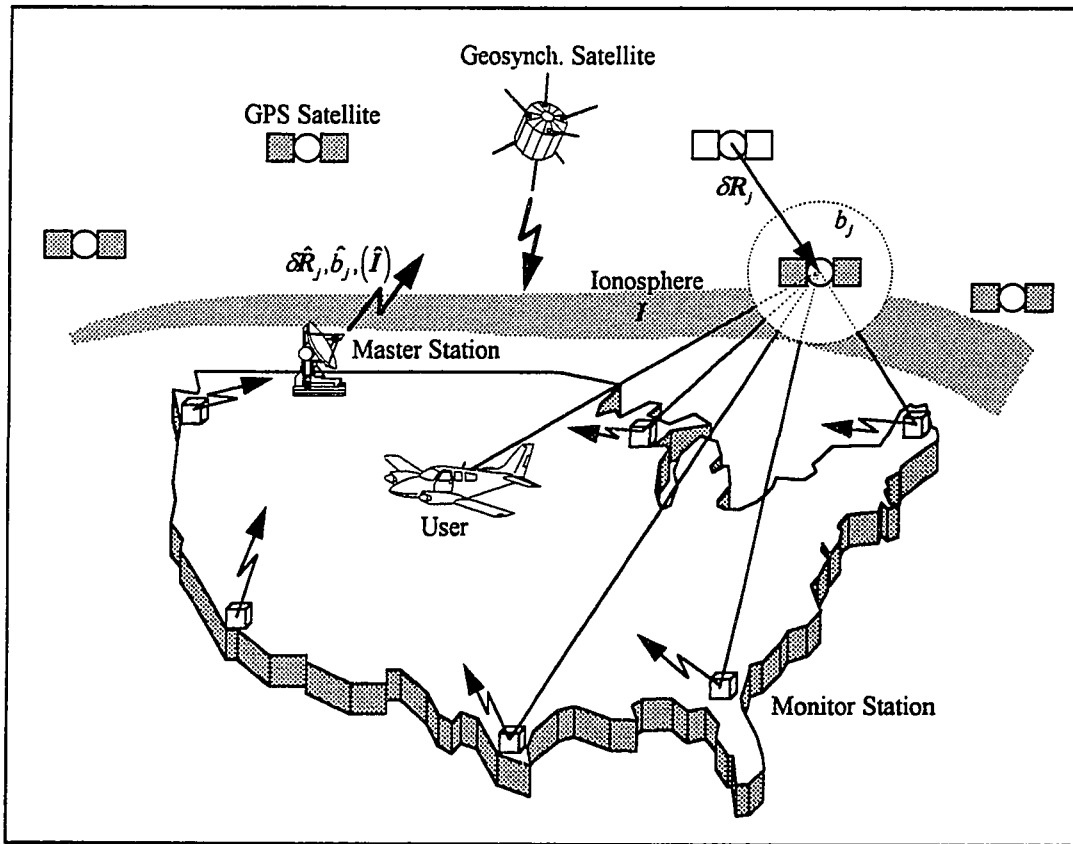
Figure 2.3 Wide Area Differential GPS Concept

The WADGPS network consists of one master station, a number of monitor stations, and a communication link. Each monitor station is equipped with a high quality rubidium clock and a GPS receiver capable of tracking all satellites within the field of view. GPS measurements taken at each local station are sent to the master station. The master station estimates ionospheric time delay parameters plus the satellite ephemeris and clock errors, based on the known location of the monitor station and the information collected. The computed error corrections are transmitted to the users via any convenient communication link such as satellite, telephone, or radio.

Figure 2.3 provides an overview of the WADGPS, and Figure 2.4 shows the flow of information between the system components. The process can be summarized as follows:

1. Monitor stations at known locations collect GPS pseudoranges from all satellites in view.

2. Pseudoranges and dual frequency ionospheric delay measurements are sent to the master station.

3. The master station computes an error correction vector.

4. The error correction vector is transmitted to users.

5. Users apply error corrections to their measured pseudoranges and collected ephemeris data to improve navigation accuracy.

The following subsections describe the monitor stations, the master station, and the typical proposed WADGPS user. The detailed function of the master station is described in the next section.
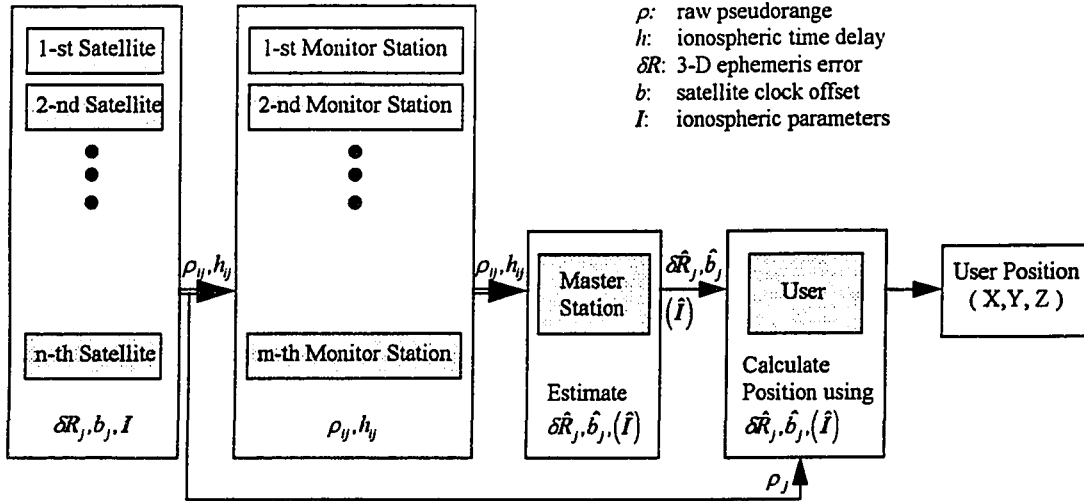
Figure 2.4 Block Diagram of WADGPS Components

2.6.1 Monitor Stations

The function of the monitor station is to collect GPS measurements from a presurveyed location and send the GPS measurements to the master station. The position of each station is known to an accuracy of centimeters, and each station is situated where it can reliably track satellites down to an elevation mask angle of five degrees.

Each monitor station is equipped with a rubidium clock, meteorological sensor, and a receiver capable of providing dual frequency ionospheric error measurements. The ionospheric errors, corrected for atmospheric errors, are transmitted together with pseudorange measurements to the master station in near real time. Tropospheric delays are corrected before data transfer to the master station based on a tropospheric delay algorithm; the inputs are from a meteorological sensor that provides temperature, pressure, and humidity and is located at the monitor station. The data may be transmitted to the master station via a communications satellite data links or telephone links.

The number of monitor stations in WADGPS should be such that WADGPS provides sufficient density for each GPS satellite to be seen by preferably more than four monitor stations, since there are three ephemeris errors and one satellite clock offset for each satellite as well as the monitor station clock offset to be estimated. Also redundancy for the monitor station function failure should be considered.

2.6.2 Master Station

The primary function of the master station is to take the ionospheric measurements and the atmospherically corrected GPS measurements from monitor stations, to estimate the ephemeris errors, satellite clock offsets, monitor station receiver clock offsets, and, optionally the ionospheric time delay parameters for single-frequency users, and to transmit those error corrections to WADGPS users. Another major function of the master station is to monitor the integrity of the signal.

Data links for broadcasting WADGPS error corrections to users can be low frequency Loran-C, UHF/VHF radio beacons, or satellite communication links. Loran-C transmits low frequency carrier (100KHz) and covers a region of 500km radius from each Loran-C station. The biggest advantage of Loran-C is that we can use the existing Loran-C stations to transmit the error corrections and as a result the implementation cost is cheaper than the others. But it has very restricted data transmission rate up to 50 bits per second and also data transmission error is one of problems to be solved to use Loran-C in WADGPS. The UHF/VHF radio beacon is one easy way to broadcast WADGPS error corrections, and it is already being used in DGPS, but since the area covered by WADGPS is very large, more than 250 radio beacons would be required for the continental United States (provided that the range of radio beacon is 200km [Enge, 1992]), which would result in a complex communication network.

Given these drawbacks, the satellite communication link may be the most simple, cheap, and reliable way to broadcast error corrections. An added advantage is that this link can also cover mountainous areas which radio beacons cannot do. The only disadvantage is that the data transmission rate is limited to 250 bps, which is available so far. However, if a 5-10 second WADGPS error correction update is used, a rate of 250bps is still usable. This will be discussed in Chapter 3.

Details of the master station estimation are given in the next section.

2.6.3 User

A typical user who would benefit from the WADGPS has a single-frequency C/A code GPS receiver with a quartz oscillator. But a dual-frequency user would derive the greatest benefit from WADGPS error corrections and would obtain more accurate positioning .

Each user collects pseudoranges and ephemeris parameters for all GPS satellites in view. In addition, it receives the error correction vector sent by the master station via phone link or satellite transmission. These corrections which are ephemeris errors and satellite clock error for each satellite, and ionospheric parameters, are applied directly to the raw measurements. The adjusted measurements are then used to form a least-squares solution for the user position and clock bias.

2.7 Master Station Error Modeling

The key to WADGPS is the formulation and computation of the error correction vector by the master station. This correction accounts for the three-dimensional ephemeris error and clock bias for each GPS satellite which is in view of one or more of the monitor stations, plus eight ionospheric time delay parameters. These parameters are

estimated based on the information gathered by the monitor stations. In addition to the error correction vector, the master station must also estimate the offset of each monitor station clock from a set reference.

The following subsections describe the sources of error, the models used by the master station, and the techniques for estimating the model parameters. The master station computes the correction vector in a two-step process. In the first step, the parameters in the ionospheric model are identified by a nonlinear static estimation (NSE) algorithm. (A recursive filter, for example an extended Kalman filter, also can be used.) The estimated ionospheric delays are then used to adjust the raw measurements from each of the local stations. The second stage solves for the ephemeris and clock errors for each of the GPS satellites observed by the network, using a batch least-squares (BLS) solution.

2.7.1 Ionospheric Time Delay

As GPS satellite signals traverse the ionosphere, their modulation is delayed by an amount proportional to the number of free ions encountered (the Total Electron Content). This is known as group delay. The ion density is a function of local time, magnetic latitude, sunspot cycle, and other factors. Its highest peak occurs at about 2:00 PM local solar time.

Klobuchar developed a simple analytical model for ionospheric time delay which we have used as the basis for the ionospheric correction model [Klobuchar, 1986] and of which parameters are being broadcast for single frequency user to correct the ionospheric time delay. His model yields an RMS correction of at least 60% for the entire northern hemisphere [Stephens, 1986]. By performing a parameter fit optimized for the US, we can improve this accuracy.

In Klobuchar's model, the vertical ionospheric time delay is expressed by the positive portion of a cosine wave plus a constant night-time bias, as follows [Stephens, 1986]:

$$T_{ij} = A_1 + A_2 \cos\left[\frac{2\Pi(\tau - A_3)}{A_4}\right]$$ (2.5)

where

T_{ij}:   ionospheric time delay in vertical direction at intersection

of ionosphere with line from i-th station to j-th satellite.

$A_1 = 5 \times 10^{-9}$ seconds (night-time value)

$A_2 = \alpha_1 + \alpha_2 \phi_M + \alpha_3 \phi_M^2 + \alpha_4 \phi_M^3$ (amplitude)

$A_3 = 14{:}00$ local time (phase)

$A_4 = \beta_1 + \beta_2 \phi_M + \beta_3 \phi_M^2 + \beta_4 \phi_M^3$ (period)

ϕ_M: geomagnetic latitude of ionosphere subpoint

α_i, β_i: ionospheric parameters (I)

τ: local time.

A typical vertical time delay profile generated by this model is shown in Figure 2.5.

The delay shown corresponds to an L1 signal coming from a satellite directly above the observer. To represent the actual ionospheric time delay (h_{ij}), for a given satellite elevation angle, one must scale T_{ij} by the appropriate obliquity factor Q_{ij} as follows:

$$h_{ij} = T_{ij}(I) \cdot Q_{ij}(\theta_{ij})$$ (2.6)

where

h_{ij}:   ionospheric time delay from i-th station to j-th satellite,

$Q_{ij} = \sec[\sin^{-1}(\dfrac{r_e}{r_e + h_{iono}} \cos\theta_{ij})]$:

obliquity factor from i-th station to j-th satellite

r_e: radius of the Earth

h_{iono}:   mean ionospheric height

θ_{ij}:   elevation angle from i-th station to j-th satellite

$I = [\alpha_1, \cdots, \alpha_4, \beta_1, \cdots, \beta_4]^T$:   ionospheric parameter.

The τ and ϕ_M of Equation (2.5) are constant at each time step.

The task of the master station is to generate the eight parameters, $[\alpha_1, \cdots, \alpha_4, \beta_1, \cdots, \beta_4]$, which, when substituted in the Klobuchar model, will yield the best ionospheric delay estimate for a single frequency.
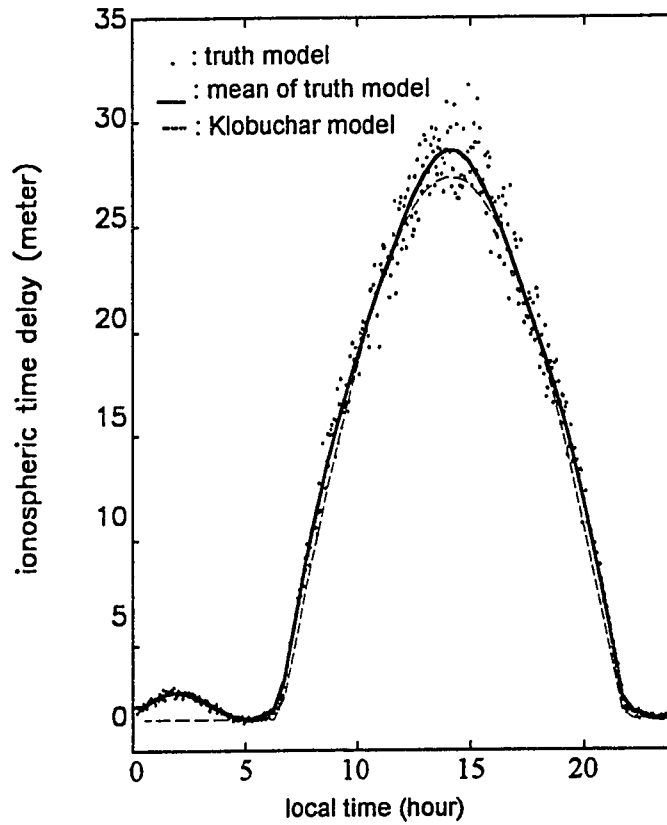
Figure 2.5 Klobuchar Model (cosine curve) and Truth Model of Ionospheric Time Delay (at Stanford, California, elevation angle = 90 deg)

2.7.1.1 Ionospheric Time Delay Measurement Equation

By collecting h_{ij} for satellite i = 1,..,m, and station j = 1,..,n, the following ionospheric time delay measurement equation can be obtained:

$$d = h(I) + v \tag{2.7}$$

where

$$d = [d_{11}, \cdots, d_{1n}, \cdots, d_{m1}, \cdots, d_{mn}]^T$$

d_{ij}:   ionospheric time delay from i-th station to j-th satellite

measured using dual frequency technique

$$h(I) = [h_{11}(I), \cdots, h_{1n}(I), \cdots, h_{m1}(I), \cdots, h_{mn}(I)]^T$$

v: measurement noise.

The linearized form of equation (2.7) is,

$$\delta d = H \cdot \delta I + v \tag{2.8}$$

where

$I = I_0 + \delta I$

$I_0 = [\alpha_{1_0}, \cdots, \alpha_{4_0}, \beta_{1_0}, \cdots, \beta_{4_0}]^T$:   nominal ionospheric parameters

$\delta I = [\delta\alpha_1, \cdots, \delta\alpha_4, \delta\beta_1, \cdots, \delta\beta_4]^T$:   increment of ionospheric parameters.

$\delta d = d - h(I_0)$

$H = \dfrac{\partial h}{\partial I}\bigg|_{I=I_0}$

$= [T_{11}^{T} \cdot Q_{11}, \cdots, T_{1n}^{T} \cdot Q_{1n}, \cdots, T_{m1}^{T} \cdot Q_{m1}, \cdots, T_{mn}^{T} \cdot Q_{mn}]^T$

$T_{ij_{\alpha_k}} = \dfrac{\partial T_{ij}}{\partial \alpha_k}\bigg|_{I=I_0}$

$$T_{ij_{\rho_k}} = \left.\frac{\partial T_{ij}}{\partial \beta_k}\right|_{I=I_0}$$

v :   measurement noise.

2.7.1.2 Nonlinear Static Estimation of Ionospheric Parameters

We applied a nonlinear static estimation technique [Bryson, 1989] developed by Bryson to the problem of fitting the ionospheric parameters to the data collected by the monitor stations. We define the state x and measurement z as,

$$x = I = \left[\alpha_1, \cdots, \alpha_4, \beta_1, \cdots, \beta_4\right]^T \tag{2.9}$$

$$z = d = \left[d_{11}, \cdots, d_{1n}, \cdots, d_{m1}, \cdots, d_{mn}\right]^T \tag{2.10}$$

The algorithm to find the solution may be formulated as follows:

(1) Guess x (e.g. use the broadcast parameters by GPS satellite)

(2) Evaluate $h(x)$ and H

(3) $P = \left(M^{-1} + H^T V^{-1} H\right)^{-1}$

(4) $\dfrac{\partial J}{\partial x} = M^{-1}(x - \bar{x}) - H^T V^{-1}\left[z - h(x)\right] \equiv GR$

(5) If $|GR| \leq \varepsilon$, then set $\hat{x} = x$ and stop. Otherwise $\bar{x} = x$.

(6) Replace x by $(x - P \cdot GR)$

(7) Go to (2).

2.7.2 Ephemeris and Satellite Clock Errors

The GPS navigation message broadcast by the satellites provides a means for computing the satellite positions in the WGS-84 Coordinate system [Green, 1989]. These reported positions are in error due to the limitations of the GPS control segment's ability to predict the satellite ephemeris, and potentially also due to intentional degradation of the reported parameters under SA. The GPS satellite ephemeris errors can be estimated through a network of monitor stations, by essentially using GPS upside down. Just as a user can determine its position and clock bias based on the ranges to the known locations of four or more GPS satellites, five or more monitor stations viewing the same satellite from known locations, can be used to estimate the satellite position, clock offset, and monitor station clock offsets.

The measured pseudorange (ρ_{ij}), from i-th monitor station to j-th GPS satellite, after being correctly adjusted for atmospheric errors and multipath errors, is modeled by,

$$\rho_{ij} = D_{ij} \cdot e_{ij} - b_j + B_i + n_{ij}$$

$$= \left[\left(R_j + \delta R_j \right) - S_i \right] \cdot e_{ij} - b_j + B_i + n_{ij} \qquad (2.11)$$

where

ρ_{ij}:   measured pseudorange from i-th monitor station to j-th satellite

D_{ij}:   range vector from i-th monitor station to j-th satellite

e_{ij}:   range unit vector from i-th monitor station to j-th satellite

R_j: j-th satellite location calculated from GPS message

δR_j: ephemeris error vector of j-th satellite

S_i: known i-th monitor station location

b_j: satellite clock offset

B_i :   monitor station clock offset

n_{ij} :   measurement noise including mismodelling of ionosphere and troposphere.

This is illustrated in Fig. 2.6.

Define x for all the monitor stations (i = 1, ..., n) and GPS satellites (j = 1, ..., m) as follows:

$$x = \begin{bmatrix} \delta R^T & b^T & B^T \end{bmatrix}^T \tag{2.12}$$

where

$$\delta R = \begin{bmatrix} \delta R_1^T & \delta R_2^T & \cdots & \delta R_m^T \end{bmatrix}^T$$

$$b = \begin{bmatrix} b_1 & b_2 & \cdots & b_m \end{bmatrix}^T$$

$$B = \begin{bmatrix} B_1 & B_2 & \cdots & B_{n-1} \end{bmatrix}^T.$$

If we gather all the measurement equations (2.11) for all the monitor stations (i = 1, ..., n) and GPS satellites (j = 1, ..., m) and rearrange them, we will get a matrix equation as follows:

$$\begin{bmatrix} E_1 & -I & I_1 \\ E_2 & -I & I_2 \\ \vdots & \vdots & \vdots \\ E_n & -I & I_n \end{bmatrix} x = D - \begin{bmatrix} E_1 & 0 & 0 & 0 \\ 0 & E_2 & 0 & 0 \\ 0 & 0 & \ddots & 0 \\ 0 & 0 & 0 & E_n \end{bmatrix} P \tag{2.13}$$

where

$$E_i = \begin{bmatrix} e_{i1}^T & 0 & 0 & 0 \\ 0 & e_{i2}^T & 0 & 0 \\ 0 & 0 & \ddots & 0 \\ 0 & 0 & 0 & e_{im}^T \end{bmatrix} \quad (m \times 3m)$$

$$I = \begin{bmatrix} 1 & 0 & 0 & 0 \\ 0 & 1 & 0 & 0 \\ 0 & 0 & \ddots & 0 \\ 0 & 0 & 0 & 1 \end{bmatrix} \qquad (m \times m)$$

$$I_i = \begin{bmatrix} 0 & \cdots & \overset{\text{(i-th column)}}{1} & \cdots & 0 \\ 0 & \cdots & 1 & \cdots & 0 \\ \vdots & \cdots & \vdots & \cdots & \vdots \\ 0 & \cdots & 1 & \cdots & 0 \end{bmatrix} \qquad (m \times (n-1)) \qquad (\text{for } i = 1, ..., n\text{-}1)$$

$$I_n = 0 \qquad (m \times (n\text{-}1)) \qquad (\text{for } i = n)$$

$$D = \begin{bmatrix} D_1^T & D_2^T & \cdots & D_n^T \end{bmatrix}^T$$

$$D_i = \begin{bmatrix} D_{i1} & D_{i2} & \cdots & D_{im} \end{bmatrix}^T$$

$$P = \begin{bmatrix} P_1^T & P_2^T & \cdots & P_n^T \end{bmatrix}^T$$

$$P_i = \begin{bmatrix} (R_1 - S_i)^T & (R_2 - S_i)^T & \cdots & (R_m - S_i)^T \end{bmatrix}^T$$

In the above equations the matrix, I_n, is set to be 0 matrix because all the clock errors are relative and are estimated on the basis of the n-th monitor station clock.

If we define the system matrix H and measurement z as,

$$H = \begin{bmatrix} E_1 & -I & I_1 \\ E_2 & -I & I_2 \\ \vdots & \vdots & \vdots \\ E_n & -I & I_n \end{bmatrix} \qquad (2.14)$$

$$z = D - \begin{bmatrix} E_1 & 0 & 0 & 0 \\ 0 & E_2 & 0 & 0 \\ 0 & 0 & \ddots & 0 \\ 0 & 0 & 0 & E_n \end{bmatrix} P \qquad (2.15)$$

then equation (2.13) become

$$z = Hx.$$ (2.16)

In case that the i-th monitor station cannot see the j-th satellite the corresponding row element of the vector z and row vector of the matrix H in the equation (2.16) must be eliminated.

The master station uses a batch least squares technique to estimate the three dimensional ephemeris error vector and clock bias for each GPS satellite within view of the network. If there are more measurements than the unknowns (three-dimensional errors, satellite clock offset, and monitor station clock offset) in the WADGPS network, the observation equation for that satellite is overdetermined, and the solution is picked to minimize the measurement residual sum of squares.

$$x = \left(H^T H\right)^{-1} H^T z$$ (2.17)

If there are fewer measurements than the unknowns, the solution is underdetermined, and the optimal estimate minimizes the two-norm of the error solution.

$$x = H^T \left(H H^T\right)^{-1} z$$ (2.18)

The simple two-norm solution and its proof is explained in Appendix B.

In the underdetermined case, the corrections for ephemeris errors and clock offsets are not accurate, but the user positioning is still accurate with these corrections because for the user only the projection of the error correction vector on the line of sight to the satellite is important.

If the monitor stations are confined to the continental U.S., users near the coastal monitor stations will be using satellites that are underdetermined, and therefore accuracy

will degrade. From this reason we recommend locating monitor stations over a wider area than the system is designed for the users.
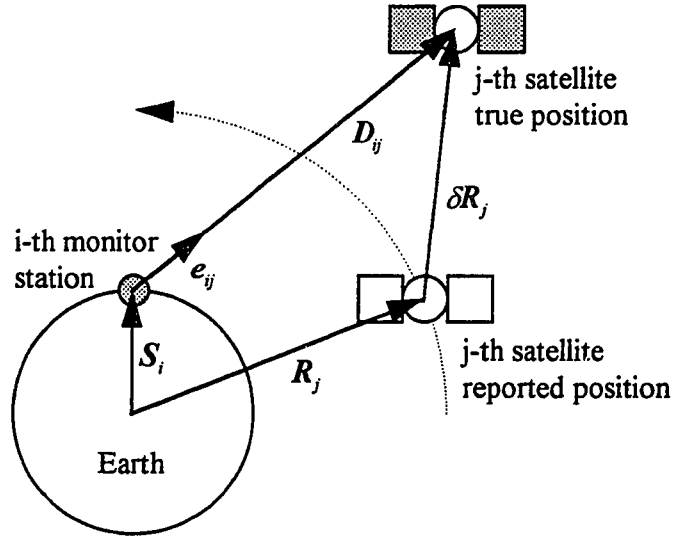
Figure 2.6 GPS Ephemeris Errors

If we use a clock with a very low drift rate, such as a rubidium clock (10^{-12}sec/sec), a cesium clock (10^{-13}sec/sec), or a hydrogen maser clock (10^{-15}sec/sec), in the monitor station instead of a quartz oscillator (10^{-8}-10^{-9}sec/sec), we do not need to estimate the monitor station receiver clock error at every epoch in the estimator. Instead, we can designate the monitor station clock error to be the latest receiver clock error and estimate the other parameters—the ephemeris errors and the satellite clock error—for certain periods of time without loss in estimation accuracy. This simplification will boost the estimation speed (because the observation matrix becomes small) and the estimation accuracy (because there are fewer unknowns than before while the number of measurements is the same), and it will give the master station more flexibility to check the integrity of the GPS signals. The simplification is possible because the drift rate of the

hydrogen maser clock is 10^{-15} sec/sec, i.e., 3×10^{-5} cm/sec, which means the clock error grows only one centimeter in 10 hours and is lower than the receiver noise (one meter for code). For the rubidium clock, the error grows nine centimeters in five minutes; we therefore need to estimate the monitor station clock error every five minutes and keep the clock error and error rate fixed in between in the estimation process.

2.8 User Message Content and Format

For an option, transmission of the WADGPS correction can be accomplished by direct geosynchronous satellite link from master station to remote users. The correction is converted to the format which is consistent to the Global Navigation Satellite System (GNSS) Integrity Channel (GIC) message format developed by the Radio Technical Commission for Maritime Service Special Committee 159 [Van Dierendonck, 1993].

Table 2.1 WADGPS Correction Message Content

Message		Update Rate
SV ID	PRN	every 5-10 seconds
Time Tag (GPS time)	Time of Transmission	
SV Clock Offset	Offset	every 5-10 seconds
	Offset Rate	
SV Position Error	X component	
(in WGS-84 frame)	Y component	every 1-5 minutes
	Z component	
SV Velocity Error	$\dot{X}$ component	
(in WGS-84 frame)	$\dot{Y}$ component	every 1-5 minutes
	$\dot{Z}$ component	
Ionospheric Parameters	eight parameters	every 2-5 minutes

Clock offsets including SA [Chao, 1993] and ephemeris errors have been observed to have variations with time constants on the order of three minutes and 12 hours respectively, and with RMS errors on the order of 25 and six meters respectively. Thus an update rate of 0.1-0.2Hz is sufficient to eliminate the clock error so that the growing positioning errors for the clock caused by latency is less than one meter, and an update rate of one to five minutes is sufficient to eliminate the ephemeris error so that the growing positioning errors for ephemeris caused by latency is less than five centimeters. Determining the appropriate update rate for the ionospheric time delay correction is more difficult. Usually the total electronic content at zenith varies very slowly (on the order of 6 to 12 hours), but the scintillation of the ionosphere, an abrupt change of the ionosphere in a small region, can make it difficult to estimate. SV ID and a time tag in GPS time are attached to the beginning of each message. The suggested message content for transmission of the WADGPS correction is shown in Table 2.1.

2.9 Latency

It is impossible for users to apply the error corrections at the same epoch at which they are estimated in the master station. The time taken to estimate the correction parameters plus the time spent for the WADGPS error corrections to arrive at the users via geosynchronous satellite can be more than a few seconds and therefore results in loss of positioning accuracy. We define this time delay as latency. The latency effect will have the same effect on both DGPS and WADGPS navigation performances.

The major source of this error is SA, which has a two to three minute time constant and is the fastest changing error source. Chao [1993] computed the statistics of SA range error from experimental data. Table 2.2 shows the SA error, the velocity and the acceleration of SA.

Table 2.2 Statistics of SA Range Errors

	SA Error $(\varepsilon_{SA}, \text{m})$	Velocity of SA $(\dot{\varepsilon}_{SA}, \text{m/sec})$	Acceleration of SA $(\ddot{\varepsilon}_{SA}, \text{m}^2/\text{sec})$
Mean	≈ 0	≈ 0	≈ 0
Standard Deviation	20-30	0.2	0.004-0.005

We used two different error correction techniques. The first technique is constant error correction which keeps the error corrections fixed and after a certain time delay applies these corrections to the users. The pseudorange error growth using this technique can be approximated as follows:

$$\delta\rho(\Delta t) = \dot{\varepsilon}_{SA} \cdot \Delta t + \frac{1}{2}\ddot{\varepsilon}_{SA}\Delta t^2 \tag{2.19}$$

where

$\delta\rho$:   pseudorange error caused by latency

Δt: latency

The second technique is error-rate correction technique which uses the error-rate corrections as well as the error corrections and applies both corrections to the users. For this technique the error-rate correction can be calculated either by the master station or by the user himself. The pseudorange error growth using this technique can be approximated as follows:

$$\delta\rho(\Delta t) = \frac{1}{2}\ddot{\varepsilon}_{SA}\Delta t^2 \tag{2.20}$$

.

The range error growth caused by latency using constant error correction and error-rate correction techniques, based on the SA statistics in Table 2.2, is shown in Figure 2.7. For five and 10 seconds of latency the range error growths using constant error correction are 1.1m and 2.3m, respectively and those using error-rate correction are 0.063m and 0.25m, respectively. Multiplying the range error growth by HDOP, VDOP, or PDOP gives the navigation accuracy degradation caused by latency.
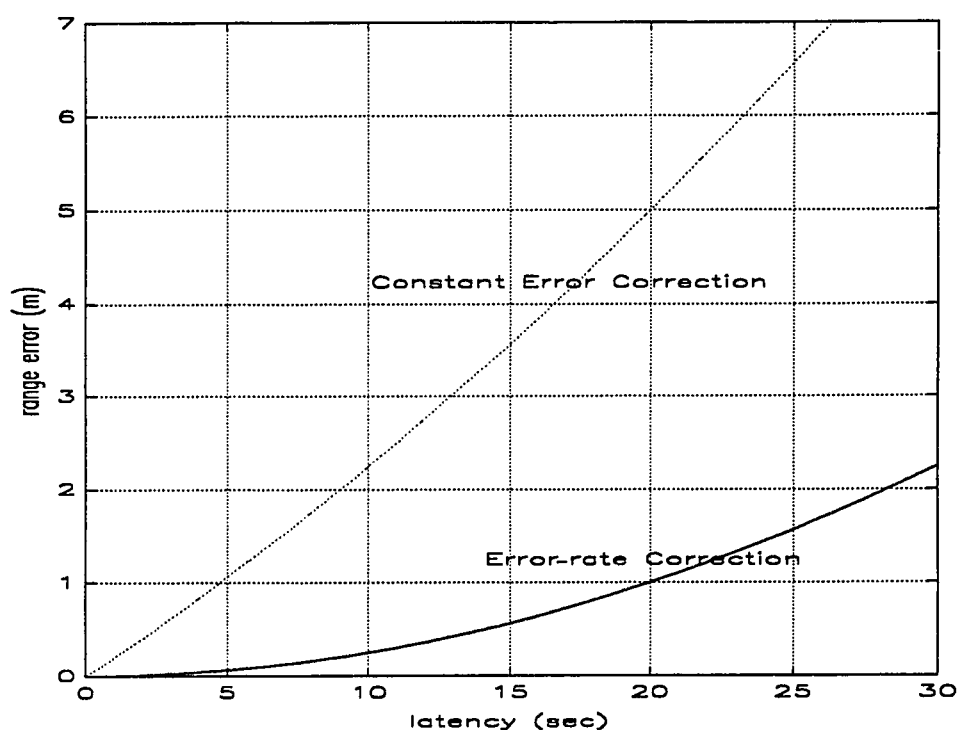
Figure 2.7 Range Error Growth Caused by Latency Using Different Error Correction Techniques.

The difference of the range errors using error-rate correction calculated by the user and the master station is not significant. Therefore the error-rate correction technique in which the user calculates the error-rate correction is recommended [Hegarty, 1993].

2.10 Summary

This chapter has introduced the basics of GPS and DGPS and given the definition of GPS observables. It has defined error sources in GPS measurements and suggested possible techniques to eliminate those errors.

It has also introduced the WADGPS concept and explained the function of the various WADGPS components, which are monitor stations, master station, and data link. Namely, in the master station ionospheric time delay parameters are first estimated using the ionospheric time delay measurements taken from monitor stations equipped with dual frequency receivers and then ephemeris errors and the satellite clock error for each satellite are estimated. The chapter has suggested Nonlinear Static Estimation for estimating the ionospheric time delay parameters and a least-squares technique for the ephemeris errors and satellite clock error.

The chapter has also proposed the WADGPS user message content and its format.

CHAPTER 3. REAL-TIME WADGPS ALGORITHMS AND IMPLEMENTATION

3.1 Introduction

The proposed WADGPS network consists of one master station, a number of monitor stations, and a communication link. GPS measurements taken at each monitor station are sent to the master station. The master station estimates the satellite ephemeris, clock errors, and, optionally, the ionospheric time delay parameters based on the known location of the monitor station and the information collected. The computed error corrections are transmitted to the users via satellite.

Several important questions must be addressed in designing the real-time WADGPS algorithm: what type of receiver (single or dual frequency) is used and where (at the user or the monitor station), how powerful a computer is used in the master station (how fast is the estimation speed), what kind of communication link (radio, telephone, computer network, or geosynchronous satellite) is used and where (between the monitor station and the master station or between the master station and the user), and how much accuracy is needed. The biggest concerns in this study are the estimation speed and the estimation accuracy in the master station.

Unlike in GPS postprocessing for surveying, in which processing time is not important and position accuracy is very important, the real-time WADGPS algorithms have to be very fast and yet provide acceptable navigation accuracy (the vertical positioning error requirement for CAT I precision approach is 4.1m 2drms).

The next section of this chapter describes and discusses real-time algorithms. It is followed by a discussion about the implementation of each component and WADGPS transmission message to decide the error correction update rate. Finally a short summary ends the chapter.

3.2 Real-time WADGPS Algorithms

In the design of WADGPS, we need to address issues such as the receiver required for monitor station and user, the estimation speed, which corresponds to the update rate of error corrections, and the navigation accuracy. Since the most important application of WADGPS may be aviation the navigation accuracy should be the major concern.

The master station estimates the three-dimensional ephemeris errors, the satellite clock errors, the monitor station receiver clock errors, and, optionally, the ionospheric time delay parameters. It does not transmit the monitor station receiver clock errors.

A single-frequency receiver normally provides L1 pseudorange and continuous carrier phase as outputs. A dual-frequency receiver provides not only L1 pseudorange and continuous carrier phase but also L2 pseudorange and continuous carrier phase from which the ionospheric time delay can be calculated as if it were an extra output, but dual-frequency receivers are far more expensive than single-frequency receivers. Using the fact that the ionospheric time delays in the pseudorange and continuous carrier phase are equal in size and have opposite signs, it has been shown that it is possible to estimate ionospheric time delay with a single-frequency receiver [Cohen, 1992] [Xia, 1992] at the expense of a loss in navigation accuracy. Since dual-frequency receivers (provided they are at both the monitor station and the user) directly give the ionospheric time delays, they can save time that would have to be spent on estimating the ionospheric time delay parameters in the master station and can therefore improve the navigation accuracy.

Table 3.1 WADGPS Algorithms

		Algorithms		
		A	B	C
Variables to be estimated	three-dimensional Ephemeris errors	yes	yes	yes
	Satellite clock error + SA	yes	yes	yes
	Ionospheric parameters	yes	yes	no
Variables to be transmitted (error corrections)	three-dimensional Ephemeris errors	yes	yes	yes
	Satellite clock error + SA	yes	yes	yes
	Ionospheric parameters	yes	yes	no
Number of master station estimators		one	two	one
Size of master station estimator		large	small	small
Required receiver	Monitor station	single frequency	dual frequency*	dual frequency*
	User	single frequency	single frequency	single frequency** dual frequency*

*: *There are a few receivers, like the Trimble 4000SSE and Rogue, that can measure the ionospheric time delay even when the P-code is encrypted.*

**: *Ionospheric time delay estimation with a single-frequency receiver has been demonstrated by Cohen, Pervan, Parkinson [4], and Xia [5].*

Three WADGPS algorithms (A, B, and C) and their characteristics are summarized in Table 3.1 and Table 3.2, respectively, and each algorithm is discussed in the following subsections.

3.2.1 Algorithm A

This algorithm allows both monitor station and user to use single-frequency receivers that do not provide ionospheric time delays as extra measurements. In this algorithm, the master station estimates the three-dimensional ephemeris errors, the satellite clock errors, and the ionospheric time delay parameters in one large filter using pseudoranges as the only measurement vector [Ashkenazi, 1992]. Processing time is the longest among the three algorithms because the observation matrix is large. The transmission message consists of the ephemeris errors, the satellite clock errors, and the ionospheric parameters. There are some advantages in terms of lower cost to using this algorithm, the penalty being lower estimation speed and accuracy.

3.2.2 Algorithm B

By using the extra measurement of ionospheric time delay from a dual-frequency receiver in the monitor station we can separate the one large estimator used in Algorithm A into two smaller estimators. The estimation of ionospheric time delay parameters is one filter and the estimation of the three-dimensional ephemeris errors, the satellite clock errors, and the monitor station receiver clock errors is another, separate, filter [Kee, 1990]. For the resulting algorithm (Algorithm B), a dual-frequency receiver is required in the monitor station but the user needs only a single-frequency receiver. Because the ionospheric time delays are separate measurements in a dual-frequency receiver, they are used to estimate the ionospheric parameters directly and the pseudoranges, adjusted for ionospheric time delay and tropospheric error, are fed into the other filter, which estimates ephemeris errors and clock errors. But a satellite interfrequency bias can be a new error source in this algorithm because it affects only dual-frequency receiver. The satellite interfrequency bias, T_{gd}, is a time delay between L1 and L2 frequencies in the GPS satellite

and is included in the ionospheric time delay measurement for dual-frequency receiver unless it is carefully calibrated and taken off from the raw ionospheric time delay measurement.

Algorithm B has advantages over Algorithm A in terms of accuracy and speed of estimation because extra ionospheric measurements are used and the filter is divided into two small ones resulting in reduced matrix sizes. The transmission message to users consists of three-dimensional ephemeris errors and satellite clock errors, as well as ionospheric parameters. Even single-frequency users can take advantage of these error corrections to improve positioning accuracy.

3.2.3 Algorithm C

If users can measure the ionospheric time delay, the ionospheric parameters do not need to be estimated in the master station and as a result only three-dimensional ephemeris errors and satellite clock errors need to be estimated there. The resulting algorithm (Algorithm C) requires a dual-frequency receiver in the monitor station. Because there is no ionospheric parameter estimation, the transmission message does not contain ionospheric parameters and therefore the estimation time is shorter than that of Algorithm B and the update rate of the transmission messages can be much higher. A user may be equipped with a dual-frequency receiver, but such a receiver may not be required. We may use a single-frequency receiver at the expense of a loss in navigation accuracy. The single-frequency technique needs further study however.

Of the three algorithms discussed, Algorithm C achieves the best accuracy because it does not fit the ionosphere to the model. Algorithm B sacrifices accuracy because of this fit, especially in the equatorial and polar region. Also the satellite interfrequency bias may be a significant error source for the Algorithm B. Thus, of the three algorithms discussed,

Algorithm C achieves the best accuracy. This algorithm provides the best accuracy for users with dual frequency receivers, but a user may opt for a single frequency receiver depending on how much accuracy is desired.

Table 3.2 Performances of WADGPS Algorithms

Performance	Algorithms		
	A	B	C
Estimation speed (estimation time in unit)*	slow (bigger than 10.0)	fast (2.0)	fastest (1.0)
Navigation accuracy (meter)**	good (3.0)	better (1-2)	best*** (<1)

*: *based on simulations*

**: *three-dimensional RMS positioning error based on simulations with no latency*

***: *users equipped with dual-frequency receivers*

3.3 Best WADGPS Design

Algorithm C, which uses a dual-frequency receiver in the monitor station and a dual-frequency for the user, provides the fastest estimation speed and the best accuracy. It will be used to demonstrate the potential of WADGPS in this dissertation. A block diagram of implementation of WADGPS is shown in Figure 3.1.

In Chapter 5 we used only dual-frequency receivers in both the monitor station and the users. we applied a Hatch/Eshenbach filter to reduce receiver noise and multipath error and used Black's model to eliminate tropospheric error. we used a combination of a batch least-squares technique and a two-norm minimum solution for the process of estimation in the master station. In the future we can also use a sequential filter in the estimation process, which estimates the correction parameters more accurately.
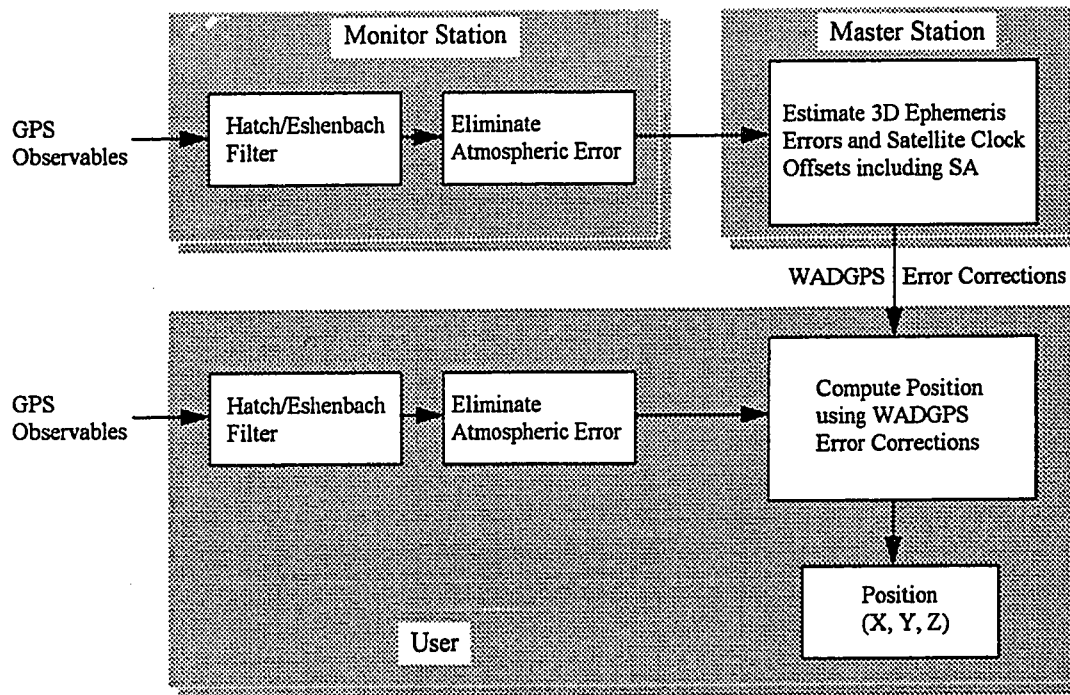
Figure 3.1 Implementation of WADGPS

3.3.1 Monitor Station

The dual-frequency receiver in the monitor station provides L1 and L2 raw pseudoranges. Because these pseudoranges have multipath errors, tropospheric errors, and receiver noise, we need to reduce or to eliminate these errors by feeding them to a series of filters to provide clean signals to the master station so that these parameters can be estimated more precisely. We first use a Hatch/Eshenbach filter to reduce the receiver noise and the multipath errors and also use a simple ionospheric formula to eliminate the ionospheric time delays. Then we use Black's model to get rid of the tropospheric errors.

We can reduce receiver noise and multipath errors in the code pseudoranges by smoothing them with the continuous carrier phases. The Hatch/Eshenbach filter [Hatch, 1982] averages the noisy code pseudoranges (1-2m noise) with the very precise carrier information (1-2mm noise) and provides lower measurement errors. This filter can be described as follows:

$$\Delta\phi_i(n) = \phi_i(n) - \phi_i(n-1) \tag{3.1}$$

$$\hat{\rho}_i(n) = \frac{(k-1)}{k}[\hat{\rho}_i(n-1) + \Delta\phi_i(n)] + \frac{1}{k}\rho_i(n) \tag{3.2}$$

where

ϕ_i: raw continuous carrier phase

ρ_i: raw pseudorange

$\hat{\rho}_i$:   estimated pseudorange

i: L1 or L2 frequency (i = 1 or 2)

n: epoch

k: averaging constant.

The Hatch/Eshenbach filter improves the pseudoranges on the order of $\sqrt{k}$. Whenever a cycle slip of continuous carrier phase occurs the filter has to be restarted. This filter can work for single-frequency receivers if we are careful to choose the averaging constant k ($k \leq$ 1-2 minutes).

For dual-frequency receivers the ionospheric time delays can be calculated as follows [Rockwell, 1987]:

$$\rho = \frac{\rho_2 - \gamma\rho_1}{1 - \gamma}$$

$$= \rho_1 - \frac{1}{\gamma - 1}(\rho_2 - \rho_1) \qquad (3.3)$$

where

ρ: pseudorange corrected for ionospheric effects in L1 frequency

ρ_1:   pseudorange in L1 frequency

ρ_2:   pseudorange in L2 frequency

$$\gamma = \left(\frac{1575.42}{1227.6}\right)^2 = \left(\frac{77}{60}\right)^2 \approx 1.65$$

There is an interfrequency bias in a dual-frequency receiver because the L1 and L2 signals are not synchronized inside the receiver and it acts like a receiver clock error. Also there is an interfrequency bias in the GPS satellite, called T_{gd}, because L1 and L2 signals are not synchronized perfectly and it acts like satellite clock error. [Wilson, et al. 1993] Since both interfrequency biases are constant for all the channels, the bias does not need to be calibrated for Algorithm C. But for Algorithm B these errors have to be calibrated in the monitor station to estimate the right ionospheric time delay parameters.

3.3.2 Master Station

The measured pseudorange (ρ_{ij}) from i-th monitor station to j-th GPS satellite (Figure 2.6), already adjusted for ionospheric error and tropospheric error, is modeled by the Equation (2.11):

$$\rho_{ij} = D_{ij} \cdot e_{ij} - b_j + B_i + n_{ij}$$

$$= [(R_j + \delta R_j) - S_i] \cdot e_{ij} - b_j + B_i + n_{ij}$$

In the above equation we have four unknowns (three three-dimensional ephemeris errors and satellite clock error) for each satellite plus one unknown (receiver clock error) for each monitor station.

The master station can use either a batch or a recursive filter to estimate the three-dimensional ephemeris error vector and clock bias for each GPS satellite within view of the network. For this study, we chose the batch estimation technique to estimate the parameters in short-time windows.

Assuming that there are n GPS satellites in view from all m monitor stations, the total number of measurements is $m \times n$ and the total number of unknowns is $n \times 4$ (three ephemeris errors and one satellite clock error), plus $(m-1)$ because clock errors can be estimated only relative to a fixed reference. Additionally, the monitor station clock offsets only need to be estimated relative to a reference clock. If there are more measurements than unknowns, the observation equation is overdetermined, and we pick the solution to minimize the measurement residual sum of squares. If there are fewer measurements than unknowns, the solution is underdetermined, and the optimal estimate minimizes the two-norm of the error solution. For a given number of monitor stations the minimum number of GPS satellites required to make the algorithm overdetermined, and vice versa, can be calculated from the inequality

$$m \times n \geq n \times 4 + (m - 1) \tag{3.4}$$

where

m: number of monitor station

n: number of GPS satellites.
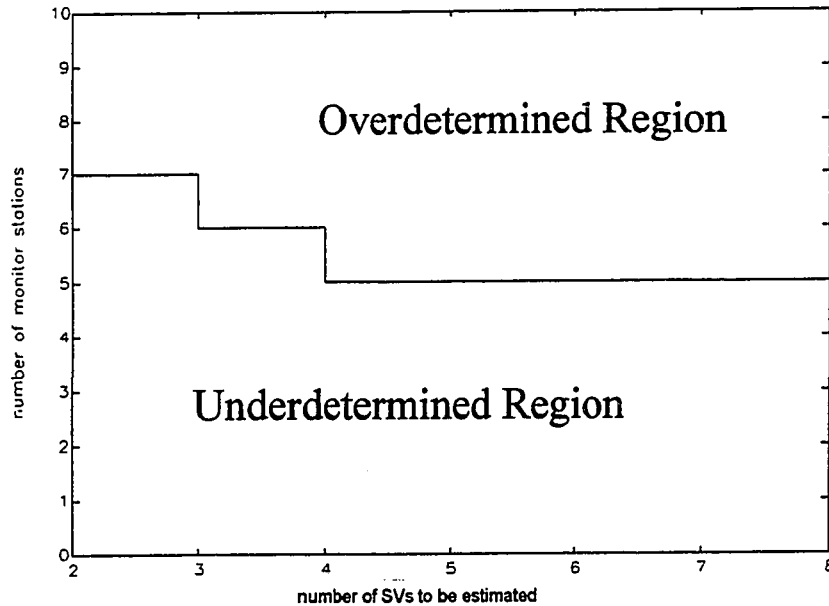
Figure 3.2 Minimum Number of Monitor Stations Required for Ephemeris and Clock Estimation.

Figure 3.2 provides the boundary of the overdetermined and underdetermined region from the above inequality. If we know the number of monitor stations available and the GPS satellites in view from the monitor stations, we can get a very rough estimate of how good the estimation process in the master station is going to be.

In fact, all the monitor stations cannot see the same set of GPS satellites. Instead, some of the satellites would be seen by five or more monitor stations and their error parameter estimation would be good. The rest of them would be seen by fewer than five monitor stations and their estimation would not be as good. Example of each case is shown in Figure 3.3.
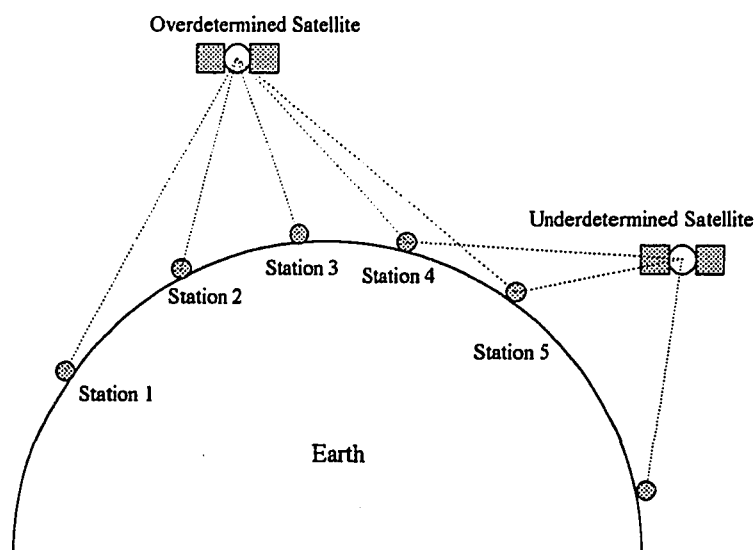
Figure 3.3 Examples of Overdetermined and Underdetermined Satellites in Estimating Ephemeris Errors.
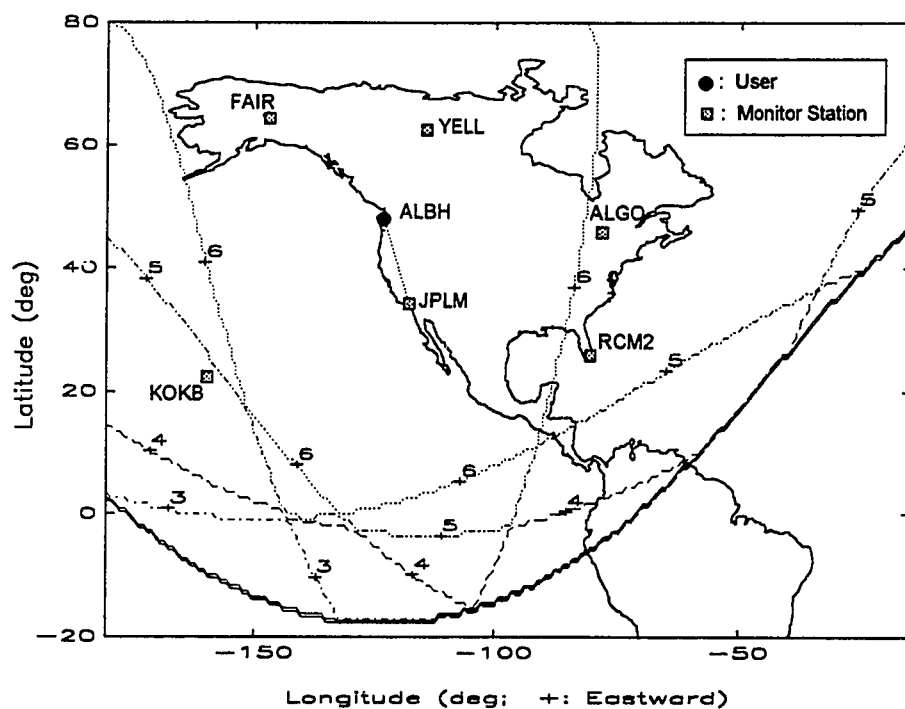
Figure 3.4 The Number of Monitor Stations in View from the GPS Satellite which is seen by the User, ALBH (Mask Angle = 10°)

Because each monitor station does not see the same set of satellites the number of measurements is less than m times n. For all m satellites we add the number of monitor stations in view from a satellite to calculate the total number of measurements. Figure 3.4 shows the number of monitor stations in view from the GPS satellite depends on where the satellite is. Each point on the map represents one of the ground track, i.e., the crossing point of the Earth surface and the line of sight from the center of the Earth to the GPS satellite. The solid line is the boundary in which satellite can be seen by the user, ALBH with 10 degrees mask angle. If any satellite is in the area inside the dotted line labeled six, six monitor stations can always see the satellite. Each line with different label can be explained in a similar way [Enge et al., 1990]. Figure 3.4 can be a design tool to select the right monitor station sites for WADGPS and from that we can predict how well the estimation of each satellite would be.

Finally the master station sends the estimated satellite ephemeris errors, satellite clock errors, and ionospheric time delay parameters to users. The satellite ephemeris and clock errors are slowly varying. A constant estimate of each, assuming that users calculate an error-rate correction using prior correction information, is therefore sufficient for the WADGPS error correction vector. [Hegarty, 1993] Ephemeris and clock errors including SA have been observed to have variations with time constants on the order of 12 hours and three minutes respectively [Chou, 1991][Chao, 1993]; hence, with a proposed update rate of 0.1-0.2Hz, this assumption is valid.

3.3.3 User

Each user collects pseudoranges and ephemeris parameters for all GPS satellites in view. In addition, the user receives an error correction vector sent by the master station via a geosynchronous satellite link. We first use a Hatch/Eshenbach filter to reduce the

receiver noise and the multipath errors and also use a simple ionospheric formula to eliminate the ionospheric time delays. Then we use Black's model to get rid of the tropospheric errors as we did in the monitor station. The error corrections are applied to the measurements, already adjusted for the atmospheric errors and reported ephemeris data. The corrected measurements are then used to form a least-squares solution for the user's position and clock bias. Interfrequency bias does not need to be calibrated for the user because it acts like a receiver clock error in the navigation solution.

3.4 WADGPS Message Transmission

The master station transmits the WADGPS error correction message to users via a geosynchronous satellite. The message content is shown in Table 2.1, which is consistent to GIC content [Enge, 1992] which is a GPS-like signal and will be broadcast from the same geosynchronous satellite. In Algorithm C the message content is the same as that in Algorithm A and B except that ionospheric parameters are deleted. The ionospheric parameters are not broadcast in Algorithm C because the users have dual-frequency receivers to correct the ionospheric time delays. The International Maritime Satellite (INMARSAT) system has a data service suitable for WADGPS message transmission and this service has the capability of broadcasting 250bps data to the civilian users. If we use a data compression technique we can save an average of 20-30% of the transmission time. Parity and detailed discussions of WADGPS message transmission are in the reference [Van Dierendonck, 1993].

Table 3.3 WADGPS Correction Message Update Rate Calculation

(0.2Hz Update Rate)

message	quantity	bits/quantity	bits	updates/min	bits/min
SV ID	1	5	5	12	60
time tag (ms)	1	16	16	12	192
SV clock offset (cm, mm/sec)	2	18	36	12	432
SV position error (cm)	3	18	54	1	54
SV velocity error (mm/sec)	3	18	54	1	54
ionospheric parameters (A & B only)	8	20	160	0.5	80
total bits/min /satellite					872

If WADGPS covers the continental US, about 16 GPS satellites will be in view for the users in the region and we need to transmit the message of 16 satellites to the users. SV identification (ID) and a time tag should be transmitted at the beginning of the transmission of any group of parameters. The bit length of each parameter should be minimized. For example, the SV ID has only a 5 bit length because only 32 different SV IDs exist and the time tag has 16 bits because we already know it occurs once a minute in GPS time and a millisecond unit is precise enough for the WADGPS correction purpose. Table 3.3 shows each parameter length in bits and the total number of bits. This number is used to compute the update rate of the correction message.

We have 872 bits/minute per satellite, which corresponds to 13,953 bits/minute for 16 satellites. This translates to 233 bits/second for a 0.2Hz error correction update rate,

which is already lower than the lowest INMARSAT transmission rate of 250bps. This is true for Algorithm C as well as for Algorithm A and B. If we use the data compression technique on the message transmission, this update rate is still feasible even if we include a parity checking procedure for error detection in the technique.

3.5 Summary

This chapter discussed three different real-time WADGPS algorithms that depend on receiver type in the monitor stations and users, and broadcasting parameters from the master station to the users. Among the three algorithms, Algorithm C, which uses dual-frequency receivers for in both monitor station and user, provides the best navigation accuracy.

The chapter also discussed WADGPS design and introduced techniques to eliminate the multipath error, receiver noise, and ionospheric time delay error. Then it introduced a simple plot that provides the boundary of the overdetermined and underdetermined region and from which we can judge how good the estimation process in the master station can be.

The chapter finally discussed the WADGPS transmission message from the master station to the users to find that 0.2Hz is a feasible error correction update rate.

CHAPTER 4. WADGPS SIMULATIONS

4.1 Introduction

The advantages of WADGPS simulations are that they can test the accuracy of the error models and evaluate the performance of the estimation algorithms even before experiments. Comparing each component of real error data with each output of truth error models helps to find better error models and as a result the simulations will be more realistic and will give a more accurate WADGPS error budget. By evaluating different estimation algorithms in the simulations one can find the algorithm for the best performance. WADGPS simulations can thus contribute to the success of WADGPS experiments.

The Simulations in this chapter is based on the Algorithm B. The error sources in the WADGPS simulations of this research are satellite ephemeris errors, satellite clock offset including SA, ionospheric time delay, receiver clock offset, and receiver noise. Tropospheric error and multipath error are assumed to be included in the receiver noise and satellite interfrequency bias is not considered. The state vector of the estimation consists of ionospheric time delay parameters, three-dimensional ephemeris errors, satellite clock offsets, and monitor station receiver clock offsets. We evaluated the performance of the WADGPS network in the United States with 15 monitor stations evenly distributed all across the US including Hawaii and Alaska stations using a computer simulation. Each simulation was run for 12 hours starting at 6:00 AM Pacific Standard Time (PST).

The next section of this chapter defines and describes the four different simulation modules used. They are the GPS satellite module, the monitor station module, the master station module, and the user module. Then, the results of the ionospheric time delay estimation are given and discussed and the total estimation results of ionospheric, ephemeris and satellite clock errors, i.e., WADGPS navigation performance, are also discussed. Next, the mask angle sensitivity to the navigation performances is analyzed. Finally the chapter ends with a summary of the results.

4.2 Simulation Modules

The simulation is composed of four modules describing the GPS satellites, the monitor stations, the master station, and the users. The GPS satellite module generates a realistic GPS pseudorange including the ephemeris errors, the satellite clock offset, and the ionospheric time delay; the monitor station module measures ionospheric time delays and pseudoranges from the GPS satellite module; the master station module estimates the ionospheric time delay parameters, satellite ephemeris errors, and satellite clock offset using all the data from the monitor station module; finally, the user module takes the GPS signal, compensates for each GPS error using the vector of error correction estimated in the master station module, and solves for its position. Details of each module are given in the following subsections. A block diagram of the simulation is shown in Figure 4.1. The truth model error specifications used in the simulation are listed in Table 4.1.
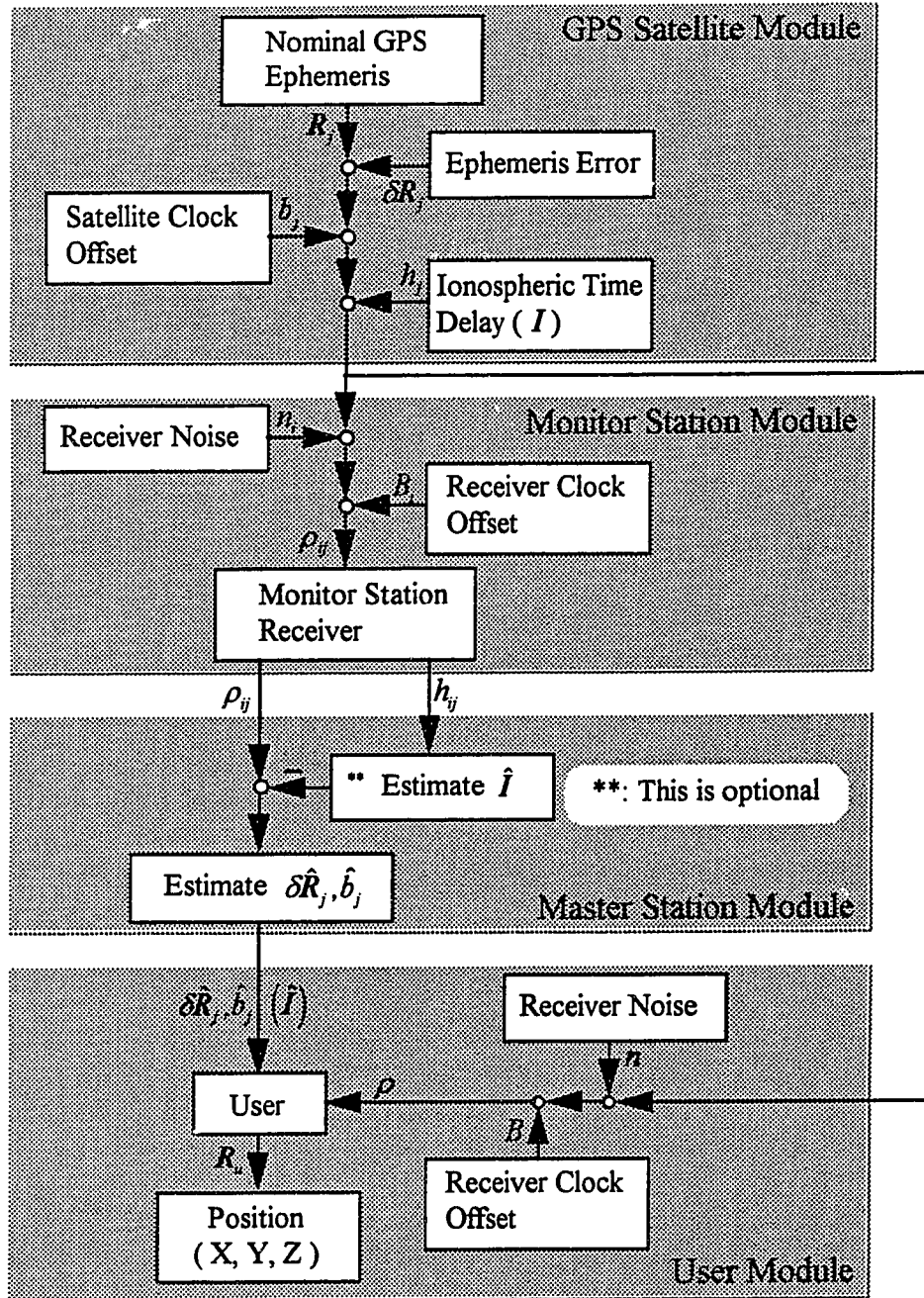
Figure 4.1 Block Diagram of WADGPS Computer Simulation.

4.2.1 GPS Satellite Module

The GPS 21 Primary Satellite Constellation [Green, 1989] is modeled in the simulation. The ephemeris reported by the GPS module to the monitor stations and the users is equal to the true ephemeris corrupted by a three-dimensional error vector. We modeled each ephemeris error vector component by passing white noise through a first-order shaping filter with time constant of 1800 sec and standard deviation of 20 m [Well, 1987].

Each satellite clock offset was also modeled by white noise input to a first-order shaping filter, this time with t = 200 sec [Chou, 1990], and standard deviation of 30 m. These values are somewhat conservative to account for possible effects due to SA.

The ionospheric delay is modeled according to the Klobuchar model discussed in Chapter 2.7.1. The nighttime value and the phase of the half cosine are assumed to be fixed constants. Specifically, it is assumed that the vertical delay is always 1.5m at night and the maximum delay always occurs at 2:00 PM local time every day. An average ionospheric height of 190 nautical miles is assumed in the simulation. In addition to the delay predicted by this model, two terms are included in our truth model to account for higher frequency ionospheric variations, which have been observed in experimental data. The first is a sinusoidal error with amplitude of 5% of the cosine peak, and period of one fifth of the cosine period of equation (2.4). The second is a random error with zero mean and standard deviation equal to 5% of the sum of the cosine terms. Ionospheric parameters (I) vary from the nominal values with time constant of six hours and result in a maximum vertical ionospheric time delay of 30m and a minimum of 1.5m. A typical vertical time delay profile at Stanford, California generated by this model is shown in Figure 2.5.

Table 4.1 True Model Error Specifications

Error Source	Error Model	Time Constant (sec)	min. (meter)	max. (meter)	RMS errors (meter)
Three dim. Satellite Ephemeris Errors	1st order Markov process	1800			20
Satellite Clock Offset	1st order Markov process	200			30
Ionospheric Time Delay *	Klobuchar's model plus spatial sinusoidal bias and white noise	6 hours	1.5 at zenith	30 at zenith	
Tropospheric Error	Modeled as Receiver noise**				
Monitor Station Receiver Clock Offset	2nd order Markov process	$h_0 = 2.0 \times 10^{-22}$ $h_{-1} = 4.0 \times 10^{-26}$ $h_{-2} = 1.5 \times 10^{-33}$			
User Receiver Clock Offset	2nd order Markov process	$h_0 = 9.4 \times 10^{-20}$ $h_{-1} = 1.8 \times 10^{-19}$ $h_{-2} = 3.8 \times 10^{-21}$			
Receiver Noise	white noise				0.2
Multipath	Modeled as Receiver noise				

*: *Ionosphere is varying with time constant of 6 hours, and 5% of one fifth period spatial sinusoidal bias* $\left(0.05\left\{ A_1 + A_2 \cos\left[\frac{2\Pi(\tau - A_3)}{0.2A_4} \right] \right\} \right)$ *and 5% of white noise* $(0.05 T_{Ji} \times N(0,1)$,

$N(0,1)$ *is Gaussian noise that has zero mean and one standard deviation) were added.*

** : *A more sophisticated model is under development*

4.2.2 Monitor Station Module

The monitor station module generates the pseudorange measurements and ionospheric delays observed by the monitor station receivers. The monitor station receiver clock error is modeled by white noise input to a second-order Markov process based on Dierendonck's model [Dierendonck, 1984], as follows:

$$\begin{bmatrix} x_1 \\ x_2 \end{bmatrix}_{k+1} = \begin{bmatrix} 1 & \tau \\ 0 & 1 \end{bmatrix} \begin{bmatrix} x_1 \\ x_2 \end{bmatrix}_k + \begin{bmatrix} w_1 \\ w_2 \end{bmatrix}_k \tag{4.1}$$

$$Q = E\{w \cdot w^T\} = \begin{bmatrix} Q_{11} & Q_{12} \\ Q_{12} & Q_{22} \end{bmatrix}$$

$$Q_{11} = \frac{h_0}{2}\tau + 2h_{-1}\tau^2 + \frac{2}{3}\pi^2 h_{-2}\tau^3$$

$$Q_{12} = 2h_{-1}\tau + \pi^2 h_{-2}\tau^2$$

$$Q_{22} = \frac{h_0}{2\tau} + 2h_{-1} + \frac{8}{3}\pi^2 h_{-2}\tau$$

$$h_0 = 2.0 \times 10^{-22} \;^*$$
$$h_{-1} = 4.0 \times 10^{-26}$$
$$h_{-2} = 1.5 \times 10^{-33}$$

where

x_1 :   clock offset (second)

x_2:   average frequency

τ :   sampling time

and the receiver clock offset values are based on a typical rubidium standard.

---

* The drift rate of receiver clock offset can be approximately calculated as $\sqrt{(2 \cdot \ln 2 \cdot h_{-1})}$.

Table 4.2 Locations of Monitor Stations.

Location	Latitude	Longitude	LORAN site	VOR site
1. George (WA)	47:04 N	119:45 W	√	
2. Middletown (CA)	38:47 N	122:30 W	√	
3. Fallon (NV)	39:33 N	115:50 W	√	
4. Searchlight (NV)	35:19 N	114:48 W	√	
5. San Diego (CA)	33:00 N	117:00 W		√
6. El Paso (TX)	31:30 N	106:20 W		√
7. Raymondville (TX)	26:32 N	97:50 W	√	
8. Grangeville (LA)	· 30:43 N	90:50 W	√	
9. Jupiter (FL)	27:02 N	80:07 W	√	
10. Carolina Beach (NC)	34:04 N	77:55 W	√	
11. Cape Race. (Newfoundland, Canada)	46:47 N	53:10 W	√	
12. Dana (IN)	39:51 N	87:29 W	√	
13. Baudette (MN)	48:37 N	94:33 W	√	
14. Narrow Cape (Kodiak Is., AK) (not shown on the map)	57:26 N	152:22 W	√	
15. Upolo Pt. (HI) (not shown on the map)	20:15 N	155:53 W	√	

The receiver noise is assumed to be white with zero mean and standard deviation of 0.2 m. This is based on averaging over 10 measurements at one second intervals.

The pseudoranges and the ionospheric time delay measured in the monitor station module are a combination of the GPS signals generated in the GPS satellite module and the receiver noise and receiver clock offsets.

The number and locations of monitor stations play a very important role in the performance of WADGPS. The more monitor stations are available the better the WADGPS performance is. To cover all of the US to the desirable positioning accuracy, the monitor stations should be located at the periphery of the continental US and on available islands in the Pacific and Atlantic. Evenly distributed monitor station sites are preferable to concentrated sites.

For the simulation discussed here, 15 monitor stations are assumed, located at already existing LORAN or VOR stations across the US including Alaska and Hawaii. Figure 4.2 illustrates the locations. In this figure the outline represents the continental US. Some of the monitor stations seem to be located in the ocean or one the Great Lakes because of the quantization effect arising from the limited number of mesh grids in the US map. Table 4.2 lists the latitude and longitude of each station. All monitor stations are assumed to have an elevation mask angle of 5.0 deg.
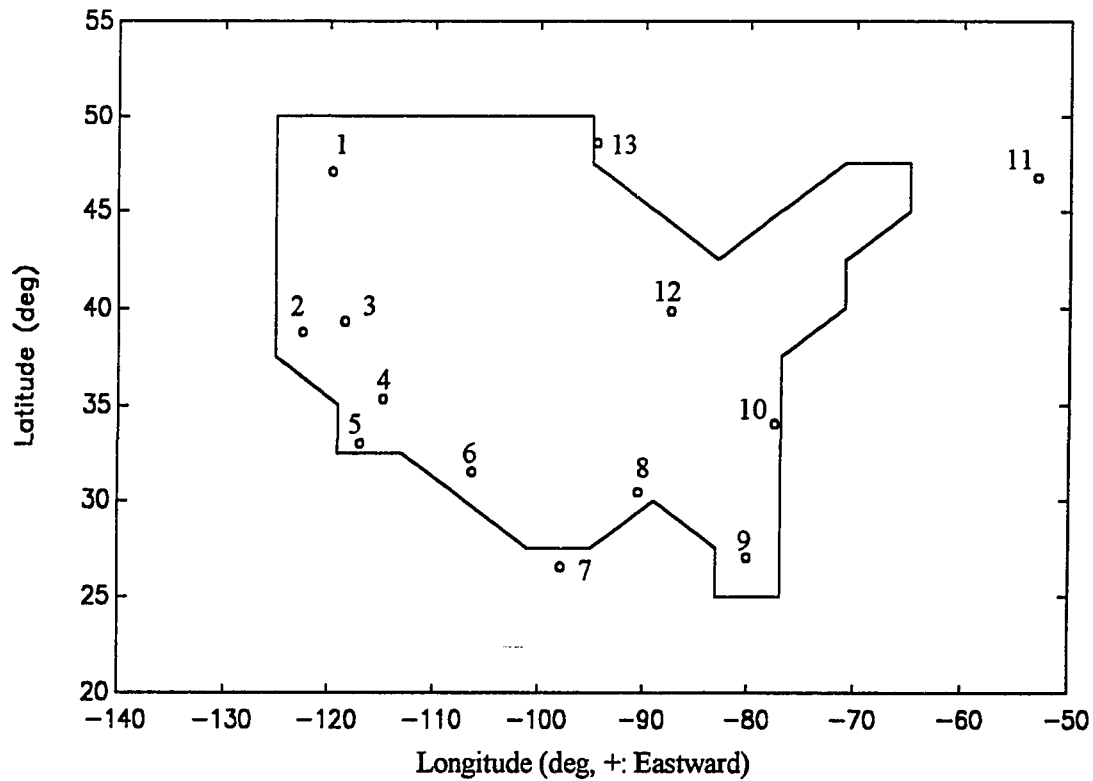
Figure 4.2 Locations of Monitor Stations in US (Narrow Cape, Alaska and Upolo Pt., Hawaii are not shown on the map).

4.2.3 Master Station Module

The master station module collects inputs from the monitor station module and implements the ionospheric and ephemeris error estimation algorithms described in the previous chapter. It consists of two submodules, the ionospheric parameter estimator submodule and the satellite parameter estimator submodule. The flow of the data can be explained as follows: First, the ionospheric parameter estimator collects the ionospheric delay measurements from the monitor station module, estimates ionospheric parameters, and generates the estimated ionospheric delays using the parameters already calculated. Second, the satellite parameter estimator collects the pseudoranges, subtracts from them

the estimated ionospheric delays, and uses these data to estimate satellite ephemeris errors, satellite clock offsets, and monitor station clock offsets. Finally, ionospheric delay parameters, estimated ephemeris and clock errors are provided to the user module.

In the simulation discussed here, algorithm B, which was explained in the previous chapter, is used to get a better understanding of how each ionospheric time delay, satellite ephemeris, and satellite clock error affects the navigation performance of WADGPS.

4.2.4 User Module

The user module simulates the operation of the user receiver. The user clock error is simulated by white noise input to a second-order Markov process based on Van Dierendonck's model [Van Dierendonck, 1984], with equation (4.1),

$$h_0 = 9.4 \times 10^{-20}$$
$$h_{-1} = 1.8 \times 10^{-19}$$
$$h_{-2} = 3.8 \times 10^{-21}$$

and the receiver clock offset values are based on a typical quartz standard. The receiver noise is assumed to be white with zero mean and a standard deviation of 0.2m. This is based on averaging over 10 measurements at one second intervals.

The user applies the eight parameters from the master station module in the Klobuchar model to the raw pseudorange and adjusts the ephemeris parameters received from the GPS satellite module using the correction vector sent by the master station module. It then forms a least-squares position solution using measurements to all the satellites within its field of view. The performance of the WADGPS is evaluated by comparing the error in this solution to the error that would have been present if the raw measurements had been used directly.

In this simulation a typical user that would benefit from the WADGPS has a single frequency C/A code GPS receiver and a quartz oscillator. Eighty-one stationary users are modeled at locations distributed uniformly across the continental US. In Figure 4.3 the bulged grid represents the continental US, and each user is shown as a grid point on it. All users are assumed to have an elevation mask angle of 6.5 deg, which is a representative mask angle for aircraft.
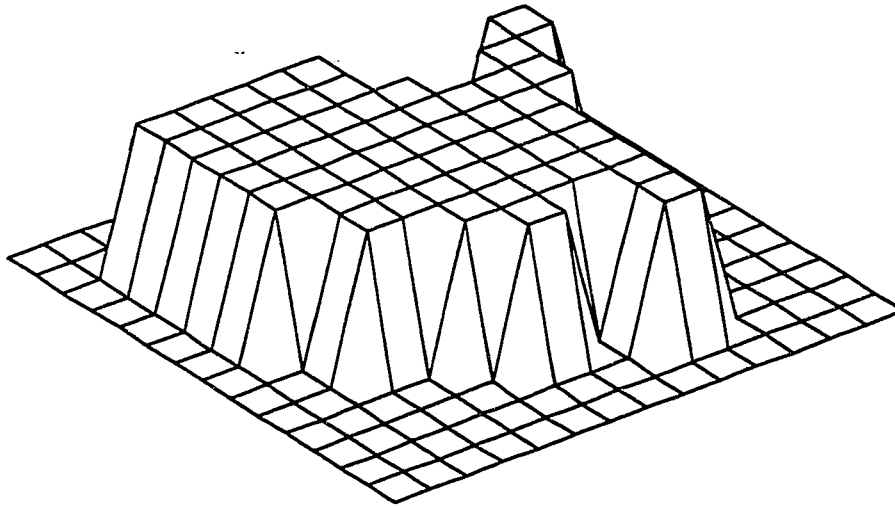
Figure 4.3 Mesh Plot of the Continental US

Each point on the grid represents one of the 81 simulated user's positions.

4.3 Results of Ionospheric Error Estimation

The first step in evaluating the performance of the WADGPS is to see how well it determines the ionospheric errors. Figures 4.4 and 4.5 show contour plots of the actual simulated and estimated vertical ionospheric delays, superimposed on a map of the US. These represent snapshots from 12hour simulations at respectively 5:00PM PST and 2:00PM PST. The contour lines are labeled according to the ionospheric delay in 3m

increments. Notice that the actual values of the ionospheric delay increase from east to west as we get closer to 2:00PM local.

Figure 4.4 Ionospheric Time Delay Estimates (5:00PM PST)

This figure shows the vertical ionospheric delay in meters as generated by the truth model and the NSE. A map of the US and the monitor station locations is also shown. The dotted line is the delay contour from the truth model; the dashed line is the NSE estimate.

The 5:00PM plot (Figure 4.4) shows that the NSE algorithm does well at estimating the delay since the estimated contours are within 1.5m of the true error contours. The performance results are summarized in Table 4.3.

Figure 4.4 also shows an improvement in ionospheric delay estimates toward the center of the country. This can be attributed to the fact that more measurements are available for the central part of the country than for the eastern or western part because

the monitor stations can observe more satellite signals passing through the central region than satellite signals passing through the far eastern or western parts of the sky.
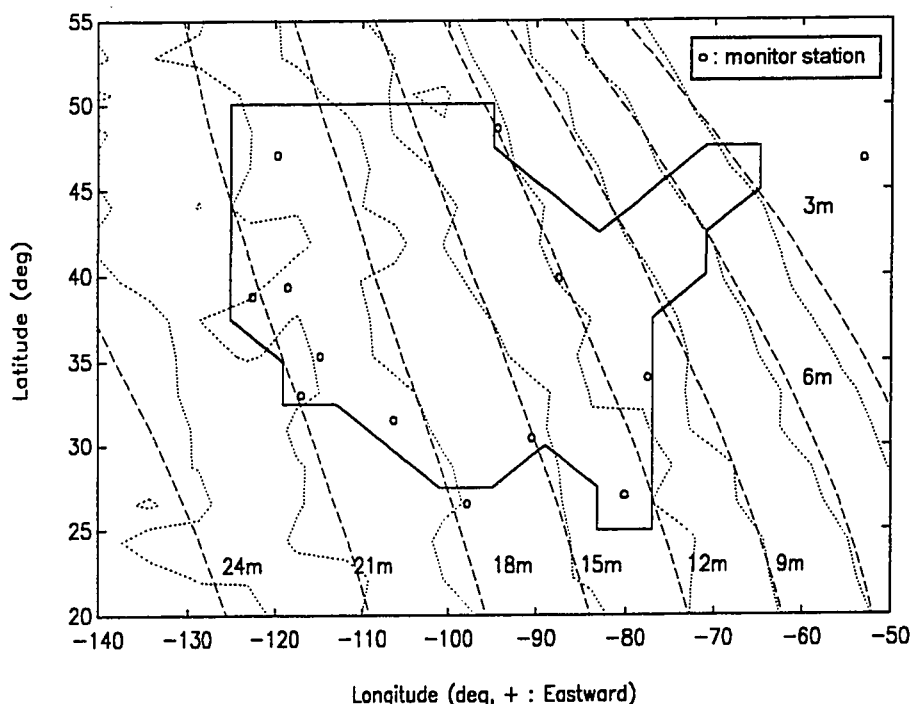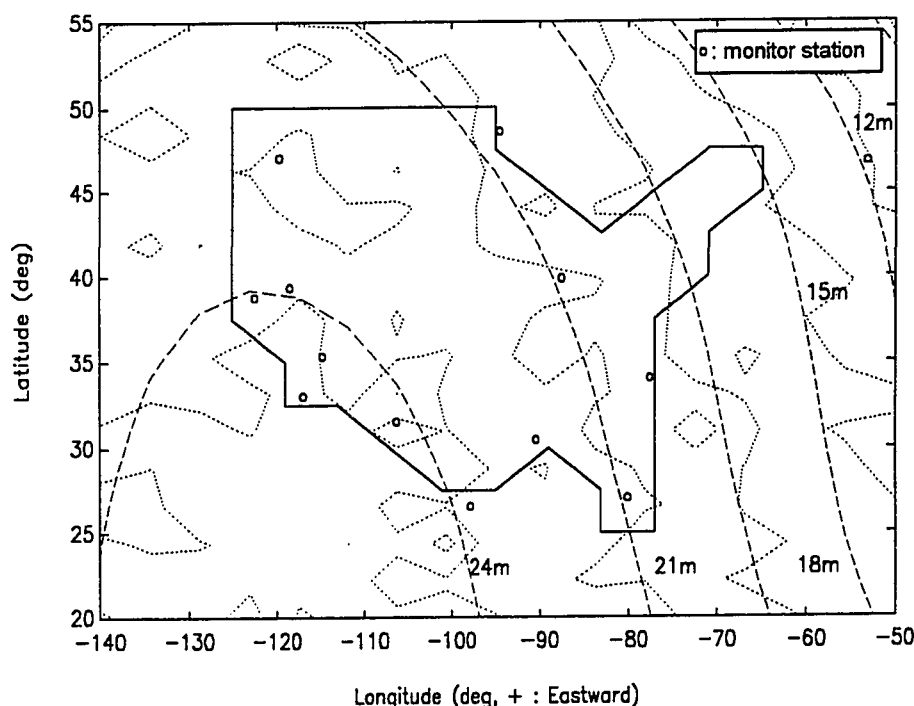

Figure 4.5 Ionospheric Time Delay Estimates (2:00PM PST)

This figure shows the vertical ionospheric delay in meters as generated by the truth model and the NSE. A map of the US and the monitor station locations is also shown. The dotted line is the delay contour from the truth model; the dashed line is the NSE estimate.

Figure 4.5 shows the same types of results for 2:00 PM PST. In this case, however, local contours of varying heights appears, which are not estimated. These small areas of variation in the ionospheric delay are generated by the random noise introduced in the truth model. Because the standard deviation of this variation is set at 5% of the nominal value for the local time of day, the maximum random error is as much as 4.5m at 2:00 PM.

It is not possible for the WADGPS network ionospheric model to estimate these random, high-frequency, localized components of the ionospheric error.

Table 4.3 RMS and Maximum Errors in Ionospheric Estimates

PST Local Time		7:00- 8:00 AM	10:00- 11:00 AM	1:00- 2:00 PM	4:00- 5:00 PM
Nonlinear Static	max * (meter)	1.0	1.4	1.3	1.3
Estimation	RMS ** (meter)	0.3	0.5	0.5	0.4

max^* : $max(abs(z_i - \hat{z}_i))$ where z_i is the true vertical ionosphere measurement and $\hat{z}_i$ the estimated value

RMS^{**}: $RMS(z_i - \hat{z}_i)$

4.4 Navigation Performance

The objective of the WADGPS system is to improve the navigation accuracy for users. The simulation results suggest that this goal can be achieved using the WADGPS system, provided that a high enough bandwidth data link is used.

Figures 4.6 through 4.13 provide a very compact summary of the simulation results that show the accuracy with no latency. The (a) and (b) sets of figures show mesh plots and contour plots of the error distributions across the country. In the mesh plots, (a), each grid point within the outline of the US represents one of the eighty-one user locations we considered. The height of the grid point above the surface corresponds to the magnitude of the error at the grid location. These heights reflect the RMS or maximum error for that user over the entire 12hour simulation period. The (b) set of figures are contour plots that show lines of constant error magnitude corresponding to the heights of the mesh plots on the left.

(a)   (b)   (5m/line)

max of rms=93.1m
continent rms=82.1m

Latitude (deg)

40

20

−100

Longitude (deg)
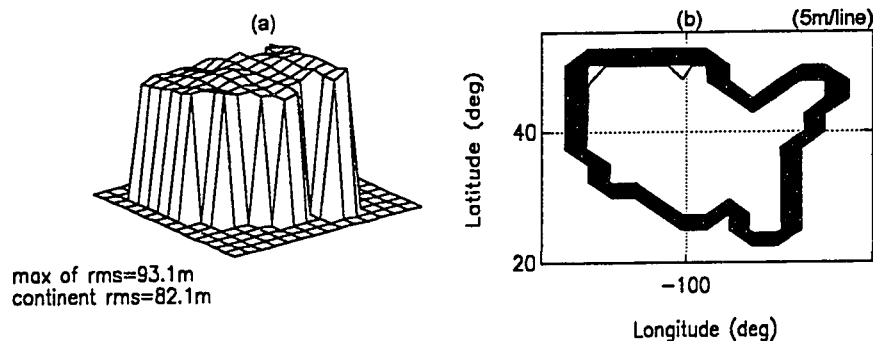
Figure 4.6 RMS Value of Stand-alone GPS Vertical Positioning Errors

The positioning errors were computed inside the boundaries of the continental U.S. Outside the continental U.S., the positioning errors grow slowly with distance. On the contour plot the steep gradient in the boundaries of the continental U.S. is just the representative of the mesh plot on the left hand side and is not real gradient of the positioning error.

(a)   (b)   (0.3m/line)

max of rms=1.9m
continent rms=1.5m

Latitude (deg)

40

20

−100

Longitude (deg)
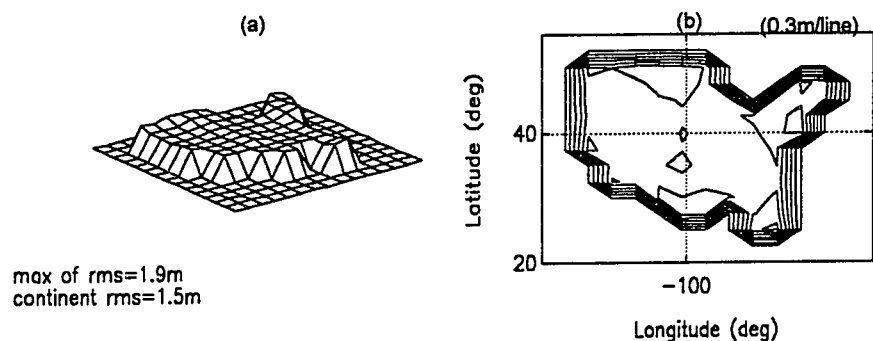
Figure 4.7 RMS Value of WADGPS Vertical Positioning Errors

(a)   (b)   (0.3%/line)

max=2.6%
continent rms=1.9%

Latitude (deg)

Longitude (deg)
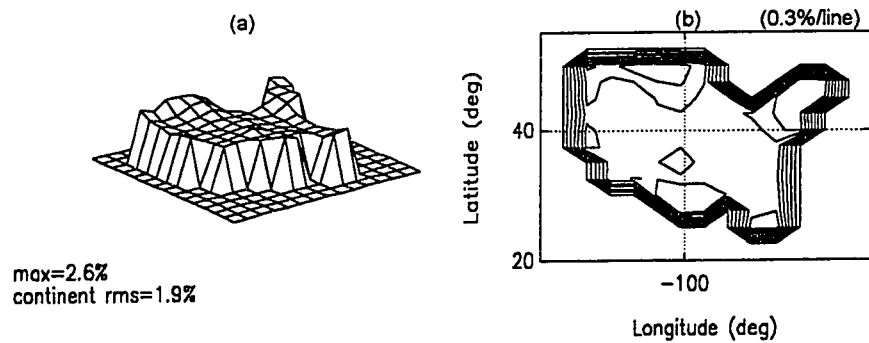
**Figure 4.8 Vertical Positioning Error Ratio
(WADGPS Error)/(Stand-alone GPS Error)**

(a)   (b)   (1m/line)

max of max=9.1m
continent rms of max=6.3m

Latitude (deg)

Longitude (deg)
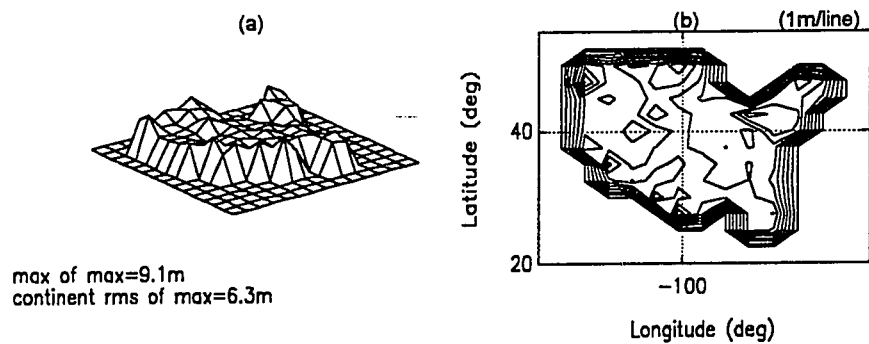
Figure 4.9 Maximum WADGPS Vertical Positioning Errors

(a)   (b)   (5m/line)

max of rms=45.4m
continent rms=42.3m

Latitude (deg)

Longitude (deg)
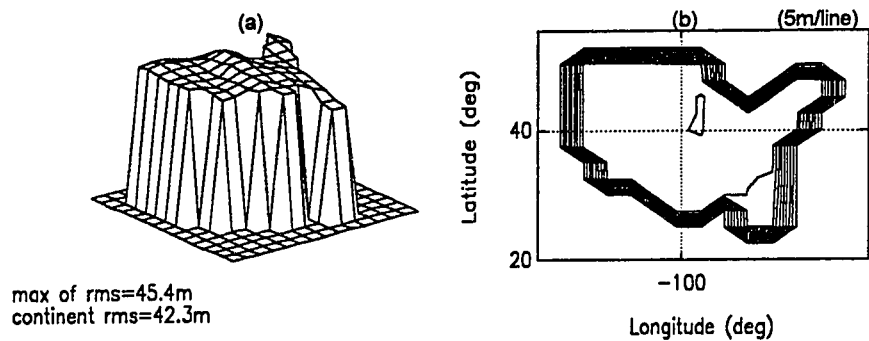
Figure 4.10 RMS Value of Stand-alone GPS Horizontal Positioning Errors

(a)   (b)   (0.3m/line)

max of rms=1.5m
continent rms=1.1m
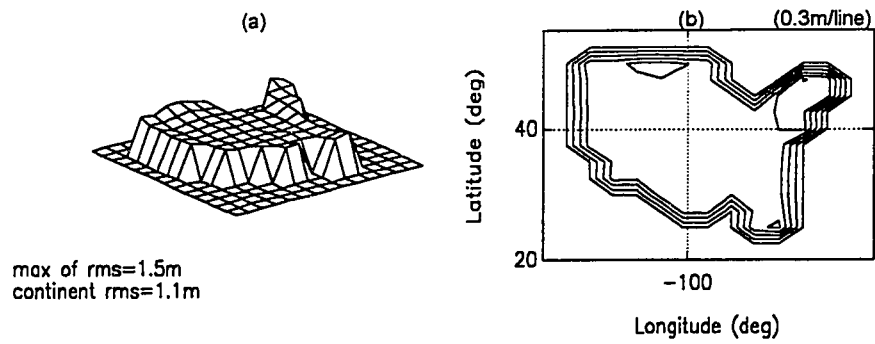
Figure 4.11 RMS Value of WADGPS Horizontal Positioning Errors

(a)   (b)   (0.3%/line)

max=3.0%
continent rms=2.1%
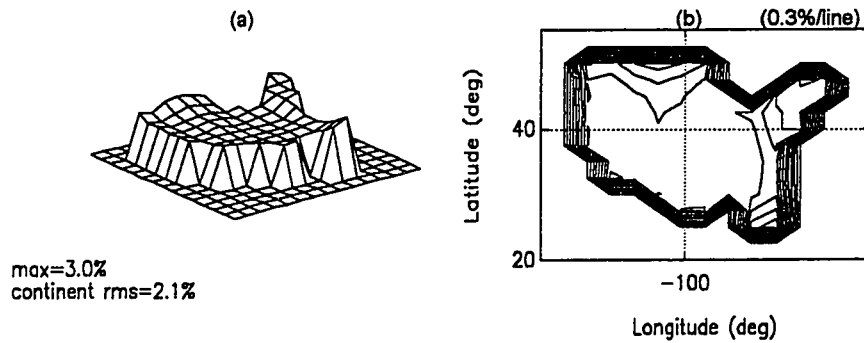
**Figure 4.12 Horizontal Positioning Error Ratio
(WADGPS Error)/(Stand-alone GPS Error)**

(a)   (b)   (0.5m/line)

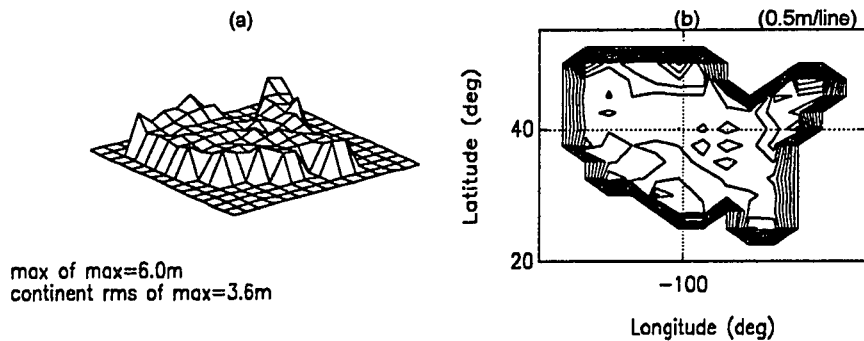max of max=6.0m
continent rms of max=3.6m

Figure 4.13 Maximum WADGPS Horizontal Positioning Errors

Figures 4.6 and 4.10 show the stand-alone navigation performance of typical users across the US. The RMS of the positioning errors for all user locations, over the entire 12hour period, is 82m in the vertical direction, and 42m in the horizontal direction. As one might expect, the error magnitudes are fairly uniform over the entire area. As is common in GPS navigation, the vertical error is approximately two times larger than the horizontal error due to the larger geometrical dilution of precision in the vertical direction (VDOP).

Figures 4.7 and 4.9, and 4.11 and 4.13 show that navigation accuracy is significantly improved through the use of WADGPS with the NSE ionospheric estimation algorithm and ephemeris and clock bias BLS algorithm. Continental RMS averages of the vertical and horizontal position errors have been reduced to 1.5m and 1.1m respectively. This dramatic decrease in the error magnitudes is emphasized in Figures 4.8 and 4.12, which show the percentage difference between the stand-alone and WADGPS solutions. Continental percentage RMS averages of the vertical and horizontal position errors have been reduced to 1.9% and 2.1% respectively.

Figures 4.9 and 4.13 show the maximum values of the errors for each user over the entire 12 hr period. The largest vertical and horizontal errors anywhere in the US over the entire 12 hr period are 9.1m and 6.0m, respectively.

One of the most striking features of the plots of WADGPS-corrected errors is the concave shape of the error mesh. In general, the navigation performance at the center of the US is better than along the coasts. This is because the satellites viewed by users in this region are also visible from a large number of monitor stations, and with better geometry (lower GDOP) than for their coastal counterparts.

One exception to this observation occurs in the southwestern US. This region exhibits better positioning accuracies than other edges of the country because of the high density

of monitor stations (Figure 4.7-4.9 and 4.10-4.13). Likewise, the north central part of the country is noticeably worse than average because of the relative sparsity of monitor stations.

The ability of WADGPS to model ionospheric delay in the master control station algorithm has a profound effect on the navigation performance. Figures 4.14 and 4.15 illustrate the RMS vertical and horizontal positioning errors for all users as a function of time. Figure 4.14 shows the time history of the stand-alone RMS vertical and horizontal positioning errors; both curves of the errors are flat and random, as they should be. In Figure 4.15 the peak of the WADGPS positioning errors occurred between 12:00-1:00 PM PST — the time of day when the largest ionospheric time delays, accompanied by the greatest variations in the delay, occur over the center of the WADGPS network.

Another indication of the influence of ionospheric errors and their estimation is given by the observation that WADGPS achieves greater improvement in RMS vertical positioning accuracy than in RMS horizontal positioning accuracy. The difference arises because measurements from satellites that are lower on the horizon have a larger obliquity factor, and consequently an amplified random error component, which is used in generating the simulated ionospheric time delays. Thus, since the unmodeled random part is larger in the horizontal direction, the horizontal positioning error is not lowered as much as the vertical positioning error by the ionospheric correction. The WADGPS vertical error is reduced to 1.9% of its stand-alone value, whereas the horizontal error is reduced to 2.1%.
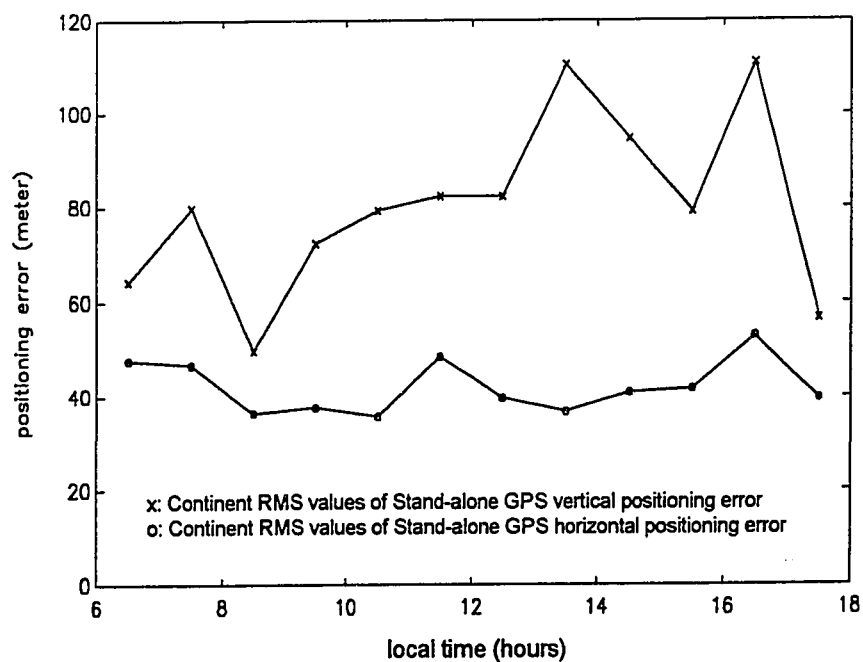
Figure 4.14 Continental RMS Values of Stand-alone GPS Vertical and Horizontal Positioning Errors for each hour period (6:00AM-6:00PM PST)
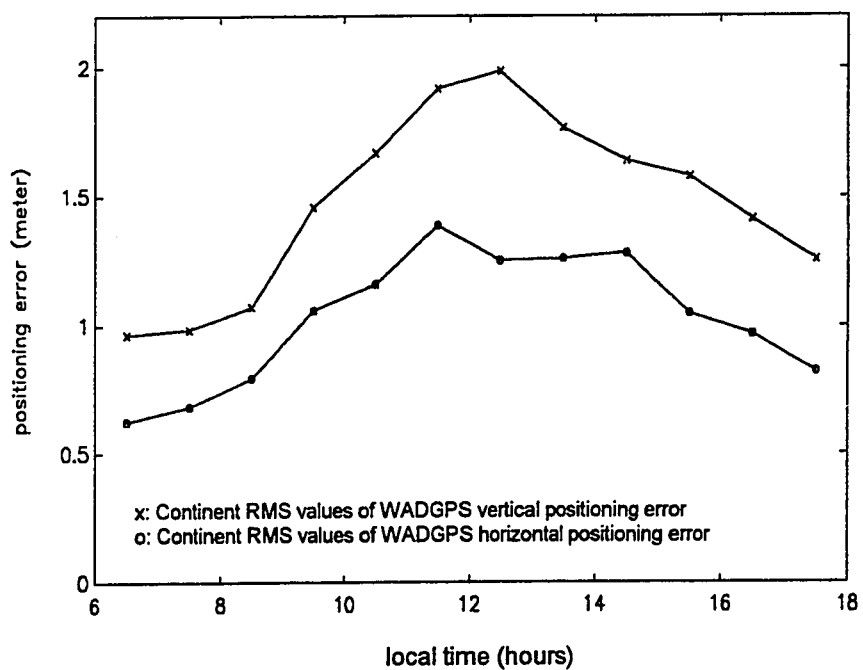

Figure 4.15 Continental RMS Values of WADGPS Vertical and Horizontal Positioning Errors for each hour period (6:00AM-6:00PM PST)

4.5 Summary of Navigation Results

We ran a 12hour simulation starting at 6:00AM PST and ending at 6:00PM PST. The NSE technique was used to determine the ionospheric delay parameters. Table 4.4 lists a summary of navigation accuracies, Table 4.5 shows WADGPS navigation accuracies with different receiver noise, and Table 4.6 shows a WADGPS navigation comparison of users in the center and users near the perimeter of the network. We used a mask angle of 5 degrees for the monitor stations and 6.5 degrees for the users.

Simulation results over a 12hour period indicate that stand-alone GPS positioning errors can be reduced to about one meter in horizontal positioning error using WADGPS without significant degradation caused by distance between monitor station and users. Continental RMS averages of the vertical and horizontal position errors have been reduced to 1.5m and 1.1m respectively.

Table 4.4 Summary of Positioning Errors (with no Latency)

Monitor mask angle = 5.0° User mask angle = 6.5°			RMS value of stand-alone positioning error (meter)	RMS value of WADGPS positioning error (meter)	(stand-alone error) /(WADGPS error) (%)	max value of WADGPS positioning error (meter)
Nonlinear Static Estimation	vertical	max *	93.1	1.9	2.6	9.1
		RMS **	82.1	1.5	1.9	6.3
	horiz.	max *	45.4	1.5	3.0	6.0
		RMS **	42.3	1.1	2.1	3.6

* : *maximum for the continental US*

** : *RMS value for the continental US*

The contribution of receiver noise to the WADGPS navigation accuracy is important because we may use different kinds of receivers and different mode (cross-correlation mode [Keegan, 1990][Lorenz, 1992][Enge, 1994] or P-code mode), and they have different receiver noise statistics. Three-dimensional WADGPS navigation accuracies for the receiver noises, 0.3m and 0.4m, are 2.6m and 3.1m respectively, which are 44% and 72% increases respectively, compare to 1.8m for 0.2m of receiver noise.

Vertical and Horizontal WADGPS positioning errors for the users near the perimeter of the network have mean values of 1.59m and 1.13m respectively, which are 10.7% and 18.5% higher errors than those for the users in the center of the network, 1.44m and 1.13m respectively (Table 4.6).

These results indicate that WADGPS can provide accurate ionospheric delay estimates as well as positioning errors, typically on the level of standard differential GPS operations.

Table 4.5 WADGPS Navigation Accuracies with different Receiver Noise (with no Latency)

Receiver Noise (m)	Positioning Error (m)			Increase in 3-D (%)
	Vertical	Horizontal	3-D	
0.2	1.5	1.1	1.8	0
0.3	2.1	1.6	2.6	44
0.4	2.2	2.14	3.1	72

Table 4.6 WADGPS Navigation Comparison of Users In the Center and Users Near the Perimeter of the Network (with no Latency)

WADGPS	Vertical positioning error			Horizontal positioning error		
	Perimeter (m)	Center (m)	$\frac{(\text{Perimeter} - \text{Center})}{\text{Center}}$ (%)	Perimeter (m)	Center (m)	$\frac{(\text{Perimeter} - \text{Center})}{\text{Center}}$ (%)
Mean	1.59	1.44	10.7	1.13	0.95	18.5

4.6 Sensitivity of Navigation Performance to Mask Angle

We investigated the sensitivity of navigation performance to mask angle by using different mask angles of the monitor stations and the users in the simulations. The mask angle of the users should be bigger than that of the monitor stations because the monitor stations have to see all the GPS satellites that are in view for users across the US. If this is not the case, then GPS satellites whose parameters are not estimated may be used to calculate the navigation solution in the users, which may result in very big positioning errors. This can happen on the boundary of the US. In most simulations we use a 1.5 degrees larger mask angle for the users than that for the monitor stations. Table 4.7 shows the simulation results for different mask angles.

From the above table we see that the RMS stand-alone GPS positioning errors do not change with the mask angle but the RMS WADGPS positioning errors increase by 20-30%, when the user mask angle changes from 5.0 to 11.0 degrees. The maximum WADGPS positioning errors increase by 30-50% with the same change of the user mask angle. For both of these increases, the errors in WADGPS remain much smaller than the errors in stand-alone GPS. These results confirm that the edges of the continental U.S. are the region most sensitive to the mask angle.

Table 4.7 Navigation Performance with Different Mask Angles (with zero latency)

		Monitor Station Mask Angle/ User Mask Angle (deg)							
		5.0/ 6.5	5.0/ 7.0	6.0/ 7.5	7.0/ 8.5	8.0/ 9.5	9.0/ 10.5	10.0/ 11.5	11.0/ 12.5
RMS vertical position errors	stand-alone GPS (m)	82.1	87.3	64.8	74.3	74.4	66.9	73.9	89.8
	WADGPS (m)	1.51	1.09	1.07	1.11	1.33	1.28	1.28	1.39
	WADGPS/ (stand-alone GPS) (%)	1.85	1.74	1.73	1.71	1.82	1.95	1.76	1.90
	max WADGPS errors (m)	6.30	2.64	2.93	3.01	3.58	3.52	3.57	4.19
RMS horizontal position errors	stand-alone GPS (m)	42.3	56.8	51.2	48.6	39.3	74.9	45.0	53.6
	WADGPS (m)	1.06	0.76	0.68	0.73	0.79	0.78	0.87	0.89
	WADGPS/ (stand-alone GPS) (%)	2.51	1.46	1.55	1.68	2.06	1.59	1.95	1.68
	max WADGPS errors (m)	3.62	1.69	1.56	1.82	2.00	1.92	2.41	2.23

If the mask angle of the user is bigger than 12.0 degrees there are several short periods of time a day when the user sees fewer than four GPS satellites and therefore its positioning errors are extremely large. When the mask angle of the user is 6.5 degrees and that of the monitor station is 5.0 degrees the RMS WADGPS positioning errors became large, but as the mask angle of the user increases to 7.0 degrees while that of the monitor station remains at 5.0 degrees, the errors become small. This can be explained as follows: When the mask angle of the user is too small the user may use the satellite in its navigation solution when it is at a very low elevation angle and only one monitor station can see it; as a result the estimation of this satellite's parameters is bad and the positioning errors become large.

From this study we recommend 6.0 degrees for the typical mask angle of the monitor station and 7.5 degrees for that of the user. However, when P-code is encrypted and we want to use cross-correlation mode at low elevation angle (below 10°) the signal to noise ratio (SNR) may not be adequate. This will be further discussed in Chapter 5.

4.7 Summary

This chapter introduced and described four different simulation modules: the GPS satellite module, the monitor station module, the master module, and the user module. Then it gave and discussed the results of the ionospheric time delay estimation: The RMS value of the ionospheric delay estimation error determined using the NSE technique was less than 0.5m.

We discussed the WADGPS navigation performance and introduced the time history plot of the WADGPS navigation performance: In the simulations we used a monitor station mask angle of 5.0 degrees and a user mask angle of 6.5 degrees and found WADGPS vertical and horizontal positioning errors of 1.51m and 1.06m, respectively,

and WADGPS positioning errors for the users near the perimeter of the network was about 15% bigger than those in the center of the network. Then, we analyzed the sensitivity of the navigation performance to angle mask and concluded that the mask angle is not significant for WADGPS. We recommended a mask angle of 6.0 degrees for the monitor station mask angle and a mask angle of 7.5 degrees for the user.

CHAPTER 5. WADGPS TEST RESULTS

5.1 Introduction

In Chapter 4, we discussed how we separated the ephemeris error from the satellite clock error in WADGPS and used simulations to show the potential of WADGPS to provide a 1-2m positioning accuracy. But the simulations themselves cannot model the error sources accurately and therefore the positioning error caused by unmodeled errors cannot be detected in the simulations. A test of the WADGPS, which uses field data, will be the best way to prove the potential of WADGPS.

We conducted a number of field tests to evaluate WADGPS performance. We used existing networks for the tests rather than the monitor stations used in the simulations because it was impossible to install the GPS receivers at the particular locations we chose, and to conduct our own WADGPS experiment would have been too costly. The available networks were the Cooperative International GPS Network (CIGNET), the International Earth Rotation Service (IERS) '91 Campaign, and the GPS Global Tracking Network coordinated by Jet Propulsion Laboratory (JPL). Stations in CIGNET are available all year and are globally distributed, but were too sparse to be used for WADGPS experiments. More stations, including CIGNET stations, were used in the IERS '91 Campaign and the GPS Global Tracking Network, and thus we used data collected in both the IERS '91 Campaign and the GPS Global Tracking Network in our field tests. The GPS Global Tracking Network has the same five monitor stations that were used in the IERS '91 Campaign plus one additional station, and it is equipped with ROGUE dual-

frequency receivers. For the tests, we used P-code data and employed Algorithm C, which uses a dual-frequency receiver in both the monitor stations and the users because it provides the best accuracy (for details see Chapter 3).

This chapter consists of two parts. The first discusses the field tests we performed using the IERS '91 Campaign data; the second discusses the tests we performed using the GPS Global Tracking Network data. The first part starts with a discussion of the IERS '91 Campaign when SA was off, giving the receiver locations, and showing the test results, and ends with a test result summary. The second part describes the field tests using the data from the GPS Global Tracking Network from December 10, 1992 till February 12, 1993 when SA was on. It compares stand-alone, DGPS, and WADGPS navigation accuracy and also discusses the latency effect and the comparison of cross-correlation vs. P-code in the WADGPS experiment. Finally a short summary ends the chapter.

5.2 IERS '91 Campaign

The IERS '91 Campaign was deployed between January 22nd and February 13th, 1991 as part of a cooperative global scientific geophysical experiment. The purpose of the IERS Campaign was to determine the precise location of the earth's center and the speed of the earth's rotation, in addition to establishing the drift of continental plates. A total of 49 P-code receivers were used. Of these, 21 were Rogues, five were Wild Magnavox WM-102s, 11 were Texas Instrument seven-channel TI-4100s, and 12 were four-channel TI-4100s. All the receiver sites are shown in Figure 5.1. After we analyzed the quality of the field data, we chose only Rogue receivers for our test. The field data from all receiver sites were collected at JPL and converted from receiver-dependent formats to a Receiver-Independent-Exchange (RINEX) format in ASCII.

During this period SA was off. Sampling time for most of the Rogue sites was 120 seconds and the available measurements were L1 & L2 P-code pseudoranges and L1 & L2 continuous carrier phases. C/A-code pseudoranges, Doppler (velocity) and meteorological data were not available.
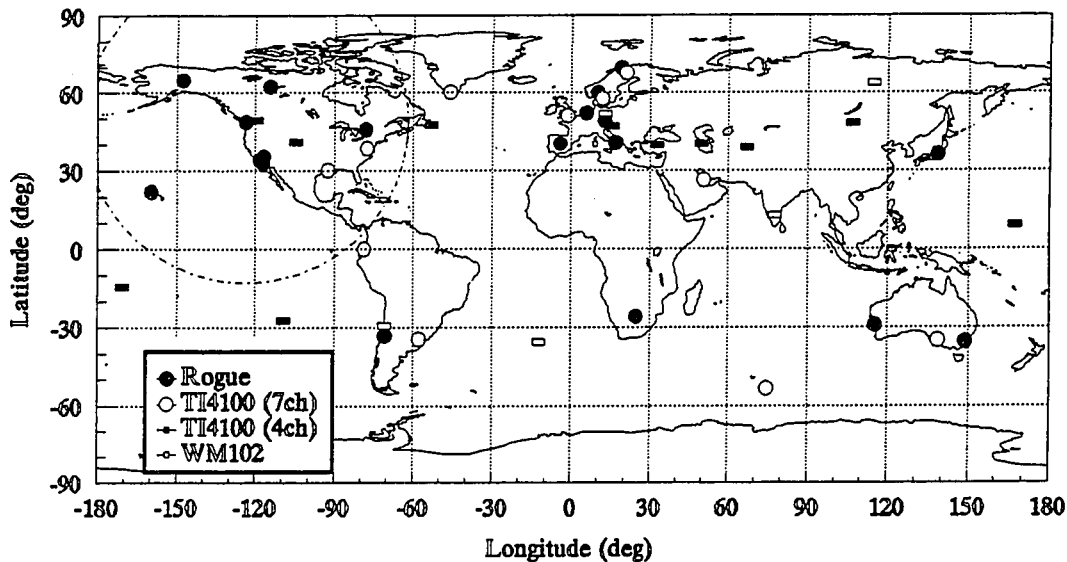

Figure 5.1 IERS '91 Campaign Receiver Locations.

5.2.1 Receiver Locations

Among the 21 Rogue receiver sites, seven sites were picked in North America and Hawaii. Five stations were chosen as monitor stations because their sites are evenly distributed and their geometry constitutes a rim, and two stations were chosen as users. Of the user stations, the first (PGC1) is near the center and was chosen to illustrate the potential of WADGPS; the second station (SCRI) is located near and outside the

boundary of the network and was chosen to show how WADGPS navigation accuracy degrades on the perimeter. Both user sites have Cesium clocks. The locations of the receiver sites are listed in Table 5.1 and the corresponding map is in Figure 5.2. The outline in this figure represents the US continent.

In the previous chapter the number of monitor stations necessary to make WADGPS overdetermined was found to be five but in the field tests the distances between the user (PGC1) and the monitor stations are so far (maximum 4261km and minimum 1633km) that all the monitor stations cannot observe the same satellite all the time. Therefore there may be only a small improvement in WADGPS navigation accuracy.

All the coordinates of the receiver locations were given in the SV5 coordinate frame [Murray, 1990] instead of the WGS-84 frame in which the GPS ephemeris is computed. The ephemeris errors of WADGPS calculated in the SV5 frame are different from those calculated in the WGS-84 frame, but the WADGPS navigation errors caused by treating the ephemeris errors in the WGS-84 frame as if they were in the SV5 frame is negligible.

Table 5.1 Locations of the Receiver Sites

| Station Type	Station ID	City	Nation	Latitude (deg)	Longitude (deg)	Baseline from PGC1 (km)	Baseline from SCRI (km)
Monitor	ALGO	Algonquin	Canada	46.0 N	78.0 W	3354	3580
Monitor	FAIR	Fairbanks, AK	USA	65.0 N	147.5 W	2295	4046
Monitor	JPLM	Pasadena, CA	USA	34.1 N	118.1 W	1658	171
Monitor	KOKB	Kokee, HI	USA	22.1 N	159.7 W	4261	4243
Monitor	YELL	Yellowknife	Canada	62.5 N	114.5 W	1633	3262
User	PGC1	Victoria	Canada	48.7 N	123.5 W	0	
User	SCRI	Scripps, CA	USA	32.8 N	117.3 W		0
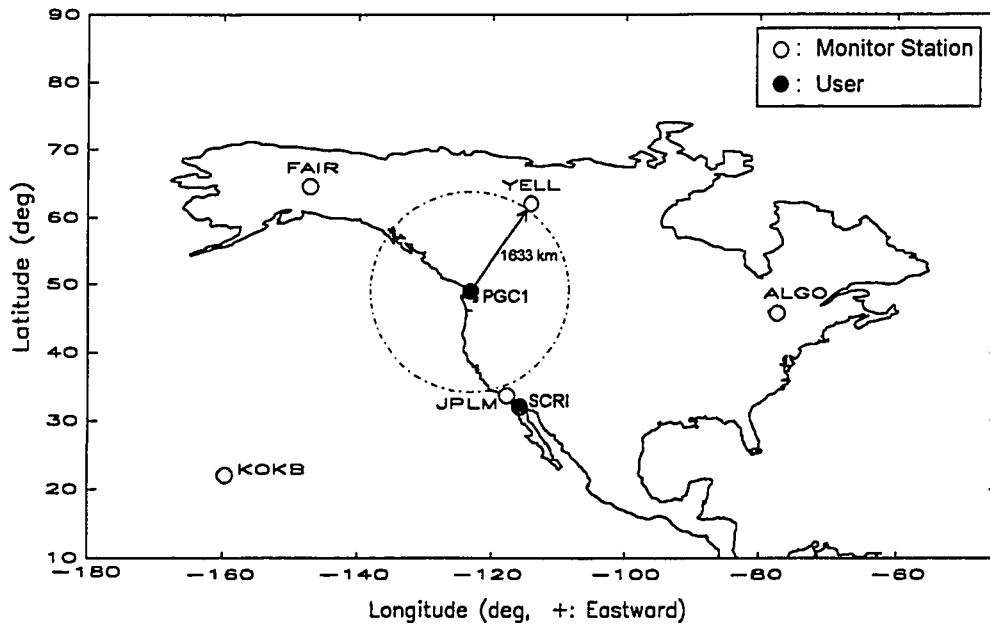
Figure 5.2 Map of Locations of the Receiver Sites

5.2.2 Test Results

We removed ionospheric time delays from all the data before the tests because we used Algorithm C, which uses dual-frequency receivers both in the monitor stations and the users and assumes that the ionospheric time delays can also be measured for the users. Since the meteorological data were not available, the temperature, the pressure, and the humidity of each site were inferred by its location and the time of day. Because there was no SA in the data, we used only P-code receivers, whose noise is lower than that of C/A-code receivers. Only five monitor stations were available; each monitor station can not see the same set of satellites and dramatic improvement in navigation accuracy with respect to stand-alone navigation accuracy could therefore not be expected.

The test was postprocessed as if it was in real time so there was no latency error. As soon as a set of data from a monitor station became available, the master station estimated the ephemeris errors and satellite clock errors from the first epoch and transmitted the

error corrections to the users. The five monitor stations used in the field test were considerably fewer than the 15 we had proposed to use (see Chapter 4). Use of this small a number of stations resulted most of time in the underdetermined case. In the underdetermined case, the corrections for ephemeris errors and clock offsets are not accurate, but the user positioning is still accurate with these corrections because for the user only the projection of the error correction vector on the line of sight to the satellite is important. A single estimation cycle typically took less than three seconds for a PC-486/25 machine.

We obtained two sets of results. The first set is for user PGC1, which is located near the center of the network; and its positioning errors are shown in Figures 5.3, 5.4, 5.5, and 5.6. The second set of results is for user SCRI, which is located just outside the perimeter of the network. Its positioning errors are shown in Figures 5.7, 5.8, 5.9, and 5.10.

Figures 5.3 and 5.5 show the PGC1 stand-alone user's positioning errors respectively in the morning and at night. The RMS horizontal positioning errors are 6.7m and 21.2m, respectively. They are quite small because there is no SA and because P-code receivers, whose noise is lower than that of C/A-code receivers, were used. Figures 5.4 and 5.6 show the improved navigation accuracy, with horizontal positioning errors of 0.7m and 4.8m, respectively in the morning and at night, that the user at the center of the network achieves by employing WADGPS error corrections. The shortest baseline from the monitor station to PGC1 is 1633km, which is very long, but WADGPS provides non-spatially degrading error corrections to the user. The reason why the results in the morning are better than those at night is that, as explained in Chapter 3, the estimation used in the night test is more underdetermined than that used in the morning test. Underdetermination can also explain the three bumps of positioning errors in Figure 5.4 at different times. In Figure 5.4 a bump at 16.4 hour can be explained as follows: three

satellites were seen by four or more monitor stations but two satellites were seen by only

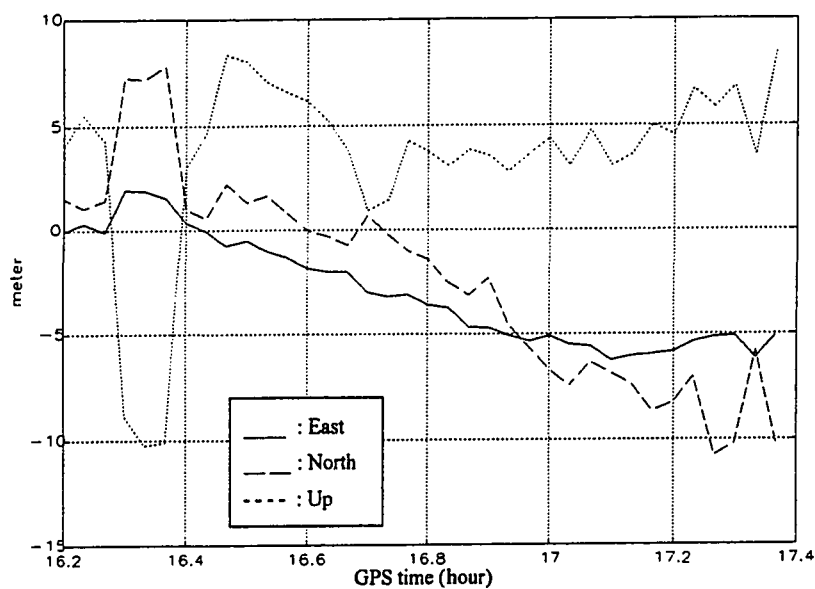three or less monitor stations during the bump period.

Figure 5.3 Stand-alone User's Positioning Errors (9:00AM local time, 2/10/91 at PGC1)
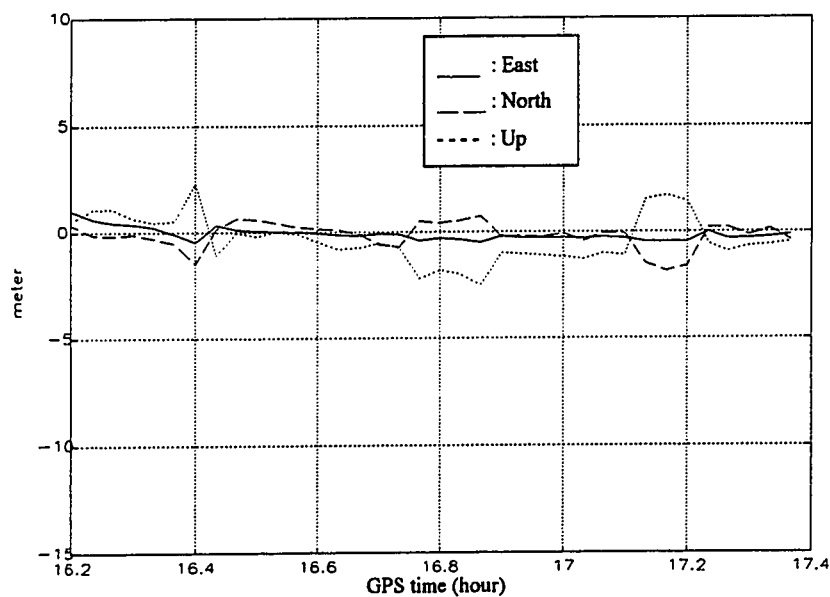

Figure 5.4 WADGPS User's Positioning Errors (9:00AM local time, 2/10/91 at PGC1)
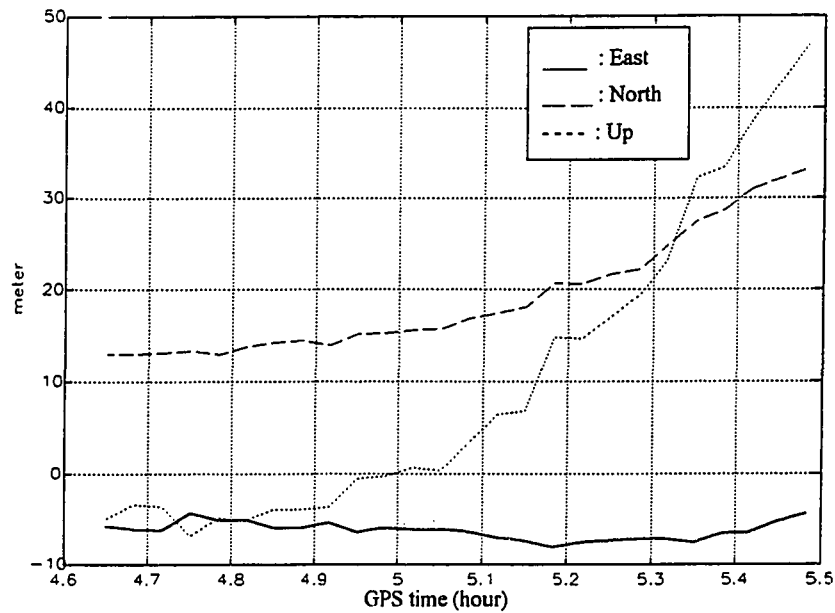
Figure 5.5 Stand-alone User's Positioning Errors (9:00PM local time, 2/9/91 at PGC1)
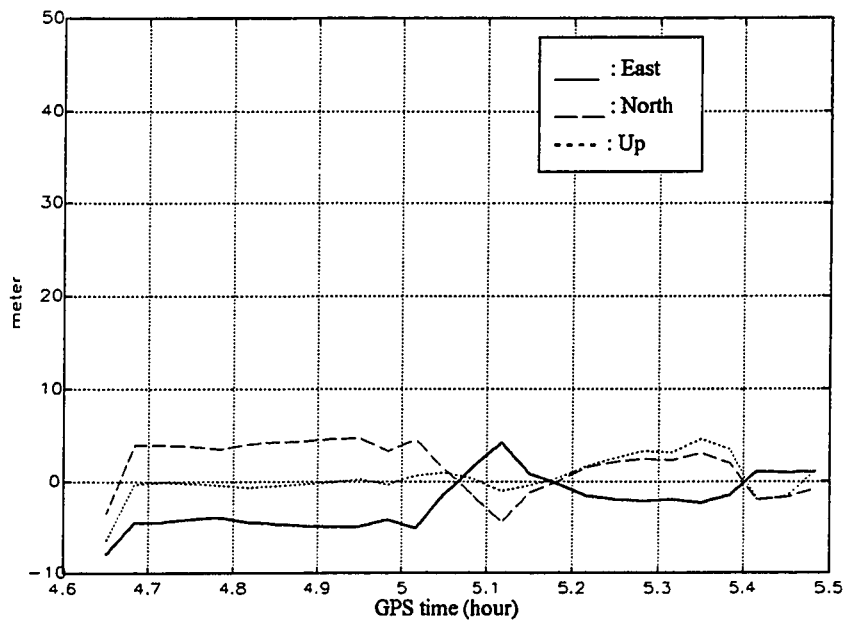

Figure 5.6 WADGPS User's Positioning Errors (9:00PM local time, 2/9/91 at PGC1)

The improvement in navigation accuracy at PGC1 is not very significant because the number of monitor stations is only five, whereas we had proposed 15 monitor stations to achieve a substantial improvement (see Chapter 4). Despite the smaller number of stations we used, our results demonstrate that WADGPS improves navigation accuracy. Generally the improvement in the horizontal positioning error is better than that in the vertical positioning error in Algorithm C because user-satellite geometry generally lends itself to better position solutions in the horizontal plane.

Figures 5.7 and 5.9 show the SCRI stand-alone user's positioning errors respectively in the morning and at night. SCRI is located just outside the perimeter of the network. The horizontal positioning RMS errors are 7.7m and 13.6m, respectively, and the vertical positioning RMS errors are 28.2m and 20.1m, respectively.

Figures 5.8 and 5.10 show the SCRI stand-alone user's significantly improved positioning errors, respectively in the morning and at night. The horizontal positioning errors are 0.3m and 2.4m, respectively; the vertical positioning errors are 2.1m, 3.0m, respectively when WADGPS error corrections were applied at the edge of the network. The shortest baseline, which is from JPLM to SCRI, is 171km. WADGPS still provides very good error corrections even to users located close to the edge of the network.

In general, the navigation performance of users close to the center of the network is better than that for users along the perimeter. This is because the satellites viewed by users close to the center are also visible from a large number of monitor stations, whereas users at the edge have a less advantageous geometry (lower GDOPs). The error parameters for the satellites visible from all the monitor stations are well-estimated and the user in the vicinity of the center of the network sees only the satellites with well-estimated parameters. However in these tests the user (SCRI) on the perimeter has better navigation

accuracy than the user (PGC1) close to the center of the network. I speculate that this

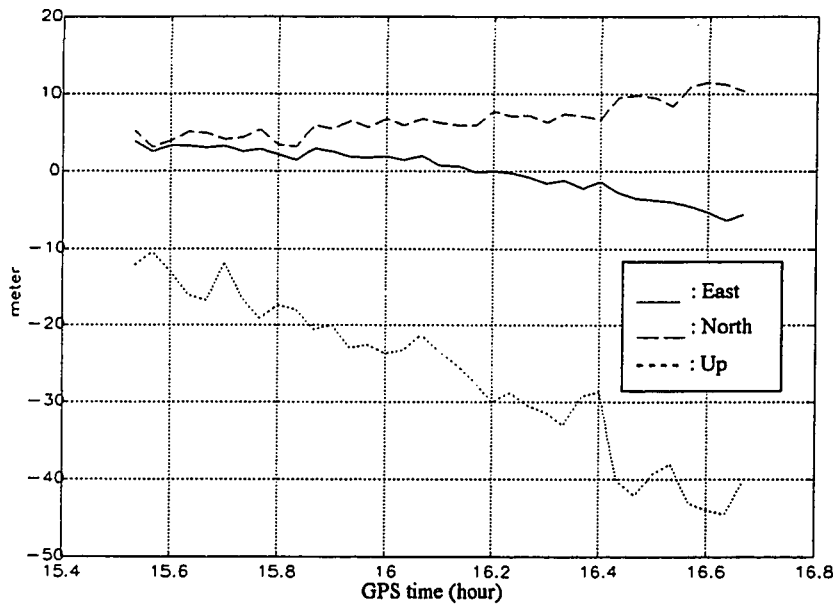occurs because SCRI is close to the monitor station.

Figure 5.7 Stand-alone User's Positioning Errors (8:00AM local time, 2/10/91 at SCRI)
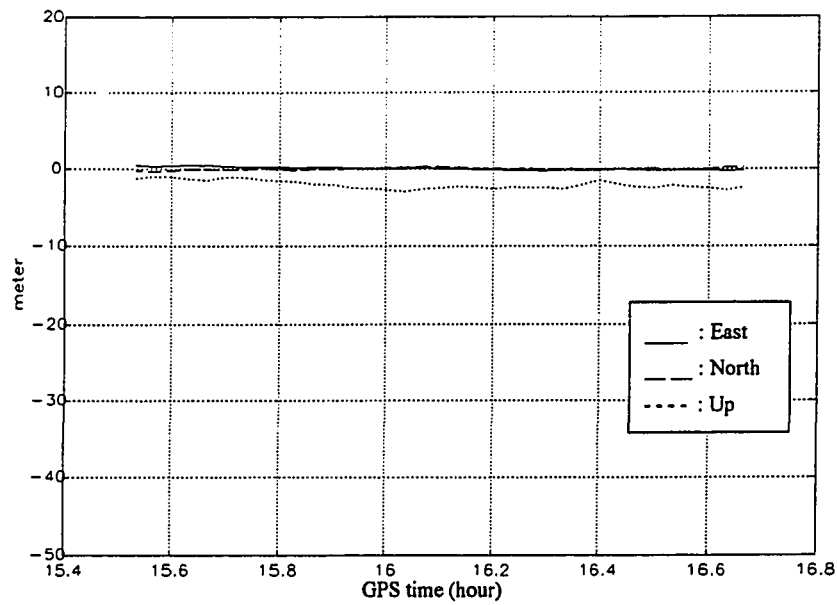
Figure 5.8 WADGPS User's Positioning Errors (8:00AM local time, 2/10/91 at SCRI)
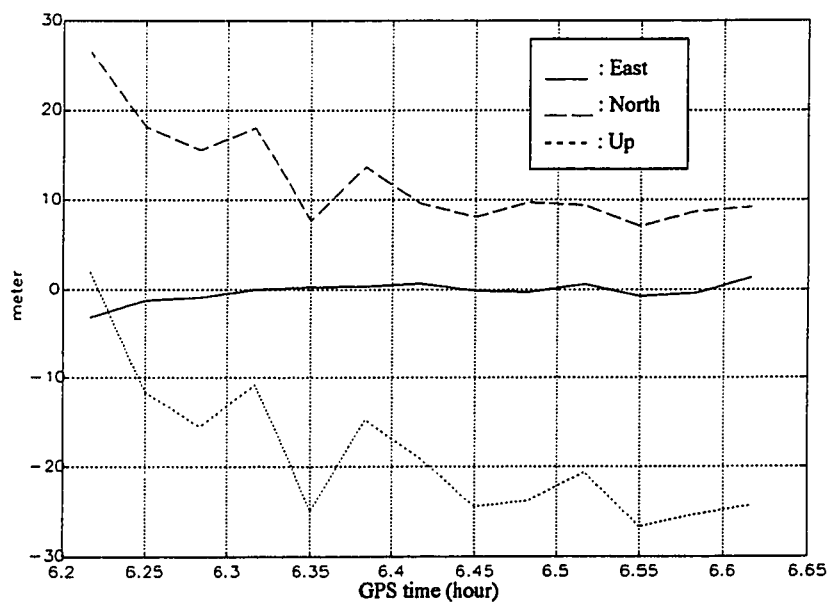

Figure 5.9 Stand-alone User's Positioning Errors (10:30PM local time, 2/9/91 at SCRI)
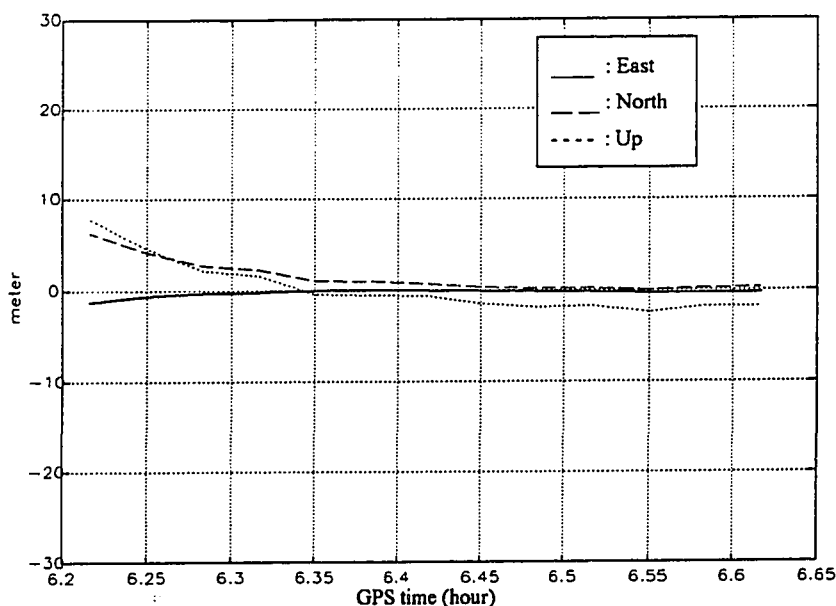
Figure 5.10 WADGPS User's Positioning Errors (10:30PM local time, 2/9/91 at SCRI)

5.2.3 Summary of the Test Results

The field test results of the IERS '91 Campaign showed the potential of WADGPS. WADGPS provides very good error corrections to users located near the center of the network with a minimum baseline of 1633km and even to users located close to the edge of the network. Table 5.2 summarizes the horizontal and vertical navigation errors at PGC1 and SCRI. Because we had only five monitor stations, only four satellites for the PGC1 test and only five satellites for the SCRI test were available, and each monitor station can not see the same set of satellites, the experiments were the underdetermined case most of time. The positioning accuracy of the PGC1 night test is a good example of the underdetermined case. The navigation accuracy will improve when more monitor stations are used and more GPS satellites are available.

We did not investigate latency effects for the field test because the sampling rate of the
IERS '91 Campaign was 120 seconds, much lower than the proposed WADGPS
correction update rate of 5-10 seconds/update discussed in Chapter 2.

Table 5.2 Summary of Navigation Errors (with no latency and SA off)

Station ID	Local Time	RMS Horizontal Positioning Errors (meters)		RMS Vertical Positioning Errors (meters)	
		Stand Alone	WADGPS	Stand Alone	WADGPS
PGC1	9:00AM	6.7	0.7	5.6	1.2
	9:00PM	21.2	4.8	19.2	2.1
SCRI	8:00AM	7.7	0.3	28.2	2.1
	10:30PM	13.6	2.4	20.1	3.0

5.3 The GPS Global Tracking Network

Previously collected field test data, which were collected from December 10th, 1992
till February 12th, 1993 using GPS Global Tracking Network, were processed to evaluate
WADGPS performance. The GPS Global Tracking Network has more than 30 sites
distributed all over the world, whose locations are known within a few centimeters. All
are equipped with ROGUE dual-frequency receivers. JPL collects data from all the
network sites and converts it from receiver-dependent formats to a RINEX format in
ASCII. The GPS Global Tracking Network data, in which more monitor stations and
more GPS satellites were available, has more potential to obtain precise positioning
accuracy than the IERS '91 Campaign data.

SA was on during the field test. Sampling time for most sites was 30 seconds and the available measurements were L1 & L2 P-code pseudoranges and L1 & L2 continuous carrier phases. C/A-code pseudoranges and Doppler measurements were not available and meteorological data were also not available.

5.3.1 Receiver Locations

Among over 30 Rogue receiver sites, seven sites were picked in North America and Hawaii for the field test. Six sites were chosen as monitor stations for WADGPS because they are evenly distributed and their geometry constitutes a rim, and one site, ALBH, was picked as user. ALBH is near the center and therefore was chosen to demonstrate the potential of WADGPS. ALBH has a Cesium clock. The minimum baseline between user (ALBH) and monitor station (JPLM) was 1632km for WADGPS, and ALBH and JPLM were also chosen as respectively user and reference stations for DGPS. The locations of the receiver sites are listed in Table 5.3 and the corresponding map is in Figure 5.11. The outline in this figure represents the continental US. In the figure, RCM2 is an additional station sited at a location that provides excellent geometry for the WADGPS estimation in the master station.

Table 5.3 Locations of the Receiver Sites

| Site Type	Station ID	City	Nation	Latitude (deg)	Longitude (deg)	Baseline from ALBH (km)
Monitor	ALGO	Algonquin	Canada	46.0 N	78.0 W	3363
Monitor	FAIR	Fairbanks, AK	USA	65.0 N	147.5 W	2318
Monitor	JPLM	Pasadena, CA	USA	34.1 N	118.1 W	1632
Monitor	KOKB	Kokee, HI	USA	22.1 N	159.7 W	4245
Monitor	RCM2	Richmond, FL	USA	25.6 N	80.4 W	4414
Monitor	YELL	Yellowknife	Canada	62.5 N	114.5 W	1661
User	ALBH	Albert Head	Canada	48.4 N	123.5 W	0
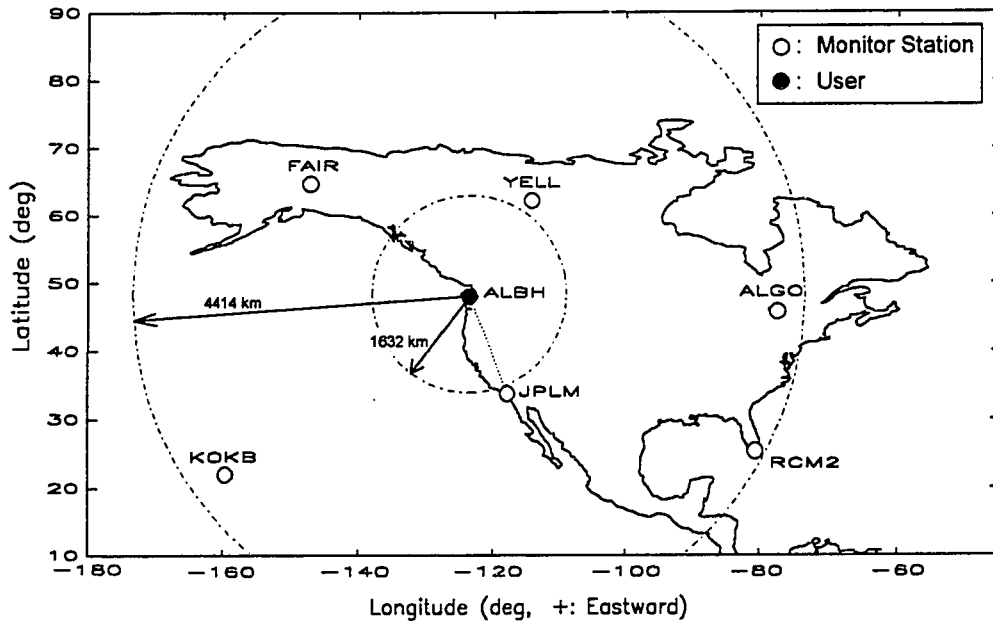
Figure 5.11 Map of Locations of the Receiver Sites

All the coordinates of the receiver locations were given in the International Terrestrial Reference Frame (ITRF) 91 coordinate frame instead of the WGS-84 frame in which the GPS ephemeris is computed. The ephemeris errors of WADGPS in the ITRF91 frame are different from those calculated in the WGS-84 frame, but the WADGPS navigation errors caused by treating the ephemeris errors in the WGS-84 frame as if they were in the SV5 frame is negligible.

5.3.2 Test Results

The GPS Global Tracking Network data were taken from December 10, 1992 till February 12, 1993. But only the results from the test on December 10th, 1992 are discussed in this subsection. All other test results are summarized in the next subsection.

Ionospheric time delays were removed from all the data because we used Algorithm C which uses dual-frequency receivers in both monitor stations and users and assumes that the ionospheric time delays are available as separate measurements. Since meteorological data were not available, the temperature, pressure, and humidity of each site were inferred by location and time of day. SA was on during the tests.

A total of seven satellites were in view from ALBH during the field test. Their elevation angles were above 18° and therefore tropospheric errors and ionospheric time delay errors are not significantly big. Of the seven satellites, PRN 28 was seen for only the first two minutes of the test; most of the other six were in view throughout the period. Typically six to nine satellites will be seen from a receiver when GPS is in full operation in 1994. Typical WADGPS navigation accuracy in 1994 should therefore be as good as or better than our test results. Figure 5.12 shows an azimuth vs. elevation plot during the test period.
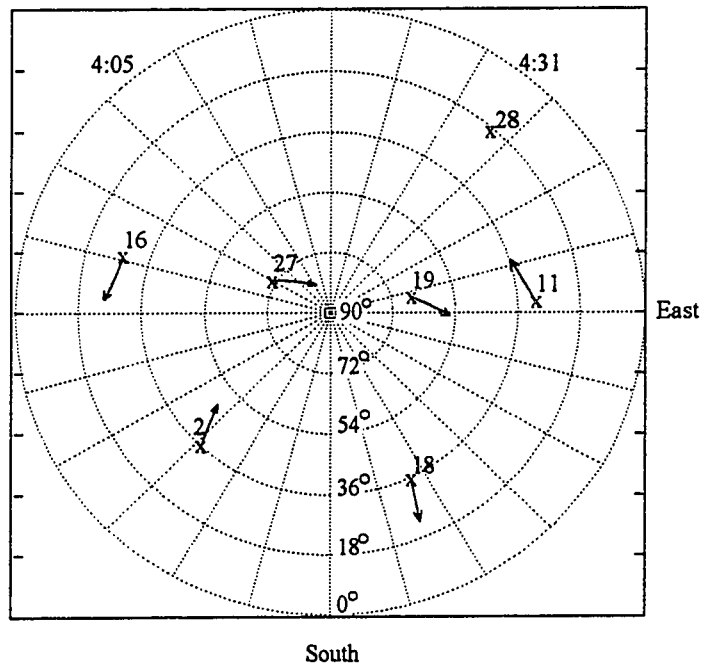

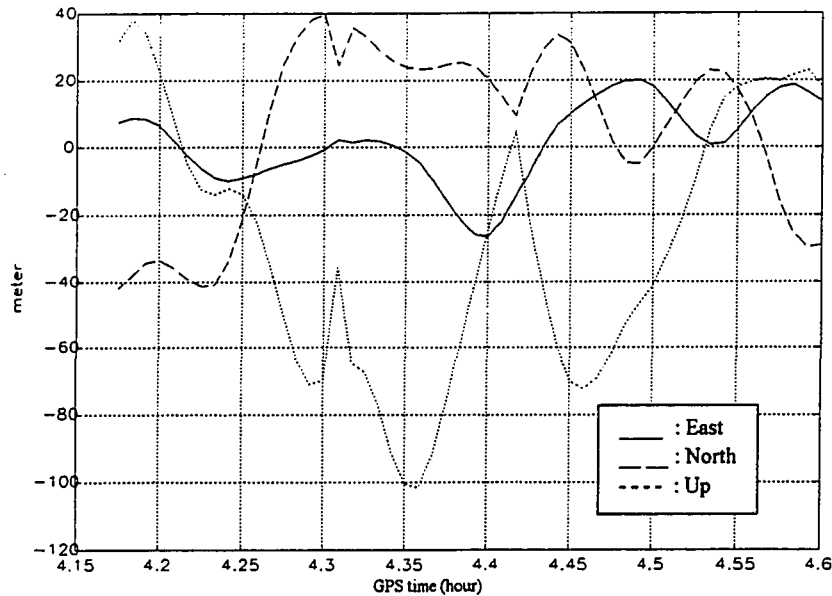**Figure 5.12 Azimuth vs. Elevation Plot (ALBH, 12/10/92)**

Figure 5.13 Stand-alone User Positioning Errors (ALBH, 12/10/92)

Six monitor stations were used in the field tests—one more than were used in the

IERS '91 Campaign, but still considerably fewer than the 15 stations we proposed (see

Chapter 4). Most of time the GPS satellites could be seen by more than four monitor

stations, but sometimes they could be seen by only four stations or fewer, which is the

underdetermined case. In the latter case, we used a two-norm minimization technique in

the navigation solution, and the absolute values of estimation results for ephemeris errors

and clock offsets were not accurate, but the user positioning was still accurate with these

corrections.

Figure 5.13 shows the stand-alone user's positioning errors at night at ALBH. The

RMS horizontal and vertical positioning errors are 29m and 49m, respectively, which is

fairly normal under SA. We can see that the navigation errors are slowly oscillating with

large magnitude indicating the existence of SA. The two sharp peaks of positioning errors in this figure are caused by changes in the satellite constellation.

Figure 5.14 shows that the DGPS navigation errors are lower than those of stand-alone GPS. Figure 5.15 shows only the DGPS positioning errors. The baseline is 1632km, which is too long for DGPS to provide high accuracy, but a substantial improvement in DGPS navigation accuracy is nevertheless achieved. The RMS horizontal and vertical positioning errors of the DGPS user are 3.7m and 12.7m, respectively. The stand-alone GPS three-dimensional positioning error is reduced by 77%, but only small improvement occurs in the vertical positioning error.
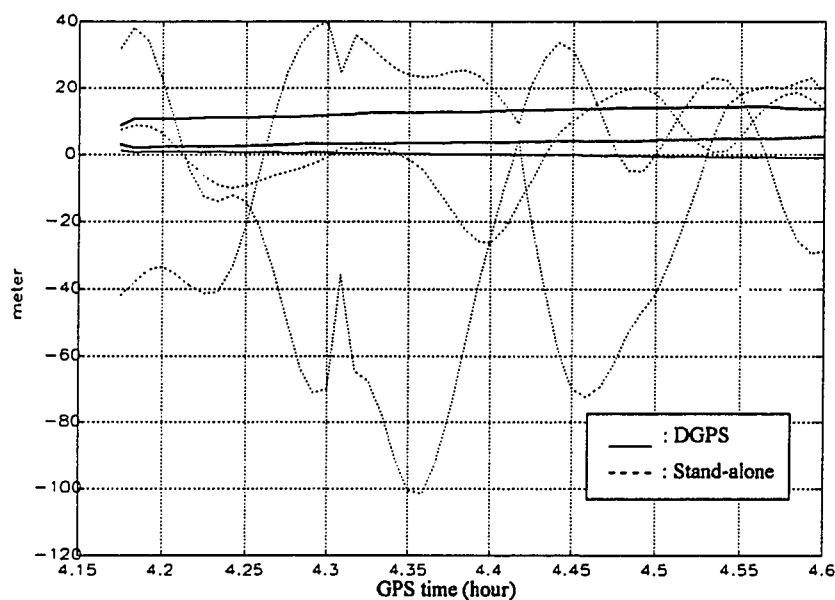

Figure 5.14 Stand-alone vs. DGPS User Positioning Errors (ALBH, 12/10/92)
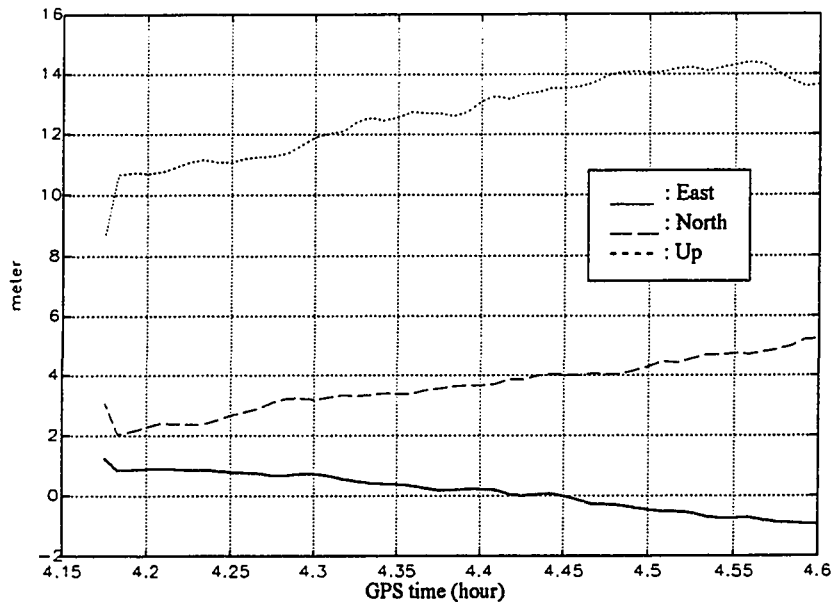
Figure 5.15 DGPS User Positioning Errors (ALBH, 12/10/92)

Figure 5.16 shows that WADGPS results in significantly smaller navigation errors than stand-alone GPS. Figure 5.17 shows only the WADGPS positioning errors. The shortest baseline from the monitor station (JPLM) to ALBH is 1632km, which is very long, but WADGPS provides non-spatially degrading error corrections to user.

The RMS horizontal and vertical positioning errors of the WADGPS user are 46cm and 54cm, respectively. The stand-alone GPS three-dimensional positioning error is reduced by 99%. In real-time applications, latency (a time delay in the error corrections) will degrade the WADGPS navigation accuracy, however. This latency will be discussed in the next section.
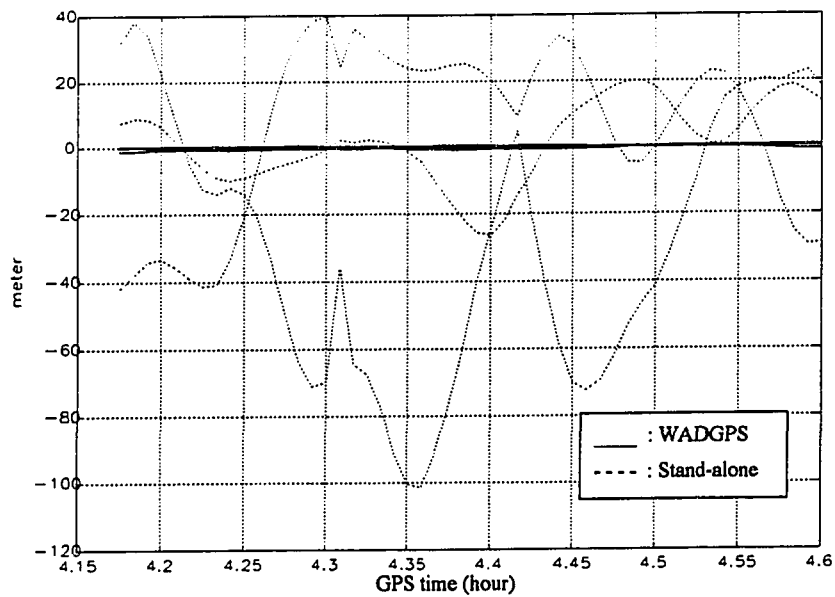
Figure 5.16 Stand-alone vs. WADGPS User Positioning Errors (ALBH, 12/10/92)
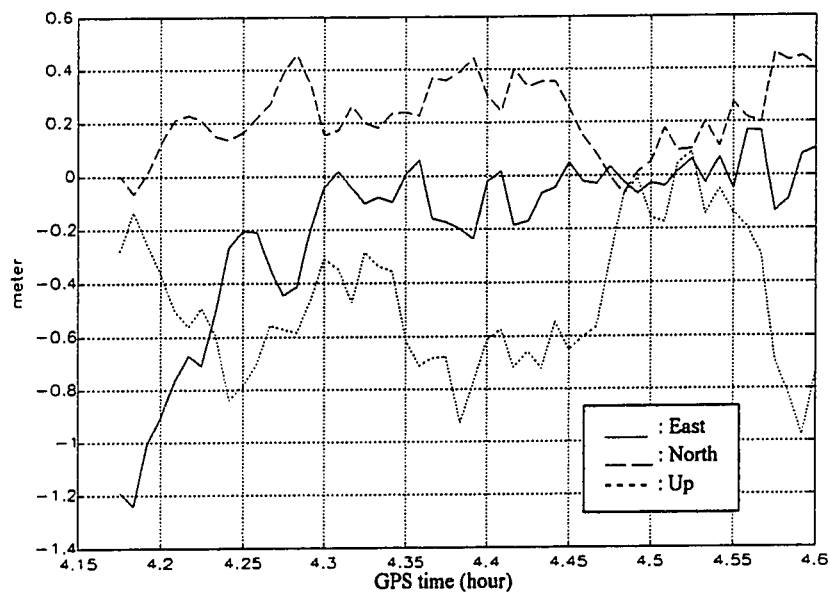
Figure 5.17 WADGPS User Positioning Errors (ALBH, 12/10/92)
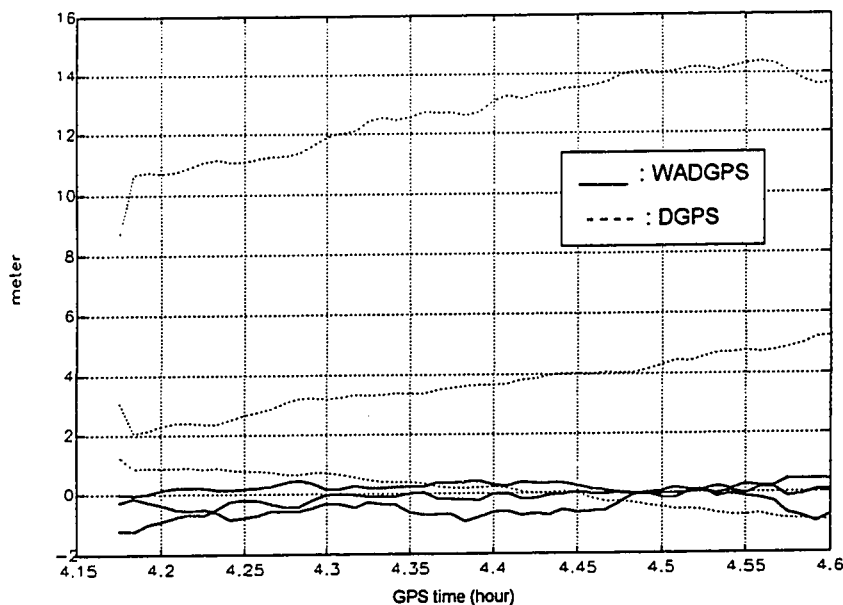
Figure 5.18 DGPS vs. WADGPS User Positioning Errors (ALBH, 12/10/92)

Figure 5.18 compares DGPS and WADGPS navigation errors. The three-dimensional positioning error of WADGPS is only 5% of that of DGPS; the largest improvement is in the vertical positioning error. DGPS has a much larger vertical than horizontal positioning error; in WADGPS by contrast, the vertical positioning error is almost the same as the horizontal positioning error even with a 1632km minimum baseline.

The horizontal and vertical navigation errors of stand-alone GPS, DGPS, and WADGPS at ALBH are summarized in Table 5.4.

Table 5.4 Summary of Navigation Errors at ALBH (1632 km Baseline, 12/10/92, with no Latency)

		GPS (m)	DGPS (m)	DGPS/GPS (%)	WADGPS (m)	WADGPS/GPS (%)
RMS errors	East	12	0.6	5.3	0.38	3.2
	North	26	3.7	14.3	0.26	1.0
	Up	49	12.7	26.2	0.54	1.1
	3-D	57	13.2	23.3	0.71	1.3

5.3.3 Summary of the Test Results

We chose algorithm C, which uses dual-frequency receivers in both monitor stations and users and estimates three-dimensional ephemeris errors and satellite clock offset including SA, to implement WADGPS because it provides the best navigation accuracy and we were interested in establishing the best possible performance for WADGPS.

The GPS Global Tracking Network data collected by P-code receivers were used to test WADGPS performance. Six monitor stations that provide good geometry, and one user site near the center of the network were picked in North America and Hawaii, to demonstrate WADGPS performance. A batch-least-squares and minimum-norm solution was used in the estimation at the master station.

Table 5.5 Summary of Navigation Errors at ALBH (1632km baseline, 12/10/92-2/12/93, with no Latency)

Date	GPS Time	GPS (3-D RMS, m)	WADGPS (3-D RMS, m)	WADGPS/GPS (%)
12/10/92	4:10AM-4:36AM	57.0	0.71	1.2
1/6/93	4:34AM-5:00AM	55.4	0.84	1.5
1/11/93	3:12AM-3:42AM	52.9	1.11	2.1
1/12/93	3:15AM-3:38AM	50.1	1.32	2.6
1/13/93	3:38AM-4:10AM	62.0	0.86	1.4
1/14/93	3:34AM-4:05AM	48.5	1.51	3.1
1/23/93	3:00AM-3:55AM	65.7	2.18	3.3
1/29/93	3:01AM-3:47AM	81.3	1.45	1.8
1/30/93	3:07AM-3:55AM	51.3	1.99	3.9
1/31/93	3:03AM-3:47AM	68.5	1.58	2.3
2/11/93	3:22AM-3:59AM	73.9	0.94	1.3
2/12/93	3:20AM-3:55AM	67.5	0.94	1.4
Total Average		61.2	1.29	2.2

The GPS Global Tracking Network data were taken from December 10, 1992 till February 12, 1993. The test results are shown in Table 5.5. The test results indicate that the three-dimensional positioning error of stand-alone GPS, which is 61.2m, can be

reduced to the order of one meter (with no latency) using WADGPS, without degradation caused by spatial separation between the monitor stations and the users.

The most likely sources of WADGPS positioning errors are multipath and tropospheric errors. Multipath errors can be reduced by using a choke ring and a Hatch/Eshenbach filter, but they cannot be totally eliminated. But a new receiver design that includes a multipath estimating delay lock loop will help eliminate multipath errors [van Nee, 1993]. A better tropospheric model will reduce tropospheric error, but the error will still exist because no model can eliminate error completely. Using satellite weather forecasts in WADGPS will prevent unexpectedly large tropospheric errors.

5.3.4 Latency and Age Concern

The results of the field test showed that WADGPS can achieve navigation accuracy on the order of one meter even for a 1632km baseline with zero latency, which is not achievable for DGPS. However, in practice it is impossible for users to apply the error corrections at the same epoch at which they are estimated in the master station. We define latency as the time taken to estimate the correction parameters plus the time spent for the WADGPS error corrections to arrive at the users via geosynchronous satellite. Actually users have to use the old correction message until the new correction message arrives. So we define age, total time delay, as latency plus the time interval from when the old correction message arrived till when users apply this correction message. Figure 5.19 shows the definition of latency and age.
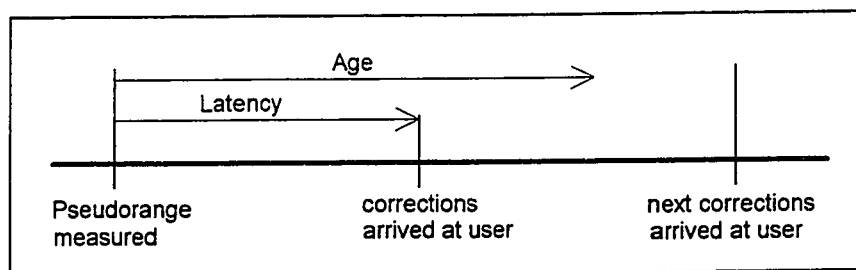
Figure 5.19 Definition of Latency and Age

Usually maximum of age for 5-10sec of latency is 10-20sec. The major source of the error caused by the time delay is SA, which has a two to three minute time constant and is the fastest changing error source.

We investigated the latency effects on WADGPS navigation accuracy. Since the sampling time of the GPS Global Tracking Network data was 30 seconds, the tests were repeated with latencies of 30 to 180 seconds with 30 second increments. We used two different error correction techniques: constant error correction and error-rate correction.

Figure 5.20 and 5.21 show WADGPS user positioning errors with 30 seconds of latency using constant error correction and error-rate correction, respectively. Figure 5.22 shows the effect of the different latency values on the three-dimensional positioning accuracies for December 10th, 1992. Table 5.6 shows the effect of latency on WADGPS navigation accuracy for December 10th, 1992 and Table 5.7 summarizes the effect of latency for all data. Figure 5.23 shows three-dimensional WADGPS positioning errors caused by the latency using the error-rate correction technique and using latency prediction technique described in Chapter 2.

Figure 5.23 indicates that an average of 2-3m of three-dimensional RMS positioning accuracy can be achieved with 5-10sec of latency, which corresponds to 10-20sec maximum age, if WADGPS is used with error-rate corrections (rather than with constant error corrections).
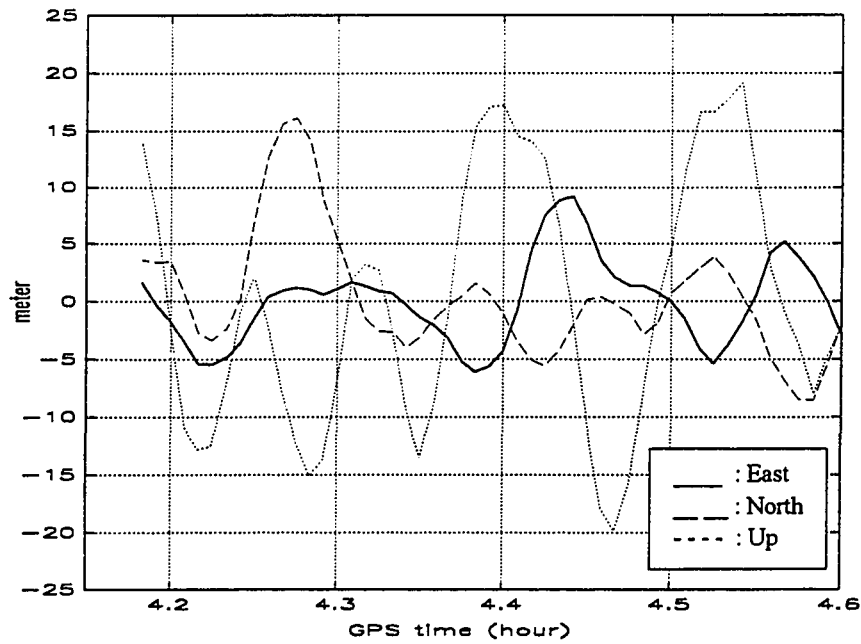
Figure 5.20 WADGPS User Positioning Error with 30 Seconds of Latency using Constant Error Correction (ALBH, 12/10/92)
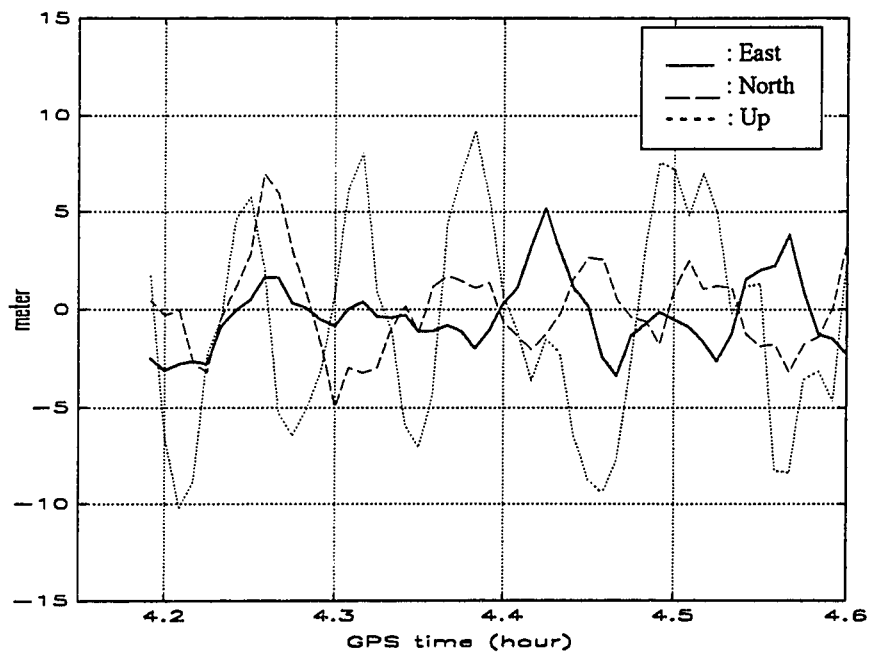
Figure 5.21 WADGPS User Positioning Error with 30 Seconds of Latency using Error-rate Correction (ALBH, 12/10/92)
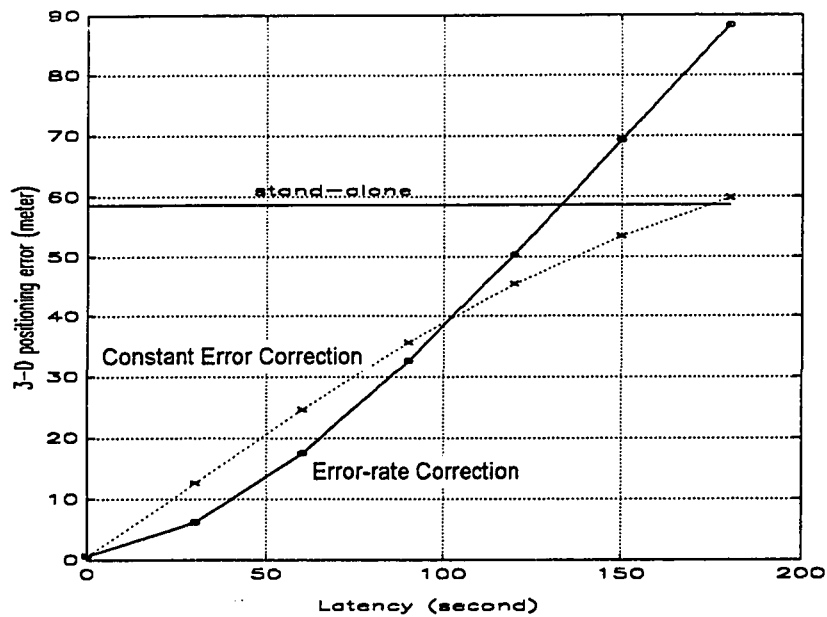
Figure 5.22 Latency Effect on WADGPS (ALBH, 12/10/92)

Table 5.6 Three-dimensional WADGPS RMS Positioning Errors in the Existence of Latency for Two different Error Correction Techniques (ALBH, 12/10/92)

Latency (sec)	0	30	60	90	120	150	180
Constant Error Correction	0.71	12.63	24.64	35.68	45.38	53.64	59.85
Error-rate Correction	0.71	6.25	17.49	32.67	50.33	69.33	88.33
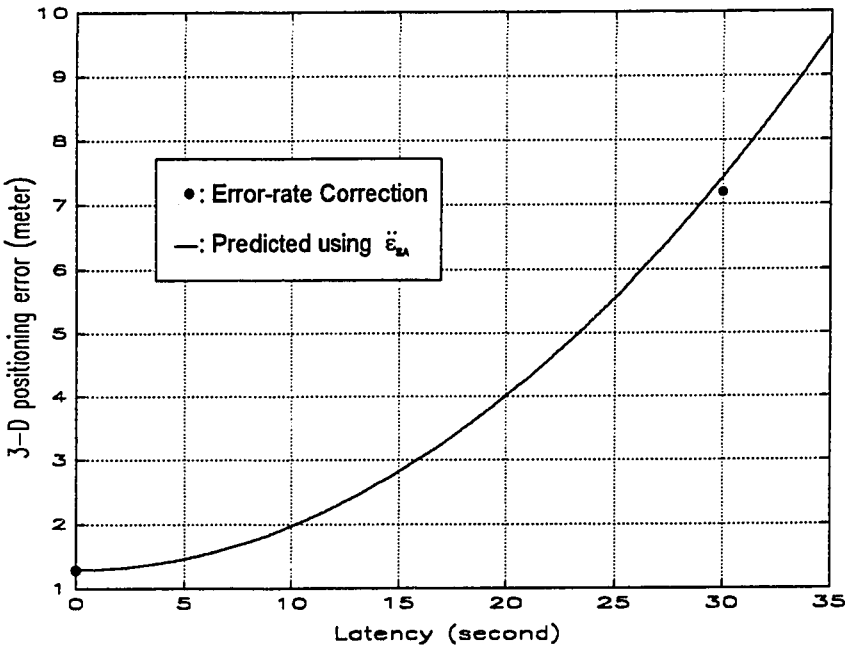
Figure 5.23 Latency Effect on WADGPS (for all data)

Table 5.7 Summary of Three-dimensional WADGPS RMS Positioning Errors in the Existence of Latency using Error-rate Correction Technique

Date	3-D WADGPS RMS Positioning Errors with Latency (m)	
	0 sec	30 sec
12/10/92	0.71	6.25
1/6/93	0.84	6.64
1/11/93	1.11	7.15
1/12/93	1.32	7.21
1/13/93	0.86	6.95
1/14/93	1.51	7.73
1/23/93	2.18	8.12
1/29/93	1.45	7.27
1/30/93	1.99	7.83
1/31/93	1.58	7.45
2/11/93	0.94	6.68
2/12/93	0.94	7.04
Total Average	1.29	7.19

5.3.5 WADGPS Navigation Accuracy for C/A-code vs. P-code

All the WADGPS field tests were done with P-code receivers and in P-code mode. But when P-code is encrypted then the receivers have to be switched to cross-correlation mode so that the receivers can still measure ionospheric time delays [Keegan, 1990][Lorenz, 1992][Enge, 1994]. The WADGPS test results with the receivers in cross-correlation mode need to be estimated because P-code will not be available all the time in the future and ionospheric time delay measurement noise in cross-correlation mode is much larger than that in P-code mode.

We have done a roof test to get the receiver noise statistics in cross-correlation mode and P-code mode. The test was done on the roof of Durand Building at Stanford University from 11:00AM till 3:30PM PST, October 21th, 1993. There were a lot of antennae on the roof and multipath errors caused by the antennae were anticipated. We used two Trimble 4000SSE P-code receivers and had them share antenna so that their multipath errors are the same. We forced one receiver to receive GPS signals in P-code mode and the other in cross-correlation mode. Experimental setup is shown in Figure 5.24.

Figure 5.25 shows elevation angle versus the statistics of ionospheric time delay measurement noise in cross-correlation mode and P-code mode. Table 5.8 summarizes the ionospheric time delay measurement noise. There are three peaks between 20° and 40° elevation angles. This is the multipath errors caused by the antennae surrounding the GPS antenna. The ionospheric time delay measurement noise in cross-correlation mode is almost the same as that in P-code mode in elevation angle above 40°, is getting bigger as elevation angle become smaller, and is 100% bigger than that in P-code mode in the elevation angle below 10°. Total average of the ionospheric time delay measurement

noise in cross-correlation mode over all elevation angle is 1.0m, which is about 70%

bigger than that in P-code mode, 0.6m.
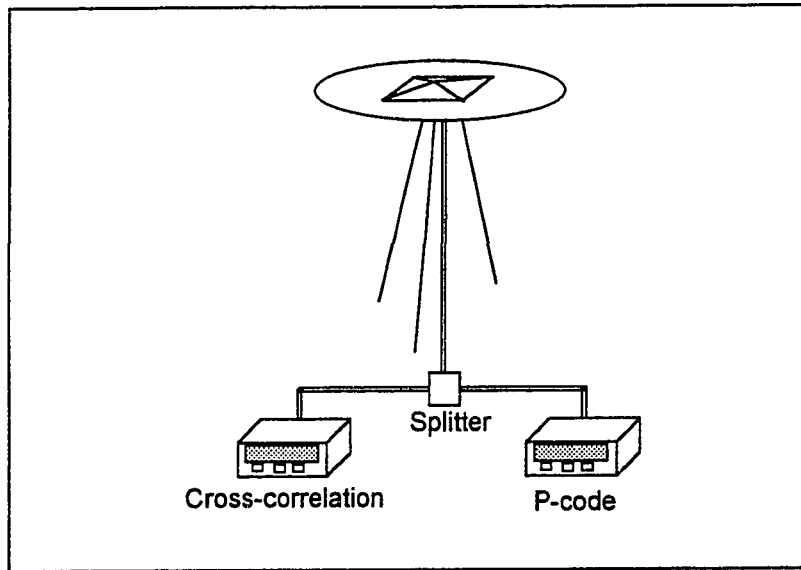
Figure 5.24 Experimental Setup for Measuring Ionospheric Time Delay Noise

The receiver noise, 0.2m, used in the WADGPS simulations were based on the

assumption that we use P-code receiver in P-code mode, use Hatch/Eshenbach filter with

the averaging constant, $k = 10$, and receiver noise improvement by the filter is a factor of

$\sqrt{10}$. The ionospheric time delay measurement noise in P-code mode, 0.6m, divided by

$\sqrt{10}$ gives 0.2m, which is the receiver noise used in the simulations.

The WADGPS test results with 5-10 seconds of latency and using the receivers in

cross-correlation mode can be predicted as 3-5m of three-dimensional positioning errors,

which is based on Table 4.5 in Chapter 4 and Table 5.8: 70% increase in receiver noise

(Table 5.8) corresponds to about 50% increase in WADGPS three-dimensional

positioning error (Table 4.5).
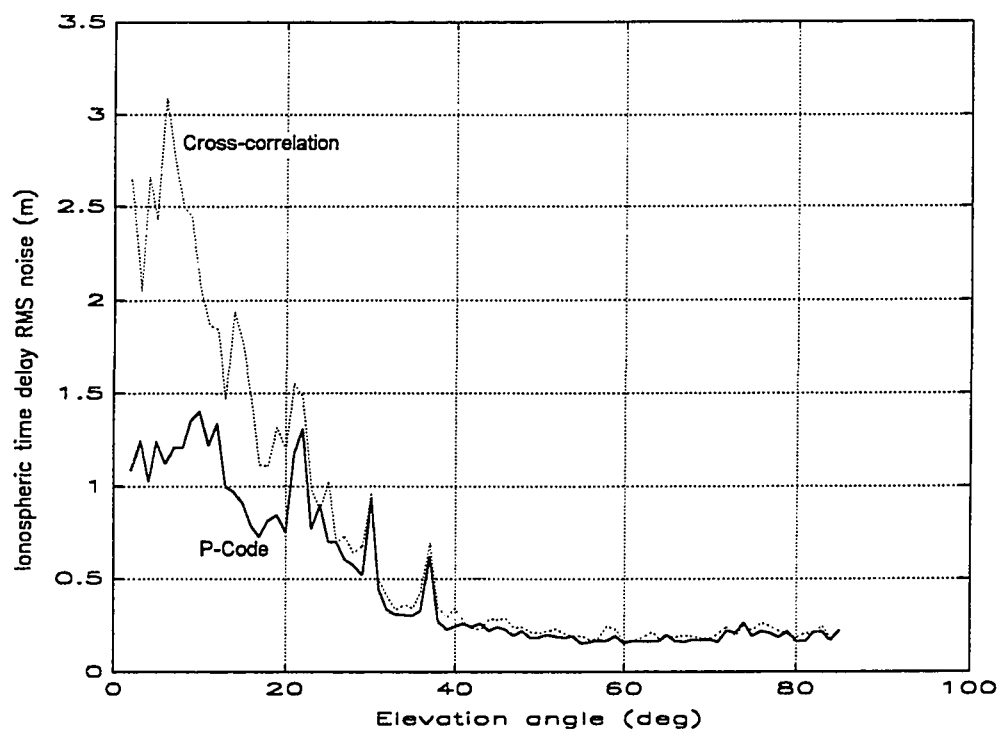
Figure 5.25 Ionospheric Time Delay Measurement Noise for Cross-correlation and P-code Mode (Trimble 4000SSE, Sampling Time = 15sec)

Table 5.8 Ionospheric Time Delay Measurement Noise Comparison for Cross-correlation and P-code Mode (Trimble 4000SSE, Sampling Time = 15sec)

Elevation angle range (deg)		0-10	10-20	20-30	30-40	40-90	0-90
Mean	Cross-correlation noise (m)	2.5	1.5	1.0	0.4	0.2	1.0
	P-code noise (m)	1.2	0.9	0.8	0.3	0.2	0.6
	$\dfrac{(Cross\text{-}corr.)\text{-}(P\text{-}code)}{(P\text{-}code)}$ (%)	108	67	25	33	0	67

5.4 Summary

This chapter showed the WADGPS field test results derived from IERS '91 Campaign data and GPS Global Tracking Network data, both of which were collected with P-code receivers in P-code mode at all sites. Cesium clocks were in user sites. Algorithm C, which uses dual-frequency receivers in both monitor stations and users and estimates three-dimensional ephemeris errors and satellite clock offset including SA, was used in the tests of WADGPS because it provides the best navigation accuracy. A batch-least-squares and a minimum-norm solution were used in the estimation.

The test results from data collected during the IERS '91 Campaign, which used only five monitor stations, indicate that WADGPS provides very good error corrections to users located near the center of the network and even to users located close to the edge of the network even though the number of monitor stations is considerably lower than the 15 we had proposed for WADGPS (see Chapter 4).

The results of the field tests using the GPS Global Tracking Network data, which used six monitor stations, shows that without latency, the positioning error of WADGPS user ALBH (1632km baseline), which is near the center of the network, was on the order of one meter while that of the DGPS user was more than 10m.

Latency will degrade the WADGPS navigation accuracy, but a study of the latency showed that 2-3m of three-dimensional RMS positioning accuracy can be achieved with 5-10 seconds of latency, which result in 10-20 seconds of maximum age, if P-code mode is selected and WADGPS is used with error-rate corrections.

The encryption of P-code will force receivers to switch to cross-correlation mode and degrade the WADGPS navigation accuracy. A statistics of the ionospheric time delay measurement noise for P-code and mode led us to predict the WADGPS test results with

5-10 seconds of latency and using the receivers in cross-correlation mode as 3-5m of

three-dimensional positioning errors.

CHAPTER 6. CONCLUSIONS AND SUGGESTIONS FOR FURTHER RESEARCH

The conclusions drawn from this research are as follows:

1. The Wide Area Differential GPS (WADGPS) concept is feasible in both simulations and experiments.

2. Using WADGPS we can reduce the number of monitor stations substantially while achieving the same accuracy that DGPS can achieve.

3. We used Algorithm B to simulate WADGPS. The accuracy of the WADGPS correction is consistent within the monitored region, and degrades gracefully on the perimeter.

4. The most accurate implementation is Algorithm C, which estimates only geometric errors (ephemeris errors and clock bias errors). The Algorithm C was chosen to postprocess real data.

5. The test results indicate that WADGPS can reduce stand-alone GPS positioning errors to the order of one meter (with a 1632km baseline) without severe degradation caused by spatial separation between the monitor stations and the users.

6. Since the time constant of SA, which is the fastest changing among the GPS error sources, is currently about three minutes, we propose an update rate of 5-10 seconds per update for error corrections.

7. A study of the latency showed that 2-3m of three-dimensional RMS positioning accuracy can be achieved with 5-10 seconds of latency, which result in 10-20 seconds of maximum age, if P-code mode is selected and WADGPS is used with error-rate corrections.

8. A statistics of the ionospheric time delay measurement noise for P-code and cross-correlation mode led us to predict the WADGPS test results with 5-10 seconds of latency and using the receivers in cross-correlation mode as 3-5m of three-dimensional positioning errors.

Suggestions for future research are as follows:

1. Aircraft should be used for dynamic tests to confirm the potential of WADGPS and to evaluate the performance of WADGPS.

2. More research should be done to model and estimate SA because this is the major error source for WADGPS. By transmitting SA parameters instead of SA errors themselves we should be able to increase the accuracy of WADGPS and shorten the transmission data contents.

3. Ionospheric time delay estimation using a single frequency receiver needs to be studied further, to enable single frequency users to use the WADGPS error correction (Algorithm C).

4. Orbit estimation, tropospheric modeling, and multipath calibration should be investigated to make WADGPS achieve decimeter accuracy.

5. A sequential filter needs to be concerned in correction parameter estimation to improve the performance of WADGPS.

APPENDIX A. NONLINEAR STATIC ESTIMATION

Given $x = N(\bar{x}, M)$,

$\quad\quad\quad z = h(x) + v$,

$\quad\quad\quad v = N(0, V)$, and M, V are symmetric covariance matrices.

Find x which minimizes,

$$J = \frac{1}{2}(x - \bar{x})^T M^{-1}(x - \bar{x}) + \frac{1}{2}[z - h(x)]^T V^{-1}[z - h(x)].$$

Solution:

Define $H = \dfrac{\partial h}{\partial x}$.

$$J = J_0 + dJ, \tag{A.1}$$

where

$$dJ = (x - \bar{x})^T M^{-1} dx - [z - h(x)]^T V^{-1} H dx$$

$$+ \frac{1}{2} dx^T \left[M^{-1} + H^T V^{-1} H - \{z - h(x)\}^T V^{-1} \left\{ \frac{\partial^2 h}{\partial x^2} \right\} \right] dx + h.o.t. \tag{A.2}$$

If $\{z - h(x)\}^T V^{-1} \left\{ \dfrac{\partial^2 h}{\partial x^2} \right\}$ and the higher order term ($h.o.t.$) are small,

$$dJ = (x - \bar{x})^T M^{-1} dx - [z - h(x)]^T V^{-1} H dx + \frac{1}{2} dx^T \left[M^{-1} + H^T V^{-1} H \right] dx. \tag{A.3}$$

118

Since the solution x cannot be expressed in analytic form, x should be found numerically. J can be minimized by making equation (A.3) a perfect square in dx. In each numerical step dx should be found to make $\frac{\partial J}{\partial x} = 0$, i.e., to minimize J.

The algorithm for the Nonlinear Static Estimation is

(1) Guess x

(2) Evaluate $h(x)$ and H

(3) $P = \left(M^{-1} + H^T V^{-1} H\right)^{-1}$

(4) $\frac{\partial J}{\partial x} = M^{-1}(x - \bar{x}) - H^T V^{-1}\left[z - h(x)\right] \equiv GR$

(5) If $|GR| \leq \varepsilon$, then set $\hat{x} = x$ and stop. Otherwise $\bar{x} = x$.

(6) Replace x by $(x - P \cdot GR)$

(7) Go to (2).

APPENDIX B. MINIMUM NORM PROBLEM

Given $Hx = z$ where H is an m by n matrix $(m \leq n)$ and has full rank, find the solution x that satisfies above linear system and minimizes $J = \frac{1}{2}x^T x$.

Solution: $\qquad\qquad\qquad\qquad x = H^T(HH^T)^{-1}z$.

Proof:

Define the Hamiltonian $\mathcal{H} = \frac{1}{2}x^T x + \lambda^T(z - Hx)$ where λ^T is a Lagrangian

multiplier. To get a minimum norm solution x should satisfy the two equations

$$\frac{\partial \mathcal{H}}{\partial x} = 0,$$ (B.1)

$$\frac{\partial \mathcal{H}}{\partial \lambda} = 0.$$ (B.2)

Those equations give

$$x = H^T \lambda,$$ (B.3)

$$Hx = z.$$ (B.4)

By substituting equation (B.3) into equation (B.4), we obtain

$$HH^T \lambda = z.$$ (B.5)

Because HH^T has full rank, the inverse of HH^T exists. Premultiplying by the inverse of HH^T gives

$$\lambda = \left(HH^T\right)^{-1} z.$$ (B.6)

Substituting equation (B.6) into equation (B.3) gives the desired minimum norm solution,

$$x = H^T\left(HH^T\right)^{-1} z.$$ (B.7)

BIBLIOGRAPHY

Ashkenazi, V., Hill, C. J., and Nagel, J., "Wide Area Differential GPS: A Performance Study," *Proceedings of ION GPS-92*, Albuquerque, September, 1992, pp. 589-598.

Beser, J. and Parkinson, B. W., "The Application of NAVSTAR Differential GPS in the Civilian Community," *NAVIGATION*, Journal of the Institute of Navigation, Vol. 29, No. 2, Summer 1982, pp. 107-136.

Bishop, G. J. and Klobuchar, J. A., "Multipath Effects on the Determination of Absolute Ionospheric Time Delay from GPS Signals," *Radio Science*, Vol. 20, No. 3, May-June 1985, pp. 388-396.

Black, H. D., "An Easily Implemented Algorithm for the Tropospheric Range Correction," *Journal of Geophysical Research*, Vol. 83, No. B4, April 1978, pp. 1825-1828.

Bryson, A. E. and Ho, Y., *Applied Optimal Control*, hemisphere publishing corporation, 1975.

Bryson, A. E., Lecture Notes, *Optimal Estimation and Control Logic in the Presence of Noise (Stanford Course AA278B)*, Spring, 1989.

Chao, Y., "The Statistics of Selective Availability and its Effect on Differential GPS," ION GPS-93, Salt Lake City, Utah, September, 1993.

Chou, H., "An Adaptive Correction Technique for Differential Global Positioning System," Ph.D. thesis at Stanford University, June 1991.

Chou, H., "An Anti-SA Filter for Non-differential GPS Users," *Proceedings of ION GPS-90*, Colorado Springs, Colorado, September, 1990.

Cohen, C., Pervan, B., and Parkinson, B. W., "Estimation of Absolute Ionospheric Delay Exclusively though Single Frequency GPS Measurements," *Proceedings of ION GPS-92*, Albuquerque, New Mexico, September, 1992, pp. 325-330.

Dixon, R. C., *Spread Spectrum Systems*, 2nd ed., John Wiley & Sons, New York, 1984.

Department of Transportation (DOT), *1990 FEDERAL RADIO NAVIGATION PLAN*, DOT-VNTSC-RSPA-90-3, 1990.

Enge, P., Levin, P., Kalafus, R., McBurney, P., Daly, P., and Nagle, J., "Architecture for a Civil Integrity Network Using Inmarsat," *Proceedings of ION GPS-90*, Colorado Springs, Colorado, September, 1990, pp. 287-296.

Enge, P., "Coverage of DGPS Radiobeacons," *Proceedings of ION GPS-92*, Albuquerque, New Mexico, September, 1992, pp. 555-564.

Enge, P., Van Dierendonck, A. J., and Kinal, G., "A Signal Design for the GIC Which Includes Capacity for WADGPS Data," *Proceedings of ION GPS-92*, Albuquerque, New Mexico, September, 1992, pp. 875-884.

Enge, P., "The Global Positioning System: Signals, Measurements and Performance," *The International Journal on Wireless Information Networks*, March, 1994.

Gelb, A., *Applied Optimal Estimation*, M.I.T. Press, 1974.

Green, G. B., Massatt, P. D., and Rhodus, N. W., "The GPS 21 Primary Satellite Constellation," *NAVIGATION*, Journal of the Institute of Navigation, Vol. 36, No. 1, Spring 1989, pp. 9-24.

Greenspan, R. L. and Donna, J. I., "Measurement Errors in GPS Observables," the 42nd Annual Meeting of the Institute of Navigation, Seattle, Washington, June 1986, pp. 55-60.

Hatch, R. R., "The Synergism of GPS Code and Carrier Measurements," *Proceedings of the Third International Geodetic Symposium on Satellite Doppler Positioning*, Las Cruces, NM, February 1982, pp. 1213-1232.

Hegarty, C. J., "Optimizing Differential GPS for a Data Rate Constrained Broadcast Channel," ION GPS-93, Salt Lake City, Utah, September, 1993.

The Institute of Navigation, *Global Positioning System Vol. I*, Papers published in NAVIGATION, Reprinted by the ION, Washington, D. C., 1980.

The Institute of Navigation, *Global Positioning System Vol. II*, Papers published in NAVIGATION, Reprinted by the ION, Washington, D. C., 1984.

The Institute of Navigation, *Global Positioning System Vol. III*, Papers published in NAVIGATION, Reprinted by the ION, Washington, D. C., 1987.

Kalafus, R. M., Van Dierendonck, A. J., and Pealer, N. A., "Special Committee 104 Recommendations for Differential GPS Service," *Global Positioning System, Vol. III*, The Institute of Navigation, 1986, pp. 101-116.

Kee, C. and Parkinson, B. W., "Wide Area Differential GPS," National Technical Meeting of the Institute of Navigation, San Mateo, California, January 1990. (Abstract was submitted and accepted.)

Kee, C., Parkinson, B. W., and Axelrad, P., "Wide Area Differential GPS," *NAVIGATION*, Journal of the Institute of Navigation, Vol. 38, No. 2, Summer, 1991.

Kee, C. and Parkinson, B. W., "Algorithms and Implementation of Wide Area Differential GPS," *Proceedings of ION GPS-92*, Albuquerque, September, 1992, pp. 565-572.

Kee, C. and Parkinson, B. W., "High Accuracy GPS Positioning in the Continent: Wide Area Differential GPS," Differential Satellite Navigation Systems 93 (DSNS-93) Conference, Amsterdam, The Netherlands, April, 1993.

Keegan, R. G., "P-Code Aided Global Positioning System Receiver," U.S. Patent No. 4,972,431, November 20, 1990.

Klobuchar, J., "Design and Characteristics of the GPS Ionospheric Time Delay Algorithm for Single Frequency Users," IEEE Plans '86 Position Location and Navigation Symposium, Las Vegas, November 4, 1986.

Knight, J. E. and Rhoades, K. W., "Differential GPS Static and Dynamic Test Results," the 1st Technical Meeting of the Satellite Division of the Institute of Navigation, Colorado Spring, Colorado, September 1987, pp. 235-242.

Kremer, G. T., Kalafus, R. M., Loomis, P. V. W., and Reynolds, J. C., "The Effect of Selective Availability on Differential GPS Corrections," *NAVIGATION*, Journal of the Institute of Navigation, Vol. 37, No. 1, Spring 1990, pp. 39-52.

Larkin, T., "GPS Services Available to Civilian Users," the 1st International Technical Meeting of the Satellite Division of the Institute of Navigation, Colorado Springs, Colorado, September 1988, pp. 67-75.

Loomis, P. V. W., Denaro, P., and Saunders, P., "Worldwide Differential GPS for Space Shuttle Landing Operations," IEEE Plans '90 Position, Location, and Navigation Symposium, Las Vegas, March, 1990.

Lorenz, R. G., Helkey, R. J., and Abadi, K. K., "Global Positioning System Receiver Digital Processing Technique," U.S. Patent No. 5,134,407, July 28, 1992.

Milliken, R. J. and Zoller, C. J., "Principle of operation of NAVSTAR and system characteristics," *Global Positioning System Vol. I*, pp. 3-14, The Institute of Navigation, 1980.

Murray, M. H., King, R. W., and Morgan, P. J., "SV5: a terrestrial reference frame for monitoring crustal deformation with the Global Positioning System," (Abstract) EOS Trans. AGU, v. 71, p. 1274, 1990.

Rockwell International Corporation ICD-GPS-200, *NAVSTAR GPS Space Segment/Navigation User Interfaces*, November 30, 1987.

Russel, S. S. and Schaibly, J. H., "Control Segment and User Performance," *Global Positioning System, Vol. I*, The Institute of Navigation, 1980, pp. 74-80.

Spilker, Jr., J. J., "Global Positioning System: Signal Structure and Performance Characteristics," *AGARD-AG-245*, July 1979.

Stephens, S. G. and Feess, W. A., "An Evaluation of the GPS Single Frequency User Ionospheric Time Delay Model," *Proceedings of the '86 Position, Location, and Navigation Symposium*, November, 1986.

Teasley, S. P., Hoover, W. M. and Johnson, C. R., "Differential GPS Navigation," PLANS 80, Atlantic City, New Jersey, December 1980, pp. 9-16.

Van Dierendonck, A. J., McGraw, J. B., and Brown, R. G., "Relationship between Allan Variances and Kalman Filter Parameters," *Proceedings of the 16th annual PTTI Applications & Planning Meeting*, Maryland, November, 1984.

Van Dierendonck, A. J., Fenton, P., and Ford, T., "Theory and Performance of Narrow Correlator Spacing in a GPS Receiver," ION National Technical Meeting, San Diego, California, January, 1992.

Van Dierendonck, A. J. and Enge, P., "RTCA Special Committee 159 Definition of the GNSS Integrity Channel (GIC) and Wide Area Differential GNSS (WADGNSS)," *ION GPS-93*, Salt Lake City, Utah, September, 1993.

Van Nee, R. D. J., "Optimum DGPS Receiver Structures," Differential Satellite Navigation Systems 93 (DSNS-93), Amsterdam, The Netherlands, April, 1993.

Ward, P., "Dispelling Some Popular Myths about GPS Receivers for Military Applications," The 2nd International Technical Meeting of the Satellite Division of the Institute of Navigation, Colorado Springs, Colorado, September 1989, pp. 281-290.

Wells, D., et al., *Guide to GPS Positioning*, Canadian GPS Associates, Fredericton, N. B., Canada, 1986.

Wilson, B. and Mannucci, A., "Instrumental Biases in Ionospheric Measurements Derived

    from GPS Data," ION GPS-93, Salt Lake City, Utah, September, 1993.

Xia, R., "Determination of Absolute Ionospheric Error using a Single Frequency GPS

    Receiver," *Proceedings of ION GPS-92*, Albuquerque, New Mexico, September,

    1992, pp. 483-490.